

University of Central Florida

STARS

Electronic Theses and Dissertations

Masters Thesis (Open Access)

Synthesis, Characterization And Antibacterial Activity Of Silver Embedded Silica Nanoparticle/nanogel Formulation

2011

Roseline Menezes

University of Central Florida

Find similar works at: <https://stars.library.ucf.edu/etd>

University of Central Florida Libraries <http://library.ucf.edu>

 Part of the [Biotechnology Commons](#), and the [Molecular Biology Commons](#)

STARS Citation

Menezes, Roseline, "Synthesis, Characterization And Antibacterial Activity Of Silver Embedded Silica Nanoparticle/nanogel Formulation" (2011). *Electronic Theses and Dissertations*. 1775.

<https://stars.library.ucf.edu/etd/1775>

This Masters Thesis (Open Access) is brought to you for free and open access by STARS. It has been accepted for inclusion in Electronic Theses and Dissertations by an authorized administrator of STARS. For more information, please contact lee.dotson@ucf.edu.



SYNTHESIS, CHARACTERIZATION AND ANTIBACTERIAL ACTIVITY OF SILVER
EMBEDDED SILICA NANOPARTICLE/NANO GEL FORMULATION

by

ROSELINE MENEZES
B.E. Biotechnology,
Shivaji University, Kolhapur, India 2008

A thesis submitted in partial fulfillment of the requirements
for the degree of Master in Science
in the Department of Biotechnology
in the Burnett School of Biomedical Sciences, College of Medicine
at the University of Central Florida
Orlando, Florida

Fall Term
2011

Major Professor: Swadeshmukul Santra

© 2011 Roseline Menezes

ABSTRACT

The antibacterial property of silver (Ag) has been known since ancient time. It is reported in the literature that silver nanoparticles (AgNPs) exhibit improved antibacterial properties in comparison to silver ions of equivalent metallic Ag concentration. Such improvement in antibacterial activities is due to the high surface area to volume ratio of AgNPs (which facilitates interaction with the bacterial cells), increased release of silver ions and direct intra-cellular uptake of AgNPs leading to localized release of Ag ions. To date, over 300 consumer products containing AgNPs are available in the market and the inventory is rapidly expanding. The antibacterial efficacy is related to the loading of AgNPs (which controls availability of active Ag ions). It is perhaps challenging to increase AgNPs loading in consumer products without compromising its aesthetic appearance. AgNPs exhibit yellow-brown color due to strong Surface Plasmon Resonance (SPR) absorption; and therefore, it is expected that an increase in loading would change the color of AgNP-containing materials. For applications, such as creating a fast-acting touch-safe surface, higher loading of AgNPs is desirable. It is also desirable to obtain a non-color forming surface. To meet the demands of desirable higher loading of AgNPs and non-color forming surface, the objective of this study is to minimize SPR by engineering Ag containing nanomaterials for potential fast-acting spray-based applications. Within this thesis several reports have been made including synthesis, characterization and antibacterial properties of Ag-loaded silica nanoparticle/nanogel (AgSiNP/NG) material containing nanoformulations. The effects of nanoformulation pH and metallic Ag content on the SPR absorption and antibacterial properties have been studied. The AgSiNP/NG materials were synthesized using silica sol-gel technique at room temperature in water. The color formation of the AgSiNP/NG

material was found to be dependent on silver ion loading (15.4 wt% and 42.3 wt %) as well as on the pH (pH 4.0 and pH 7.0). A number of material characterization techniques such as HRTEM, SEM and AFM were used to characterize particle size, crystalline and surface morphology in dry state. Dynamic light scattering (DLS) technique was used to characterize particle size and size distribution in solution. UV-VIS spectroscopy technique was applied to characterize Ag ions and AgNPs in the AgSiNP/NG material. Antibacterial studies were conducted against gram negative *E.coli* and gram positive *B.subtilis* and *S.aureus*. A number of qualitative (well diffusion, BacLight™ live-dead® viability) and quantitative (turbidity, resazurin viability) assays were used for antibacterial studies. It was observed that lower pH and low Ag loading minimized SPR absorption, resulting in no yellow-brown color formation. The HRTEM confirmed the formation of ~5-25 nm size highly crystalline AgNPs which were coated with dielectric silica layer (silica gel). AFM, SEM and DLS studies confirmed formation of AgSiNPs in the range between 100 nm – 200 nm. The AgSiNP/NG material was effective against both gram-negative and gram-positive bacteria. Based on this research it is suggested that by coating AgNPs with a dielectric material (such as silica); it is possible to suppress SPR absorption.

This thesis is dedicated to my family and friends who have always supported me and helped me through my life.

ACKNOWLEDGMENTS

I would like to take this opportunity to acknowledge my mentor and committee chair Dr. Swadeshmukul Santra for believing in me and giving me opportunity to work in his lab and for his guidance, direction and assistance. I am also very thankful to Dr. Saleh Naser and Dr. William Self for accepting to guide and support me as committee members. I will also like to acknowledge Dr. Henry Daniel for all of the help and support.

I also want to thank Dr. Padmavathy Tallury, for guiding me through this project since she developed this protocol and taught me various techniques including material synthesis and characterization part. I would like to acknowledge Dr. Helge Heinrich for helping me with HR-TEM, Kirk Scammon for helping me with SEM and Ms. Ishrath Abdulsamad, Senior lab tech, Biomed science for providing bacterial cultures for my work.

I would like to especially thank my lab mates Astha Malhotra, Andrew Teblum, Pavithra Maniprasad, Jennelle Suarez an, Srijita Basumallick, Sabrina Ghim for helping and supporting me through the process of my thesis work. I would also like to acknowledge Mona Mathew and Tanmay Bera for helping me with this project.

Finally I would like to thank all of my friends and family who in one way or the other has contributed in this work. I would also like to thank my parents for always being there for me and making me achieve my goal.

TABLE OF CONTENTS

LIST OF FIGURES	ix
LIST OF TABLES	xii
CHAPTER 1 INTRODUCTION	1
1.1 Silver as an antibacterial material	1
1.2 Mode of action of silver ions and its resistance towards bacteria	2
1.3 Silver Nanoparticles	3
1.4 Proposed Research	5
CHAPTER 2 LITERATURE REVIEW	7
2.1 What is sol-gel method?	7
2.2 Surface Plasmon Resonance.....	8
2.3 Silver-Silica composites.....	9
CHAPTER 3 MATERIALS AND METHODS	12
3.1 Materials.....	12
3.2 Synthesis.....	13
3.2.1 Silver (Ag) loaded silica nanoparticle/nanogel 200 pH 4 (AgSiNP/NG200 pH 4).....	13
3.2.2 Silver (Ag) loaded silica nanoparticle/nanogel 200 pH 7 (AgSiNP/NG200 pH 7).....	13
3.2.3 Silver (Ag) loaded silica nanoparticle/nanogel 50 pH 4 (AgSiNP/NG50 pH 4).....	14
3.2.4 Silver (Ag) loaded silica nanoparticle/nanogel 50 pH 7 (AgSiNP/NG50 pH 7).....	14
3.2.5 Controls	15
3.3 Material Characterization.....	16
3.3.1 Dynamic Light Scattering (DLS)	16
3.3.2 Atomic Force Microscopy (AFM).....	16
3.3.3 Scanning Electron Microscopy (SEM).....	17

3.3.4 UV-Visible spectroscopy.....	17
3.3.5 High Resolution Transmission Electron Microscopy.....	18
3.4 Antibacterial Studies	18
3.4.1 Well Diffusion assay	18
3.4.2 Bacterial Growth inhibition assay in broth using turbidity	19
3.4.3 Minimum Inhibitory Concentration assay using resazurin indicator	20
3.4.4 BacLight™ LIVE/DEAD® assay.....	21
CHAPTER 4 RESULTS	22
4.1 Material Morphology	23
4.1.1 Dynamic light scattering.....	23
4.1.2 Atomic force microscopy	27
4.1.3 Scanning Electron Microscopy.....	29
4.2. Confirming the production of Silver Nanoparticles.....	33
4.2.1 UV-Visible spectroscopy.....	33
4.2.2 High Resolution Transmission electron Microscopy	35
4.3 Anti-bacterial Studies.....	42
4.3.1 Well Diffusion Method.....	42
4.3.2 Bacterial Growth inhibition assay in broth using turbidity	45
4.3.3 Minimum Inhibitory Concentration assay using resazurin indicator	63
4.3.4 BacLight® LIVE/DEAD assay	66
CHAPTER 5 DISCUSSION.....	69
CHAPTER 6. CONCLUSION.....	73
REFERENCES	74

LIST OF FIGURES

Figure 1 - Proposed schematic of entrapment of silver nanoparticles in silica matrix.	6
Figure 2 - Chemical reactions in sol-gel synthesis (Adapted from Gupta R. et al(20))	8
Figure 3- Schematic of synthesis of AgSiNP/NG200 and AgSiNP/NG50 at pH 7 and pH 4	15
Figure 4 - Digital images for A) AgSiNP/NG200 pH 7 B) AgSiNP/NG200 pH 4 C) AgSiNP/NG50 pH 7 D) AgSiNP/NG50 pH 4.	22
Figure 5- DLS seen for AgSiNP/NG200 A) pH 7 B) pH 4 as synthesized C) pH 4 after a month	24
Figure 6 - DLS seen for AgSiNP/NG50 A) pH 7 B) pH 4 as synthesized C) pH 4 after a month.	25
Figure 7 - DLS seen for SiNG A) pH 7 B) pH 4 as synthesized C) pH 4 after a month.	26
Figure 8 - AFM image of AgSiNP/NG200 pH 7 with sectional analysis stating the size of particle.....	27
Figure 9 - AFM image of AgSiNP/NG200 pH 4 with sectional analysis stating the size of particle.....	27
Figure 10 - AFM image of SiNG pH 7 with sectional analysis stating the size of particle.....	28
Figure 11 - AFM image of SiNG pH 4 with sectional analysis stating the size of particle.....	28
Figure 12 - Scanning Electron microscopy of AgSiNP/NG200 pH 4	29
Figure 13 - SEM image of AgSiNP/NG200 at pH 7	30
Figure 14 - SEM Image of AgSiNP/NG50 at pH 4	30
Figure 15 - SEM Image of AgSiNP/NG50 at pH 7	31
Figure 16 - SEM Image of SiNG at pH 4	31
Figure 17 - SEM Image of SiNG at pH 7	32

Figure 18 - UV-Vis spectroscopy of A) AgSiNP/NG200 pH 4 B) AgSiNP/NG200 pH 7	33
Figure 19 - UV-Vis spectroscopy of A) AgSiNP/NG50pH 4 B) AgSiNP/NG50 pH 7	34
Figure 20 - HRTEM Image of AgSiNP/NG200 A) Formation of silver NpS uniformly in gel as seen at low magnification B) Formation of silica nanoparticles around 18nm in size is seen surrounded by amorphous silica C) The diffraction pattern confirming the presence of crystalline material (Silver) by d-spacing of analysis.	35
Figure 21 - HRTEM high magnification image of AgSiNP/NG200 pH 7 shows silver spherical silver nanoparticle crystal structure with silica matrix in background with average size ranging from 1 to 10nm.....	36
Figure 22 - HRTEM of AgSiNP/NG200 pH 4. This shows uniformly distributed silver nanoparticles through the silica matrix A) Low magnification showing uniform distribution of particles of different sizes average size being 30nm and B) showing high magnification of the nanoparticles embedded in silica gel at lower pH 4.	36
Figure 23 - Highly crystalline highly magnified silver nanoparticle can be seen in AgSiNP/NG200 pH 4.	37
Figure 24- HR-TEM EDAX for AgSiNP/NG200 pH 4 A) Selected area for diffraction (with nanoparticle) A') EDAX analysis of the area shown in A. B) Selected area for diffraction (outside particle) B') EDAX analysis of the area shown in B.....	38
Figure 25 - HRTEM of AgSiNP/NG50 pH 7-particle A) low magnification B) high magnification	39
Figure 26 - HRTEM of AgSiNP/NG50 pH 7 A) low magnification image of the gel B) Crystalline diffraction pattern of AgSiNP/NG50 pH 7 B) EDAX of ASiNG50 pH 7 taken from a point in image A.....	40
Figure 27 - HRTEM image for AgSiNP/NG50 pH 4 A) Low magnification B) high magnification	41
Figure 28 - Growth curve of <i>E.coli</i> in presence of A) AgSiNP/NG200 pH 4 B) AgSiNP/NG200 pH 7C) Silver Nitrate 200 (381µg/ml metallic silver content) pH 4 D) Silver Nitrate 200 (381µg/ml metallic silver content) pH 7.	46
Figure 29 - Comparative end point growth inhibition of <i>E.coli</i> by A) AgSiNP/NG200 pH 7 Vs Silver Nitrate 200 pH 7 B) AgSiNP/NG200 pH 4 Vs Silver Nitrate 200 pH 4.....	47
Figure 30 - Growth curve of <i>E.coli</i> in presence of A) AgSiNP/NG50 pH 4 B) AgSiNP/NG50 pH 7 C) Silver Nitrate 50 (100.8µg/ml metallic silver content) pH 4 D) Silver Nitrate 50 (100.8µg/ml metallic silver content) pH 7.....	49

Figure 31 - Comparative end point growth inhibition of <i>E.coli</i> by A) AgSiNP/NG50 pH 4 Vs Silver Nitrate 50 pH 4 B) AgSiNP/NG50 pH 7 Vs Silver Nitrate 50 pH 7.....	50
Figure 32 - Growth curve of <i>B.subtilis</i> in presence of A) AgSiNP/NG200 pH 4 B) AgSiNP/NG200 pH 7 C) Silver Nitrate 200 (381µg/ml metallic silver content) pH 4 D) Silver Nitrate 200 (381µg/ml metallic silver content) pH 7.....	52
Figure 33 - Comparative end point growth inhibition of <i>B.subtilis</i> by A) AgSiNP/NG200 pH 7 Vs Silver Nitrate 200pH 7 B) AgSiNP/NG200pH 4 Vs Silver Nitrate 200pH 4	53
Figure 34 - Growth curve of <i>B.subtilis</i> in presence of A) AgSiNP/NG50 pH 4 B) AgSiNP/NG50 pH 7 C) Silver Nitrate 50 (100.8µg/ml metallic silver content) pH 4. D) Silver Nitrate 50 (100.8µg/ml metallic silver content) pH 7.....	55
Figure 35- Comparative end point growth inhibition of <i>B.subtilis</i> by A) AgSiNP/NG50 pH 4 Vs Silver Nitrate 50pH 4 B) AgSiNP/NG50pH 7 Vs Silver Nitrate 50pH 7.....	56
Figure 36 - Growth curve of <i>S.aureus</i> in presence of A) AgSiNP/NG200 pH 4 B) AgSiNP/NG200 pH 7 C) Silver Nitrate 200 (381µg/ml metallic silver content) pH 4. D) Silver Nitrate200 (381µg/ml metallic silver content) pH 7.....	58
Figure 37 - Comparative end point growth inhibition of <i>S.aureus</i> by A) AgSiNP/NG200 pH 7 Vs Silver Nitrate 200pH 7 B) AgSiNP/NG200pH 4 Vs Silver Nitrate 200 pH 4.....	59
Figure 38 - Growth curve of <i>S.aureus</i> in presence of A) AgSiNP/NG50 pH 4 B) AgSiNP/NG50 pH 7. C) Silver Nitrate50 (100.8µg/ml metallic silver content) pH 4. D) Silver Nitrate50 (100.8µg/ml metallic silver content) pH 7.....	61
Figure 39 - Comparative end point growth inhibition of <i>S.aureus</i> by A) AgSiNP/NG50 pH 4 Vs Silver Nitrate 50pH 4 B) AgSiNP/NG50pH 7 Vs Silver Nitrate 50pH 7.....	62
Figure 40 - Resazurin assay for AgSiNP/NG200 A) <i>E.coli</i> B) <i>B.Subtilis</i> C) <i>S.aureus</i>	63
Figure 41- Resazurin assay for AgSiNP/NG50 for A) <i>E.coli</i> B) <i>B.subtilis</i> C) <i>S.aureus</i>	64
Figure 42 - <i>E.coli</i> treated for 2 hours with A) AgSiNP/NG200 pH 7 B) AgSiNP/NG200 pH 4 C) AgNO ₃ pH 7 D) AgNO ₃ pH 4 E) SiNG pH 4 F) Untreated cells.	66
Figure 43 - <i>B.subtilis</i> treated for 2 hours with A) AgSiNP/NG200 pH 7 B) AgSiNP/NG200 pH 4 C) AgNO ₃ pH 7 D) AgNO ₃ pH 4 E) SiNG pH 4 F) Untreated cells.	67
Figure 44 - <i>S.aureus</i> treated for 2 hours with A) AgSiNP/NG200 pH 7 B) AgSiNP/NG200 pH 4 C) AgNO ₃ pH 7 D) AgNO ₃ pH 4 E) SiNG pH 4 F) Untreated cells.	68

LIST OF TABLES

Table 1 - Well diffusion zones for AgSiNP/NG200.....	43
Table 2 - Well diffusion zones for AgSiNP/NG50.....	44
Table 3 - Average MIC obtained from resazurin assay	65

CHAPTER 1 INTRODUCTION

1.1 Silver as an antibacterial material

Silver is a transition metal with atomic number 47 and atomic mass 107.87. It has widely been used as an antibacterial agent for centuries because it is a non-selective toxic biocide (1). During old times, silver metal-based pots and cups were used for storage of water to inhibit the contamination. Prior to advent of antibiotics colloidal silver was used as a bactericidal agent. Silver based biocides have been used as preservatives, disinfectants, antifungal, antibacterial, and antiviral agents. Silver citrate salts have been known to treat skin infections; silver nitrate was used to treat ophthalmic infections, such as ophthalmia neonatorum for more than one hundred years (2). Several silver salts, such as silver acetate were formulated in lotions and creams to treat eye infections. To treat bladder infections silver nitrate salts were used and silver lactate was used as general antiseptic. Sulfadiazine was mixed with the silver to control the release of the silver ions. This silver sulfadiazine mixture was introduced in creams to treat burn wounds and to prevent infection (3). Silver sulfadiazine is a water insoluble, non-ionized powder used as 1% suspension as antiseptic. Colloidal preparation of silver salts is still used medically to prevent and treat numerous diseases, such as cancer, diabetes, AIDS and herpes (4). Nylon fibers coated with silver were used to treat the post operative wounds. Silver is also employed in water disinfection in order to avoid use of chlorine, which causes formation of carcinogens. Silver treated charcoal filters are used in drinking water disinfection to remove odors and organics. Due

to increase in the amount of antibiotic resistant bacterial strains, scientists today are trying to find the antibacterial materials based on metals. Since silver is a very effective antibacterial material, with little toxicity towards human cells it has been widely studied against the multiple drug resistant bacteria (5).

1.2 Mode of action of silver ions and its resistance towards bacteria

The mode of action of silver ions against bacteria is widely studied. Silver ions can kill the bacteria by various methods. Some of them are described in this section. Silver ions react with electron donors to form complexes with thiols, carboxylates, phosphates, hydroxyls, amines, imidazoles and indoles, thus inactivating the enzymes(6). It was reported by Swanson et al that respiratory chains of bacteria were inhibited by silver ions at two sites one being between cytochrome b and cytochrome d and the second being between the site where the substrate enters the respiratory chain and flavoprotein in NADH and succinate dehydrogenase (7). It was shown that silver ions at 86 μ M were able to inhibit the oxidation of carbohydrates such as glucose, fumarate, succinate and glycerol in *E.coli* (8). Reports showed that there was change in enzyme conformation within bacterial cells at concentrations between 0.001 to 1.00mM of Ag⁺ ions (9). It was also shown that Ag ion formed complexes with nucleic acid bases present in DNA (10). Silver ions were also known to form deformation of cell membranes as shown by Coward et al(11).

Even though silver is a strong and rapid acting antibacterial material, silver ion resistant bacterial strains have been isolated from various places such as clinic, silver mines as well as laboratories (12). The resistance of bacteria to silver ions is attributed to presence of resistant

plasmid which brings about active efflux of silver ions from the cell, sequestration of silver ions in periplasm, conversion of silver ions to colloidal form and reduction of the outer membrane porins which brings about the intake of silver ions (13).

1.3 Silver Nanoparticles

Due to the emerging resistance of bacteria towards antibiotics and metal ions, there is a necessity to engineer antimicrobial, biocompatible and functionalized materials, which can be effectively used. Various metallic nanoparticles, such as copper, silver, titanium and gold have been studied rigorously. The properties of these nanoparticles are different from that of the bulk material because of the large surface area to volume ratio, surface energy and spacial confinement (14). Silver nanoparticles are widely used because of its antibacterial and antiviral properties, superior catalytic activity and improved enhancement factors for Surface Enhanced Raman Spectroscopy (SERS) (15, 16). Various methods have been used to synthesize silver nanoparticles such as chemical reduction, photo reduction, sonochemical reduction, radiolytic reduction, micro emulsion, and ion beam deposition. From all of these methods, chemical reduction is widely studied. The silver nanoparticles produced by these methods have various shortcomings including aggregation of nanoparticles, which reduces the activity of the particle (17). Several methods are being investigated to reduce these problems, such as formation of silver-polymer composites as biomaterials (18). As a result, silver embedded biomaterials are raising interest that is aimed towards the broad antibacterial spectrum of silver and its potential as an anti-inflammatory agent and its wound-healing properties.

Another potential application of silver nanoparticles in biomedicine is its use as substrate for Surface Enhanced Raman Spectroscopy(SERS) (19). Silver nanoparticles are also known to enhance fluorophore emission intensity thus they are used in sensitive fluorescence screening as metal enhanced fluorescence in biomedicine.

The antibacterial effect of silver nanoparticles is stronger than the silver salts. The strong antibacterial property of silver nanoparticle is because of the increased surface area as well as increase potential to produce silver ions. The silver nanoparticles because of its small size can accumulate in the cytoplasmic membrane of the bacteria and can cause an increase in permeability of the cell wall leading to bactericidal effect. Also, surface of silver nanoparticles can produce free radicals which can cause damage to cell membrane leading to cell death (38).

Silver nanoparticles have gained various antibacterial applications in industries. More than 300 products are available in market containing silver nanoparticles (www.nanotechproject.org). They are mostly used as a surface disinfectant, anti-odor anti bacterial textiles and also to coat surgical instruments. None of these materials have claimed that they are colorless and non-staining. The common problem found in these products is the formation of color due to oxidation of silver particles, as well as increased Surface Plasmon Resonance (SPR) of silver particles. The color formation decreases the aesthetic view of the coated surface of the material creating a brown coloration that is observed around the silver nanoparticle-coated products.

1.4 Proposed Research

Many researchers have reported the synthesis of Silver containing silica (Egger et al, Kim et al, Min et al), but their synthetic methodologies are complicated, time-consuming, require heating and various complex processes. Silica is a chemically inert, stable and biocompatible material. There are various advantages to entrapping silver in silica gel, such as a better stability of silver nanoparticles in the silica matrix since their dispersion in silica matrix prevents their agglomeration and oxidation, and also higher durability of the antibacterial property of the nanocomposite because of the controlled release of the silver nanoparticles as well as its ions (17). Silica nanogel in general because of its high surface area and strong intermolecular forces has known to have good adherence to various surfaces including glass, plastics, cellulose fibers etc. We have synthesized water based silver embedded silica nanoparticle/nanogel material using simple one pot sol-gel technique. By entrapping silver in silica gel matrix it is possible produce a durable antibacterial inorganic gel with prolonged antibacterial properties. Since silica is a dielectric material, coating the silver nanoparticles with silica will shift the Surface Plasmon Resonance (SPR) absorption of the silver nanoparticles towards UV range and thus reduce the coloration or staining by silver nanoparticles at low pH or low silver ion loading. It is hypothesized that SPR absorption of silver nanoparticles can be significantly suppressed by coating with silica (a dielectric material) and the antibacterial efficacy of silver will not be compromised upon loading into silica matrix.

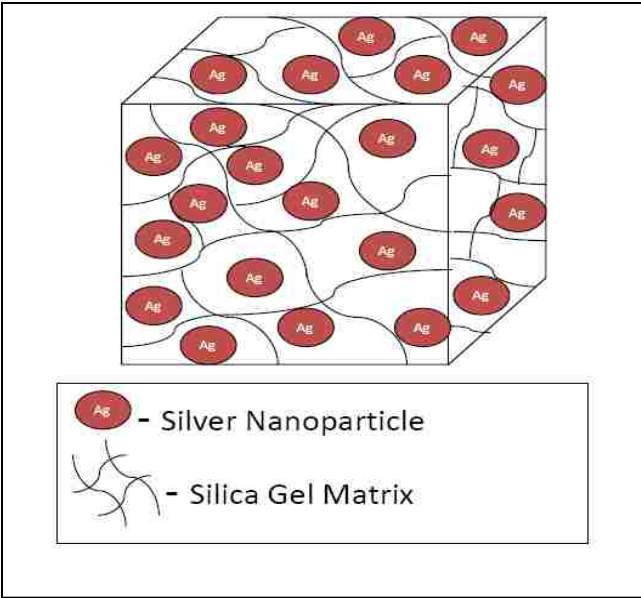


Figure 1 - Proposed schematic of entrapment of silver nanoparticles in silica matrix.

CHAPTER 2 LITERATURE REVIEW

2.1 What is sol-gel method?

Sol-gel is the technology of making glass or ceramic composites at lower temperatures allowing doping of various active agents such as inorganic, organic and biological materials during gel formation (20). The sol-gel process has recently gained momentum because of its various applications in a number of areas including optics, hydrogen storage material, semiconducting devices, sunscreen formulation, chemical and biological sensors. Sol-gel technology is ideal for fabrication of bioactive material because of low processing temperature, intrinsic biocompatibility and also environmental friendliness of the material. It manipulates the structure of the material at molecular level and can control the nature of the interfaces precisely (20). Thus this technique can be used for wide range of applications. The sol-gel process involves transition of a sol or colloidal material into solid gel material. The common silica precursors used in this technique are tetramethylorthosilicate (TMOS) and tetraethylorthosilicate (TEOS). Synthetic silica gel was first reported by Ebelmen in 1844 (21). The sol-gel reaction requires a silica or polymer precursor, water and solvent equivalent to precursor i.e. either methanol or ethanol. A base or an acid is used as a catalyst. In sol-gel reaction, hydrolysis and condensation occurs simultaneously. Silanol group ($\equiv\text{Si}-\text{OH}$) is produced by hydrolysis and condensation produces siloxane bonds ($\equiv\text{Si}-\text{O}-\text{Si}\equiv$). Water and alcohol are produced as by products. By controlling the reaction parameters i.e. the $\text{H}_2\text{O}/\text{Si}$ molar ratio and the concentration

and nature of the catalyst, the properties and structure of sol-gel silicates can be varied over wide ranges (22). Hydrolysis of alkoxy silane catalyzed by acid with low water to Si ratio produces weakly branched polymeric network, thus forming gel, whereas hydrolysis catalyzed by base having high water to Si ratio produces highly branched colloidal particles (silica particles)(23).

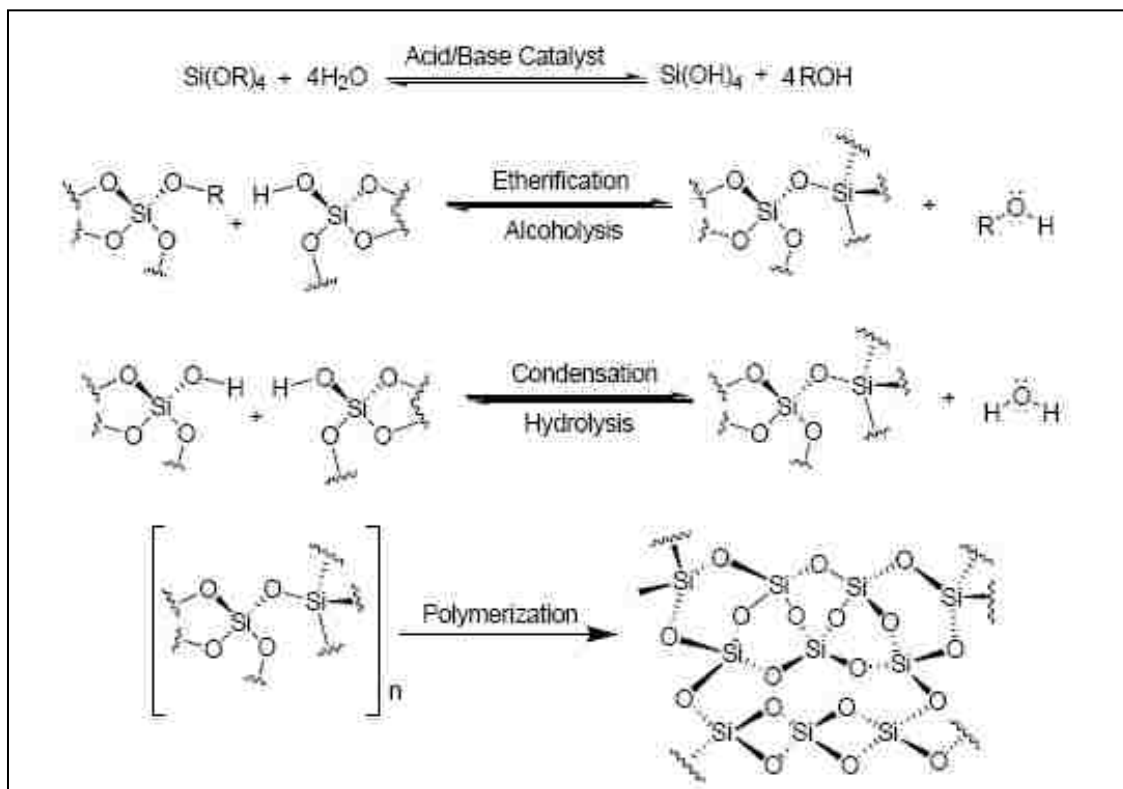


Figure 2 - Chemical reactions in sol-gel synthesis (Adapted from Gupta R. et al(20))

2.2 Surface Plasmon Resonance

Michael Faraday was the first to show that metal particles many times smaller than the wavelength of light scatter and absorb light strongly such that even the dilute solution of the particles exhibit bright colors (24). The conducting electrons within the metal particles collectively oscillate and thus enable scattering and absorption of light at that particular

frequency, giving the color to the solution in case of gold and silver nanoparticles. Surface Plasmon Resonance (SPR) is a phenomenon in which there is a collective oscillation of electrons on the surface of a metal. According to Wiley et al, the SPR peak changes according to the size and shape of the silver nanocrystal (25). The characteristic SPR of silver nanoparticle is seen at wavelengths from 390nm-450nm depending on the size of silver nanoparticle (26). The characteristic yellowish brown color of silver nanoparticle is formed because of this SPR phenomenon.

2.3 Silver-Silica composites

Various methods have been reported for the synthesis of silver-silica nanocomposites. These silver silica composites have attracted attention due to their high antibacterial activity (17). Many methods are used to synthesize silver nanoparticles including micro emulsion, sonochemical reduction, photochemical technique etc. (27-29). They mostly incorporate PVP coatings for better dispersibility of silver nanoparticles. These methods are time consuming and usage of expensive instruments is required to produce silver nanoparticles. The silver nanoparticles produced by the above methods also has a disadvantage of forming aggregations, which changes their chemical property as well as reduces its antibacterial efficacy. It was shown that silica support could solve this problem by allowing silver nanoparticles to grow on them (17). It is also shown that if Ag particles are produced on a supporting material the time required to release the silver ions will be prolonged and thus material supporting Ag have great potential in antibacterial applications (30-33). Ag is supported mainly on organic materials. These materials are not chemically durable. Inorganic materials can overcome this deficit. Various

inorganic materials are developed as a support for antibacterial Ag-containing materials including zeolites, calcium phosphate and carbon fiber (34, 35). Silica-Ag composites in form of glass and films are known to show good chemical durability and good antibacterial efficacy (36, 37). Since silica is chemically inert, stable and biocompatible material and abundantly available in nature it is advantageous to use the silver-silica composite.

In procedure explained by Kim et al (17) they used already synthesized silica nanoparticles as silica support for Ag nanoparticle formation. As explained earlier the silica on hydrolysis produces silanol group ($\equiv\text{Si}-\text{OH}$) which deprotonates under high alkaline condition to form $\equiv\text{Si}-\text{O}^-$ that reacts with electrophilic ions such as Ag, Au, and Cu etc. Thus Si-O-Ag is formed. Under basic or neutral conditions more or this electrophilic attack occurs thus increasing the Ag^+ attachment on the silica surface. Whereas in acidic condition, the process is slower since Ag^+ covalently attaches to the ($\equiv\text{Si}-\text{OH}$) and protonation occurs during acid hydrolysis. As a result a mixture of silver ions and silver nanoparticles embedded in silica gel matrix is formed.

Egger et al described the synthesis of silver-silica nanocomposite material using flame spray pyrolysis process. The advantage of embedding silver nanoparticles in silica matrix is dispersion of the silver nanoparticles through the silica matrix, thus avoiding formation of aggregates between silver particles. Smaller sized silver nanoparticles (<25nm) are also formed by this method. Very small sized silver-silica material allows uniform dispersion of material and could be incorporated on various substrates such as fibers, plastic, glass, textile etc. Silica gel conveniently works as a delivery agent to embed the fine silver particles on plastic, coatings and

textiles. Also the entrapment of silver in silica matrix limits the release and disposal of silver nanoparticles, which make the material environmentally safe(38).

Preparation of silver-silica core shell material was reported by Jiang et al to study the optical properties of the material (39). Silica nanogel/ nanoparticle has high adherence towards various surfaces including cellulose. Textile when coated with silver-silica spheres were able to show strong antibacterial properties even after ten wash cycles(40). Silver containing silica micro beads were shown to have good antimicrobial properties as described by Quang et al (41). Min et al have reported white-pigmented silver chloride nanoparticles embedded in mesoporous silica had shown stability against the reduction by photon or heat thus exhibiting antibacterial properties as well as control the color formation by silver(42).

CHAPTER 3 MATERIALS AND METHODS

3.1 Materials

Silver Nitrate; Acros organics; Cat#419360250; Tetraethyl Orthosilicate; Aldrich Chemistry; Cat# 86578; Nitric Acid solution, ACS AR, Macron; Cat# 2704-14; Sodium hydroxide, Fisher Scientific; Cat# S320-500; Hydriion pH papers; *Escherichia coli* (*E.coli*, ATCC 35218); *Bacillus subtilis* (*B.subtilis*, ATCC 9372); *Staphylococcus aureus* (*S.aureus*, ATCC 25923); Muller Hinton Agar 2 (Fulka Analytical, cat#97580); Mueller Hinton Broth 2(Fulka Analytical, Cat# 90722); Sodium Chloride (Fisher Scientific, Cat# S 271-3); Resazurin (Acros Organics, Cat# 41890-0050); Streptomycin sulfate salt (Sigma life science, Cat# S0774-256); Penicillin-G potassium salt (Sigma Life Science, P8721-108MU); eppendorff 2ml micro centrifuge tubes; BacLight™ LIVE/DEAD® bacterial viability kit (Invitrogen, Molecular Probes, Cat# L7012); Microscopic Glass slides (Fisher Scientific); Cover Slips (VWR), AFM Tips (App Nano, Cat# ACT-10); Silicon Wafers; Plastic cuvettes (Fisher Scientific); TEM Grids (Electron Microscopy Sciences, carbon film on 400 square mesh copper grids, Cat# CF 400-Cu); De Ionized sterile water; Plastic sterile petriplates (Fisher Scientific); Sterile eppendorff tips and pipettes; sterile 96 well plates (Nunc™, Nuncoln® Surface); sterile glass conical flask; magnetic stirrer.

3.2 Synthesis

Simple water based sol-gel method was used to synthesize the silver embedded silica nanogel/nanoparticle. Four formulations containing silver and silica were prepared as follows:

3.2.1 Silver (Ag) loaded silica nanoparticle/nanogel 200 pH 4 (AgSiNP/NG200 pH 4)

120mg of silver nitrate salt was dissolved in DI water. The mixing was done on a magnetic stirrer at 400rpm. After completely dissolving Silver Nitrate salt in the water, 600 μ l of Tetraethyl Orthosilicate (TEOS) (a silane precursor for silica gel) was added to the silver nitrate solution drop wise under continuous stirring condition. The above solution was allowed to mix for 5 minutes. In order to decrease the pH of the mixture to approximately 4 and induce acid hydrolysis, 1800 μ l of 1% Nitric Acid solution in DI water was added to the solution drop-wise. The prepared mixture was stirred on a magnetic stirrer for 24 hours at room temperature. After 24 hours, a transparent colorless mixture was obtained at pH 4, thus forming Ag loaded silica nanoparticle/nanogel (AgSiNP/NG) 200 at pH 4 solution.

3.2.2 Silver (Ag) loaded silica nanoparticle/nanogel 200 pH 7 (AgSiNP/NG200 pH 7)

After 24 hours 100 ml of the AgSiNP/NG200 mixture prepared above was taken in a separate flask. Under continuous stirring condition, the pH of the AgSiNP/NG200 mixture was raised from pH 4 to pH 7 by adding freshly prepared 2mM of sodium hydroxide solution in DI water in drops (approximately 200ul) under continuous stirring condition. The pH of the

AgSiNP/NG 200 was checked using Hydrion papers. The AgSiNP/NG200 mixture at 7 showed pale yellowish-brown colored transparent solution.

3.2.3 Silver (Ag) loaded silica nanoparticle/nanogel 50 pH 4 (AgSiNP/NG50 pH 4)

34mg of silver nitrate salt was dissolved in 200ml of DI water. The mixing was done on a magnetic stirrer at 400rpm. After completely dissolving Silver Nitrate salt in the water, 600 μ l of TEOS (a silane precursor for silica gel) was added to the silver nitrate solution drop-wise under continuous stirring condition. The prepared solution was allowed to mix for 5 minutes. In order to decrease the pH of the mixture to approximately 4 and induce acid hydrolysis, 1800 μ l of 1% Nitric Acid solution in DI water was added to the solution drop-wise. The above mixture was allowed to stir on a magnetic stirrer for 24 hours at room temperature. After 24 hours, a transparent colorless mixture was obtained at pH 4 forming AgSiNP/NG50 pH 4 solution.

3.2.4 Silver (Ag) loaded silica nanoparticle/nanogel 50 pH 7 (AgSiNP/NG50 pH 7)

After 24 hours 100 ml of the above-prepared AgSiNP/NG50 solution was taken in a separate flask. Under continuous stirring condition, the pH of the AgSiNP/NG50 solution was raised from pH 4 to pH 7 by adding freshly prepared 2mM of sodium hydroxide solution in DI water in drops (approximately 140ul) under continuous stirring condition. The pH of the AgSiNP/NG50 was checked using Hydrion papers. Initially this solution at pH 7 was transparent and colorless, brown coloration was observed after progression of time.

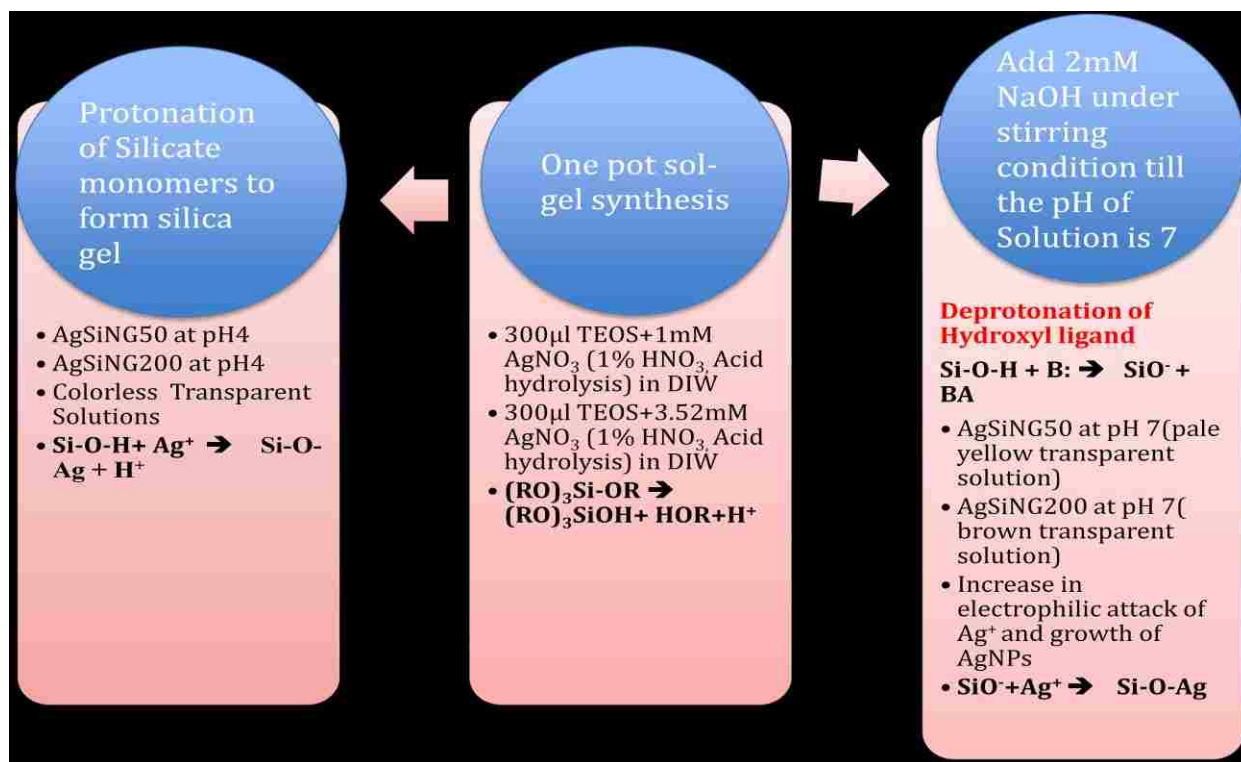


Figure 3- Schematic of synthesis of AgSiNP/NG200 and AgSiNP/NG50 at pH 7 and pH 4

3.2.5 Controls

For preparation of negative control i.e. Silica nanogel without silver 200 ml of sterile DI water was taken in a clean sterile conical flask. 600 μl of TEOS was added to the water in drops and was allowed to stir on the magnetic stirrer for 5 min. 1800 μl of 1% Nitric Acid was added to this solution drop-wise and was allowed to stir at room temperature for 24 hours. After 24 hours 100 ml of this SiNGpH 4 solution was taken in another clean sterile flask and the pH was raised to 7 by adding 2mM NaOH to get SiNGpH 7 formulations. To prepare positive control i.e. control with silver Nitrate without TEOS. The silver nitrate salt with same concentration used for

AgSiNP/NG200 and AgSiNP/NG50 was taken in DI water. Same amount of 1% nitric acid used in all the formulations was added to this solution to make pH 4 solution of silver nitrate and in order to make pH 7 silver nitrate solution 2mM NaOH was added. In the case of silver nitrate solution at pH 7, both the concentrations of silver showed blackish-brown colored formulation equivalent to silver oxide formation.

3.3 Material Characterization

3.3.1 Dynamic Light Scattering (DLS)

Dynamic Light Scattering (DLS) technique is also known as photon correlation spectroscopy. It determines the size of spherical or semi-spherical shaped particles by its Brownian motion in solution. It is a wet-characterization of the material. All the materials were characterized to determine whether there is formation of sol-gel or sol-particles. All the measurements in DLS were taken by using disposable plastic cuvettes. The DLS measurements were taken using Precision Detector/ Cool batch 4T machine.

3.3.2 Atomic Force Microscopy (AFM)

Atomic Force Microscopy (AFM) technology is used to determine the morphology of the material coated on a surface of either glass slide or cover slip. It uses the tapping mode of the cantilever on the AFM tip, which in turn deflects the angle of the laser light, which is used to image the morphology of the material. AFM was done on AgSiNP/NG200 pH 7 and pH 4

samples and also on SiNGpH 7 and pH 4 samples. All the samples were spin coated on cover slips and then analyzed by VEECO Dimensions 3100 Atomic force microscope

3.3.3 Scanning Electron Microscopy (SEM)

SEM was done on AgSiNP/NG200 pH 7 and pH 4, AgSiNP/NG50 pH 7 and pH 4, SiNGpH 7 and pH 4. All the samples were spin coated on a silica wafer and then analyzed under Zeiss ULTRA-55 FEG, which scans the surface topography of the sample suggesting the formation of either particle or gel.

3.3.4 UV-Visible spectroscopy

In order to determine the formation silver nanoparticles (because of the brown coloration) as well as to determine the Ag^+ ions and cluster formation UV-Visible spectra was done for AgSiNP/NG200 pH 7 and pH 4 and also for AgSiNP/NG50 pH 7 and pH 4. SiNG at pH 4 and pH 7 respectively was taken as baseline and blank to remove any absorbance shift observed by the presence of silica. Cary 300 bio spectrophotometer was used to do UV-Visible Spectroscopy. Disposable plastic cuvettes were used for measuring the absorbance.

3.3.5 High Resolution Transmission Electron Microscopy

HRTEM was performed to see the presence of silver nanoparticles in the silica gel matrix. HRTEM was done for AgSiNP/NG200 pH 4 and pH 7 and AgSiNP/NG50 pH 4 and pH 7. Samples were prepared by placing a drop of AgSiNP/NG/NP on a carbon coated copper grid (400 mesh size) followed by vacuum drying for 18 hours. It was made sure that no water molecules were present in the samples since it hinders with the imaging of crystalline properties viewed under HRTEM.

3.4 Antibacterial Studies

The antibacterial studies of AgSiNP/NG200 and AgSiNP/NG50 were performed on gram negative *E.Coli* and gram positive *B.subtilis* and *S.aureus*. All the antibacterial assays were done on Mueller Hinton broth 2 or Mueller Hinton agar 2.

3.4.1 Well Diffusion assay

The well diffusion assay was done to study the qualitative analysis of antibacterial properties of AgSiNP/NG200 and AgSiNP/NG50 at both pH 4 and pH 7. In order to conduct the primary study of inhibition of growth of bacteria the well diffusion assay method was done as described by Schillinger et al (43). Muller Hinton Agar plates were used for this assay. 10^8 CFU/ml of each bacterium was spread on the plate by cotton swab. 6 holes of 3mm size were punched aseptically in the plate 10 μ l of AgSiNP/NG200 both pH 4 and pH 7, Silver Nitrate 200

solution pH 4 and pH 7 and SiNG at pH 4 and pH 7 were added to each holes. Care was taken that no spillage occurred outside the hole on the agar. Similarly another plate was made in which each hole had 10 μ l AgSiNP/NG50 pH 7 and pH 4, Silver Nitrate 50 solution pH 7 and pH 4 and SiNGpH 7 and pH 4. The plates were incubated at 36°C for 24 hours. The zone of clearance was recorded after 24 hours of growth

3.4.2 Bacterial Growth inhibition assay in broth using turbidity

The inhibition studies of AgSiNP/NG were done for gram negative *E.coli* and gram positive *B.subtilis* and *S.aureus* as described by Rastogi et. al (44) with some modifications. All the organisms were grown in Mueller Hinton agar-2 plates and were cultured in Mueller Hinton broth-2 for 24 hours at 36°C. Different concentrations of AgSiNP/NG200 (381 μ g/ml of metallic silver) both pH 7 and pH 4 and AgSiNP/NG50 (100.7 μ g/ml of metallic silver) pH 7 and pH 4 were prepared in sterilized Mueller Hinton broth-2. The volume was adjusted to 0.9ml by adding sterile 0.85% saline in sterile micro-centrifuge tubes. For positive control Silica Nanogel (SiNG) without silver at both pH 7 and pH 4 was taken. The growths of bacteria were monitored with AgSiNP/NG200 pH 7 and pH 4 at metallic silver concentrations of 63.5 μ g/ml, 38.1 μ g/ml, 19.05 μ g/ml, 9.53 μ g/ml, 4.77 μ g/ml, 2.68 μ g/ml, 1.34 μ g/ml, 953ng/ml, 477ng/ml, 95.3ng/ml and 47.7ng/ml. The silver nitrate with same metallic silver content described earlier was used as negative control. Also the growths of bacteria were monitored with AgSiNP/NG50 pH 7 and pH 4 at metallic silver concentrations of 30.24 μ g/ml, 20.16 μ g/ml, 10.08 μ g/ml, 5.04 μ g/ml, 2.52 μ g/ml, 1.26 μ g/ml, 630ng/ml and 63ng/ml. The silver nitrate controls as described earlier with similar metallic silver content were used as negative control. The final volume of the

solution was made to 1ml by adding 0.1ml of 10^6 CFU/ml of bacteria making the final concentration of bacteria to 10^5 CFU/ml. Blanks without any material were also inoculated with same concentration of bacteria as second positive control. The tubes were incubated at 36°C on a 200rpm shaker. The optical density (O.D.) was measured for zero hour, every one hour until the 9th hour passed and after 24 hours at 600nm wavelength of visible spectrophotometer. The OD obtained at zero time was cancelled from the OD obtained later. Graphs were plotted for OD Vs Time (hrs) for all three bacteria with different concentrations of metallic silver in both AgSiNP/NG200 and AgSiNP/NG50.

3.4.3 Minimum Inhibitory Concentration assay using resazurin indicator

Resazurin is a non-fluorescent dye, which on oxidation produces fluorescent pink colored resorufin. The Resazurin indicator based assay is a confirmatory test for the minimum inhibitory concentration since the growing cells turns the dye in pink color whereas the non-growing ones remain blue in color. The MIC using resazurin test was done as described by Sarker et.al(45). For this assay we used 10^5 CFU/ml of *E.Coli*, *B.subtilis* and *S.aureus*. Sterile 96 well plates were taken. 100 μl of 5 times diluted samples of AgSiNP/NG200 pH 7, AgSiNP/NG200 pH 4, Silver Nitrate 200 pH 7, Silver Nitrate 200 pH 4, SiNGpH 7 and SiNGpH 4 were taken in first column respectively. For AgSiNP/NG50 sample 100 μl of the samples were taken as prepared without any dilution. As the negative control 100 μl of 1mg/ml Penicillin G and 1mg/ml of Streptomycin were used. Here Silica nanogel (without Silver, SiNG both pH 7 and pH 4) was used as the positive control. 50 μl of normal saline (0.85%) was added to all other wells. The samples were diluted 2 fold serially. Finally each well had 50 μl serially diluted sample in ascending order. 10

μl of resazurin indicator (6.75 mg/ml) was added to each well. To each well, 30 μl of Mueller Hinton broth 2 was added. 10 μl of the 10^6 CFU of bacterial suspension was added to each well so that the final bacterial concentration in 100 μl volume became 10^5 CFU/ml. The plates were incubated at 36°C for 24 hours. The color change was then visually assessed. Color change from purple to pink was considered as positive for growth. MIC was taken as the lowest concentration showing no color change to pink. The plates were prepared in triplicates.

3.4.4 BacLight™ LIVE/DEAD® assay

The BacLight™ LIVE/DEAD® assay experiment was carried out to determine the viability of *E.coli*, *B.subtilis* and *S.aureus* in presence and absence of AgSiNP/NG (44). For control experiments silver nitrate salt and silica nanogel (SiNG) without silver were taken. 10^8 CFU count of bacterial suspension was inoculated with 190.5 $\mu\text{g}/\text{ml}$ of metallic silver content of AgSiNP/NG200 pH 7 and pH 4 for two hours. The BacLight™ kit contains two dyes propidium iodide and STYO9. STYO9 (green) selectively stains cell membrane whereas propidium iodide (red) stains the nucleus. These dyes were taken in ratio of 1:1. After 2 hours of incubation the cells with AgSiNP/NG and controls, they were washed from the suspension using sterile normal saline and were then stained with the mixed BacLight™ dye for 15 minutes. 5 μl of the stained bacterial suspension was taken on a glass slide, covered with a cover slip and this slide was analyzed under a fluorescent microscope with a green filter (535nm) for live cells and red filter (642nm) for dead cells at 60X magnification.

CHAPTER 4 RESULTS

We obtained the following materials, these were characterized using various material science tools and tested for antibacterial properties:

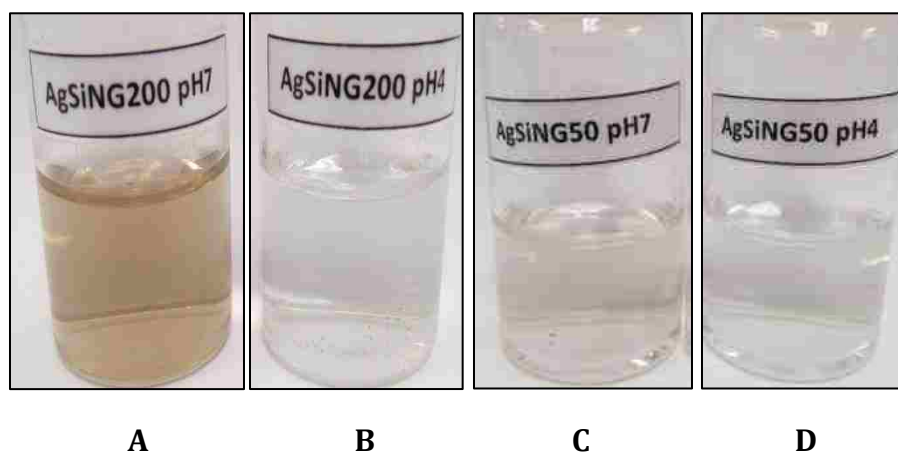


Figure 4 - Digital images for A) AgSiNP/NG200 pH 7 B) AgSiNP/NG200 pH 4 C) AgSiNP/NG50 pH 7 D) AgSiNP/NG50 pH 4.

From the digital images it can be clearly seen that there is a formation of yellowish brown color solution similar to that seen for silver and silver oxide nanoparticles. The color formation can be because of addition of NaOH triggering the formation of electrophiles and thus increasing the formation of silver nanoparticles, which are further oxidized to form silver oxide particles.

At pH 4 clear, transparent and colorless formulation can be observed; this is because of the dielectric layer of silica around the silver nanoparticles. Silica acts as a reducing agent for formation of silver nanoparticles within the gel.

4.1 Material Morphology

4.1.1 Dynamic light scattering

The results obtained from DLS shows formation of sol-particles at both pH 7 and pH 4, but after a month, for pH 4 particles there is formation of gel because the solution was not allowed to condense by adding a base to change the pH to neutral. As a result aggregations can be seen leading to gel formation at a lower pH. For AgSiNP/NG200 pH 7 the particle size average of 191nm is recorded, whereas that of pH 4, as synthesized, shows the particle size average of 67.8nm corresponding to sol particles. For AgSiNP/NG50 pH 7 the particle size seen is 111nm whereas that of pH 4, as synthesized, is 67.2nm. For SiNG200 the particle size is 168 and 216 nm for pH 7 and pH 4 respectively.

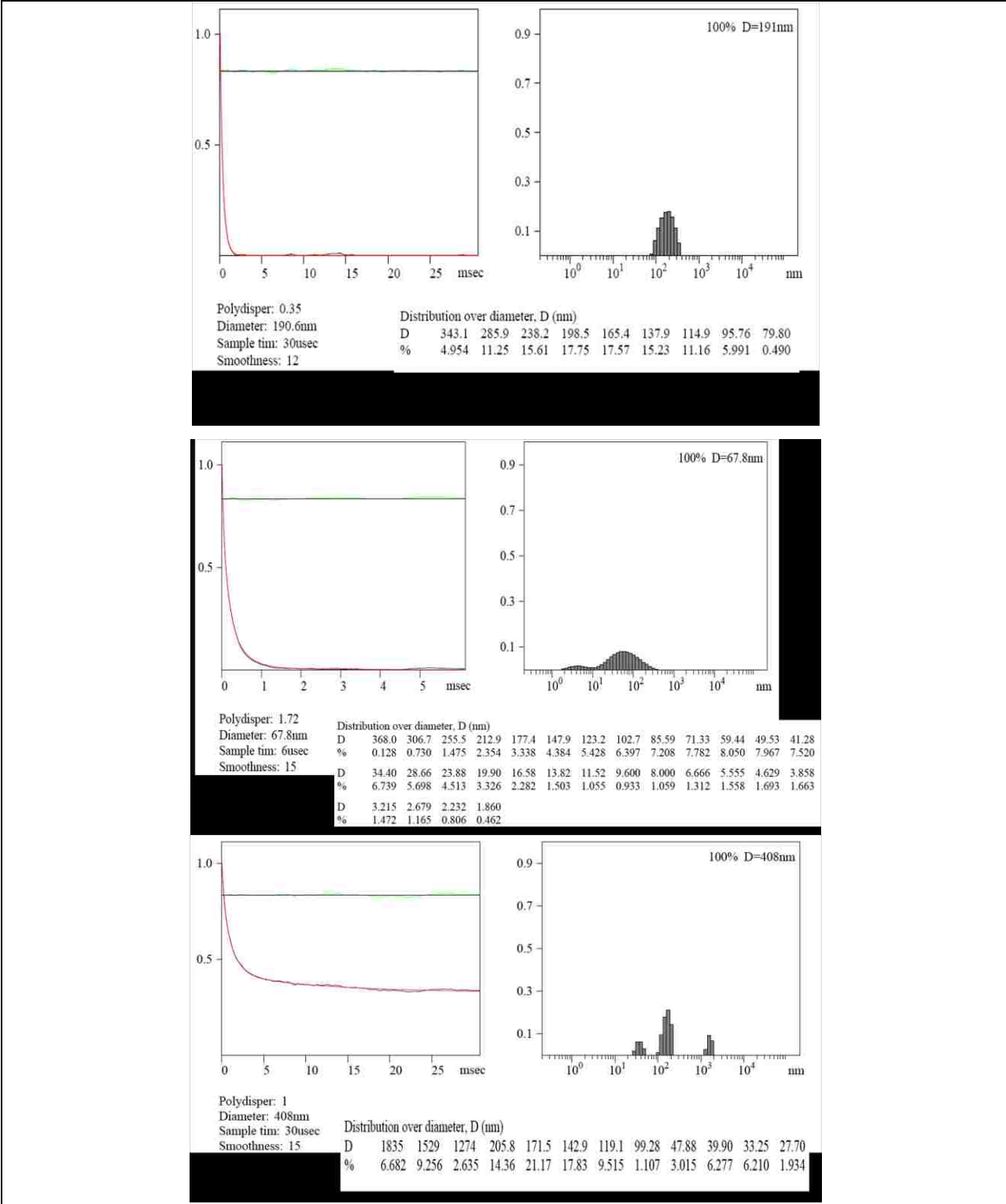


Figure 5- DLS seen for AgSiNP/NG200 A) pH 7 B) pH 4 as synthesized C) pH 4 after a month

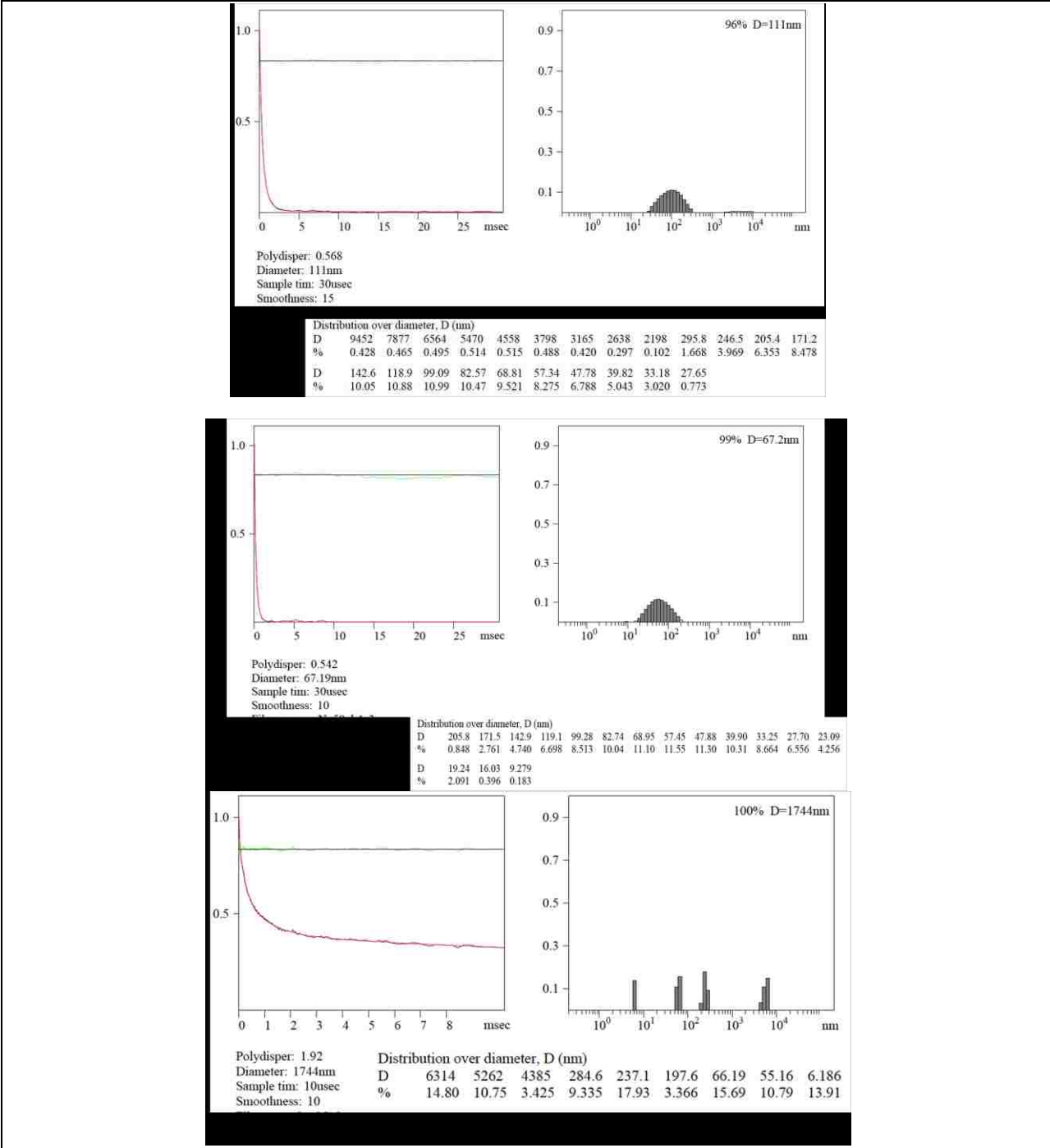


Figure 6 - DLS seen for AgSiNP/NG50 A) pH 7 B) pH 4 as synthesized C) pH 4 after a month.

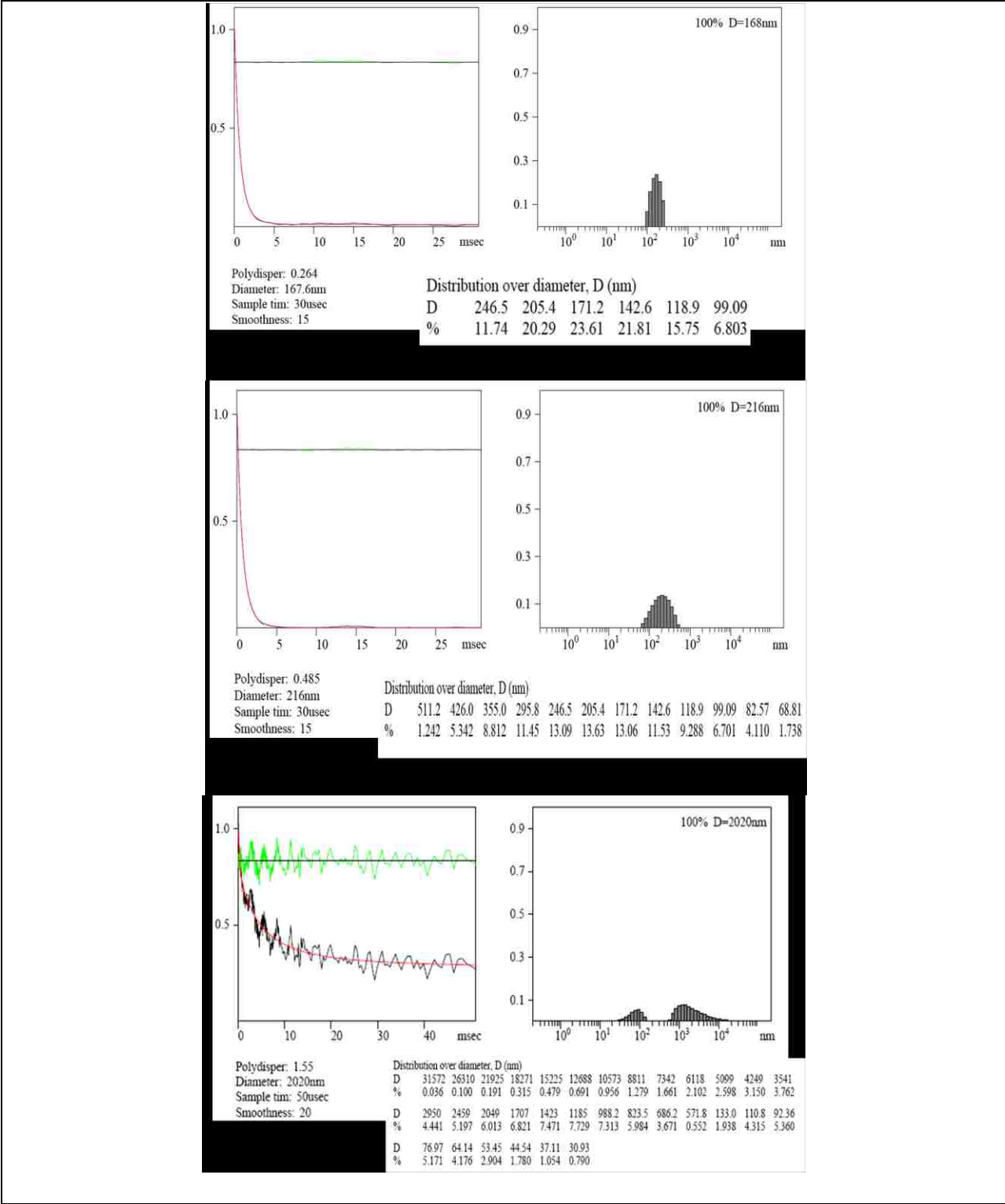


Figure 7 - DLS seen for SiNG A) pH 7 B) pH 4 as synthesized C) pH 4 after a month.

4.1.2 Atomic force microscopy

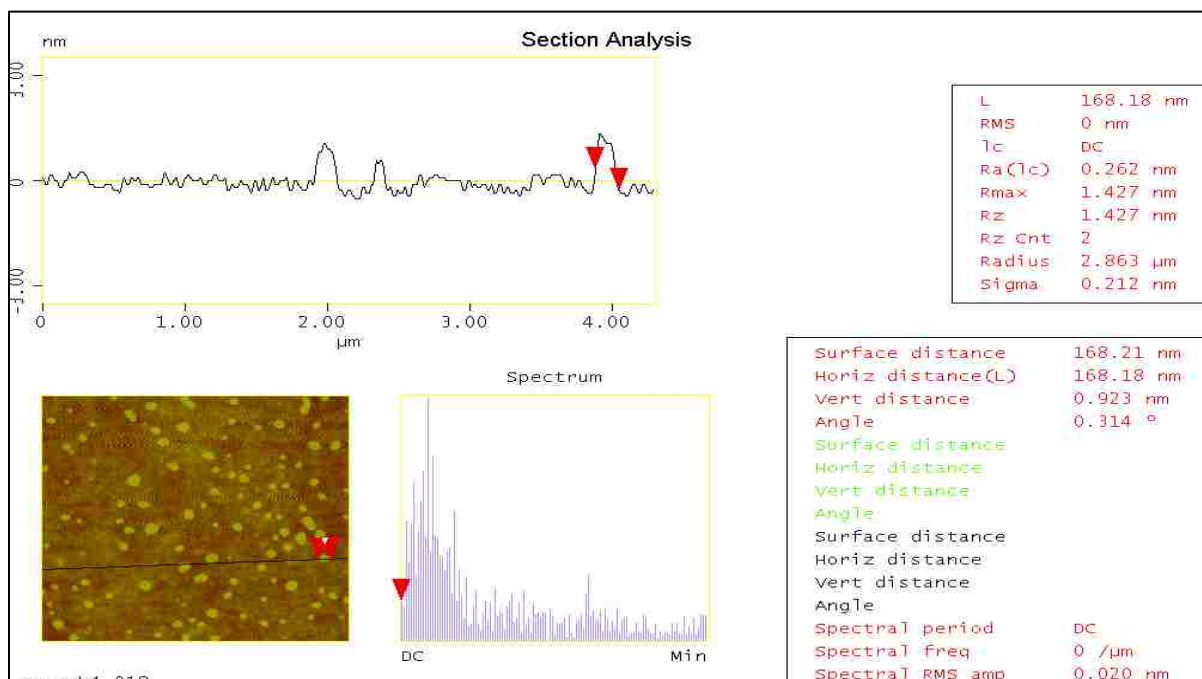


Figure 8 - AFM image of AgSiNP/NG200 pH 7 with sectional analysis stating the size of particle.

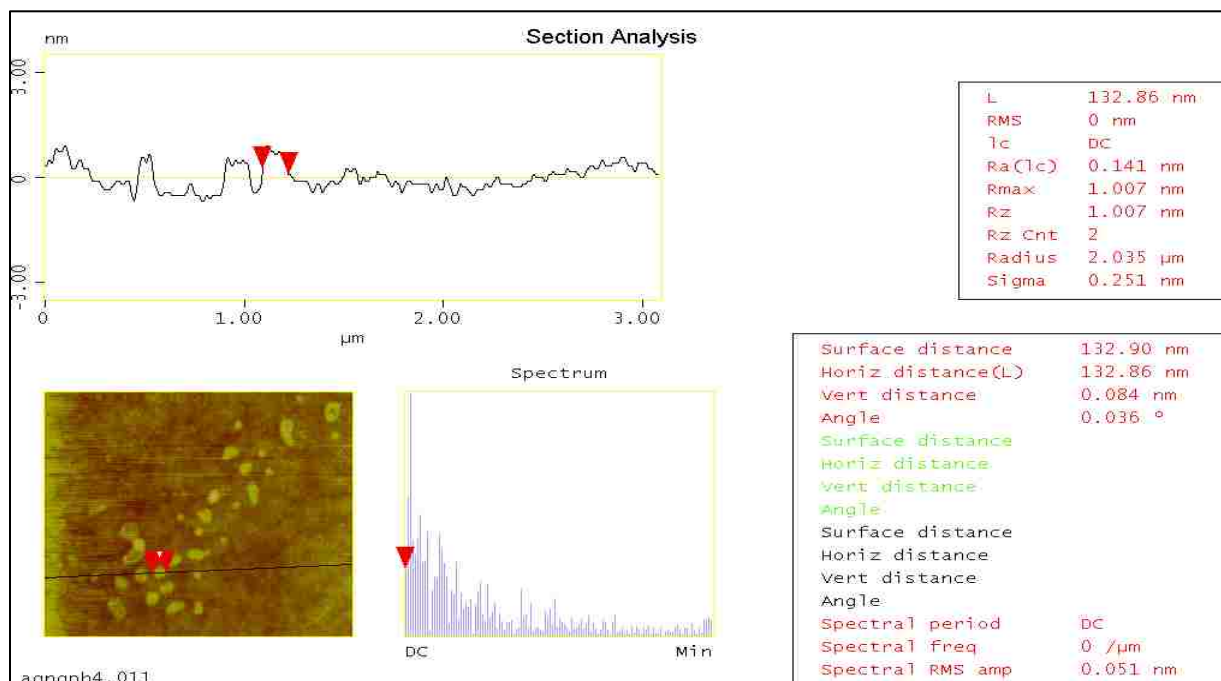


Figure 9 - AFM image of AgSiNP/NG200 pH 4 with sectional analysis stating the size of particle.

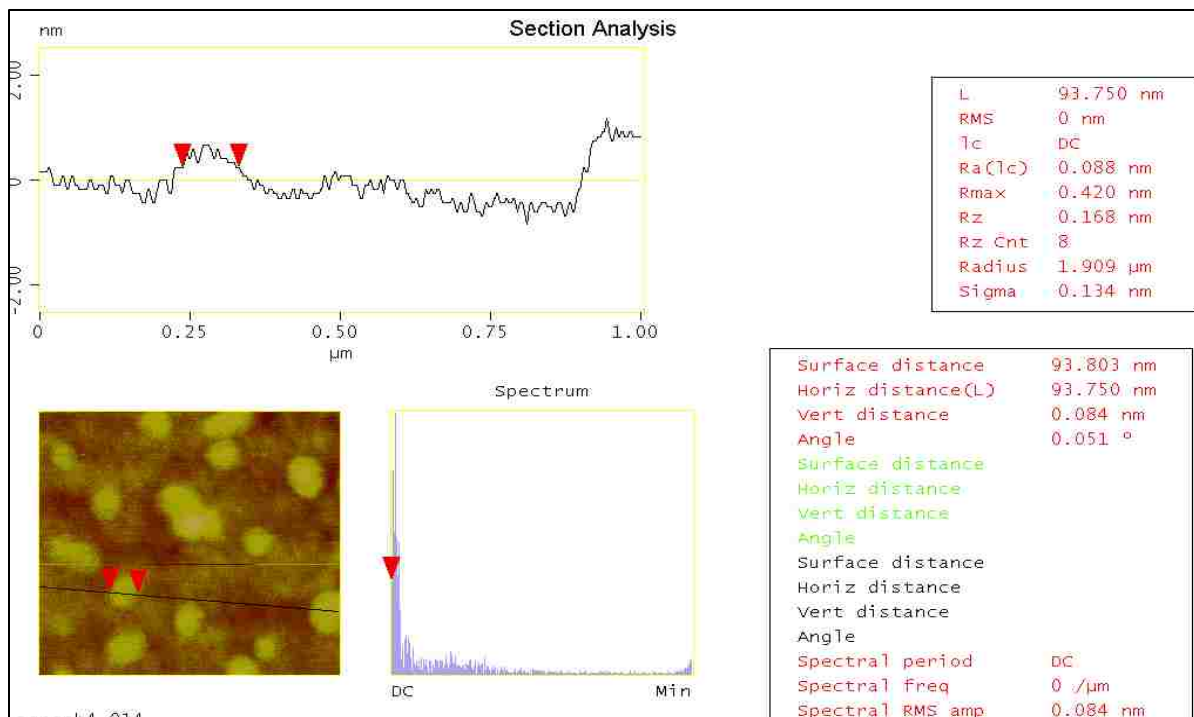


Figure 10 - AFM image of SiNG pH 7 with sectional analysis stating the size of particle.

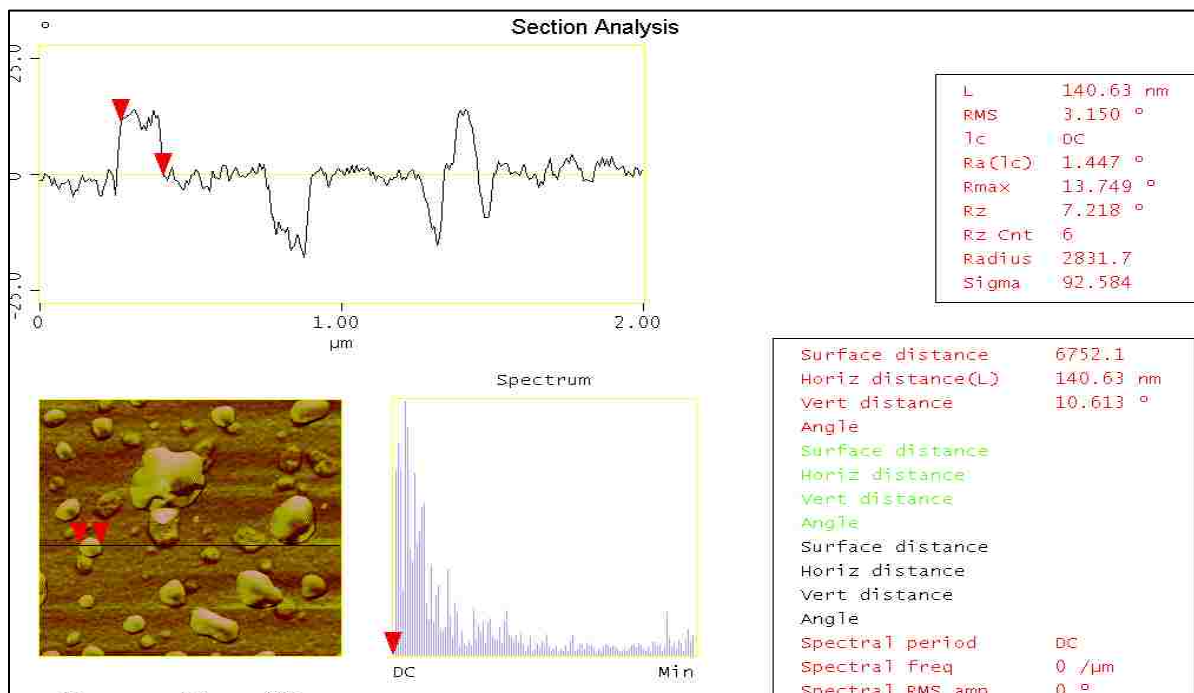


Figure 11 - AFM image of SiNG pH 4 with sectional analysis stating the size of particle.

From the AFM images the DLS results are proved. It can be clearly seen that there is a formation of distinct particles for the pH 7. The pH 4 formulations show mixture of gel and particle formations at the nanoscale range. AgSiNP/NG200 pH 7 shows particle formation of approximately 168nm, which are distinct and not aggregated, but for AgSiNP/NG200 pH 4 shows particles as well as gel like formation on the cover slip.

4.1.3 Scanning Electron Microscopy

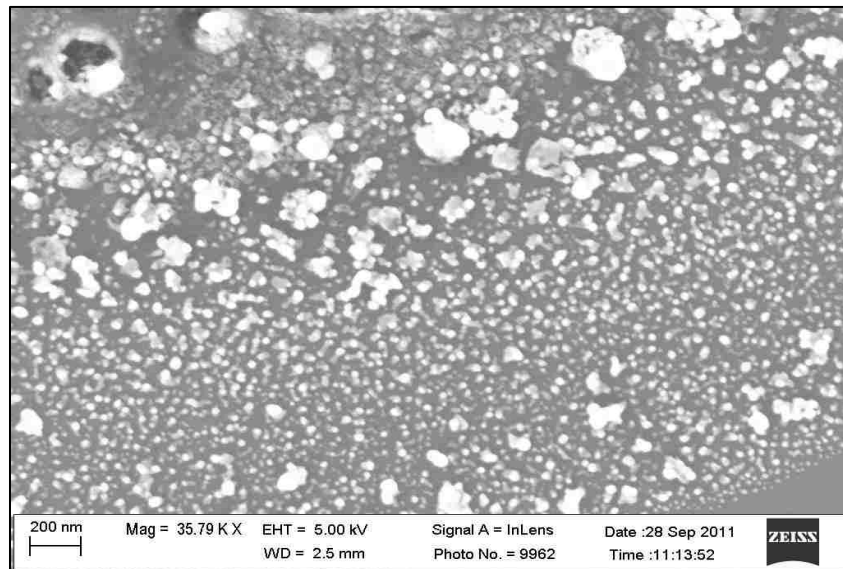


Figure 12 - Scanning Electron microscopy of AgSiNP/NG200 pH 4

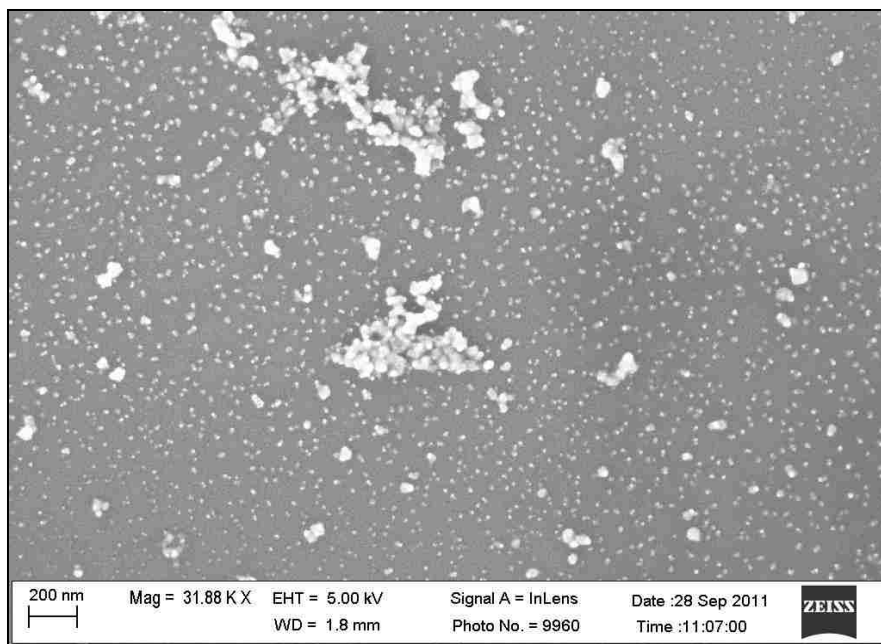


Figure 13 - SEM image of AgSiNP/NG200 at pH 7

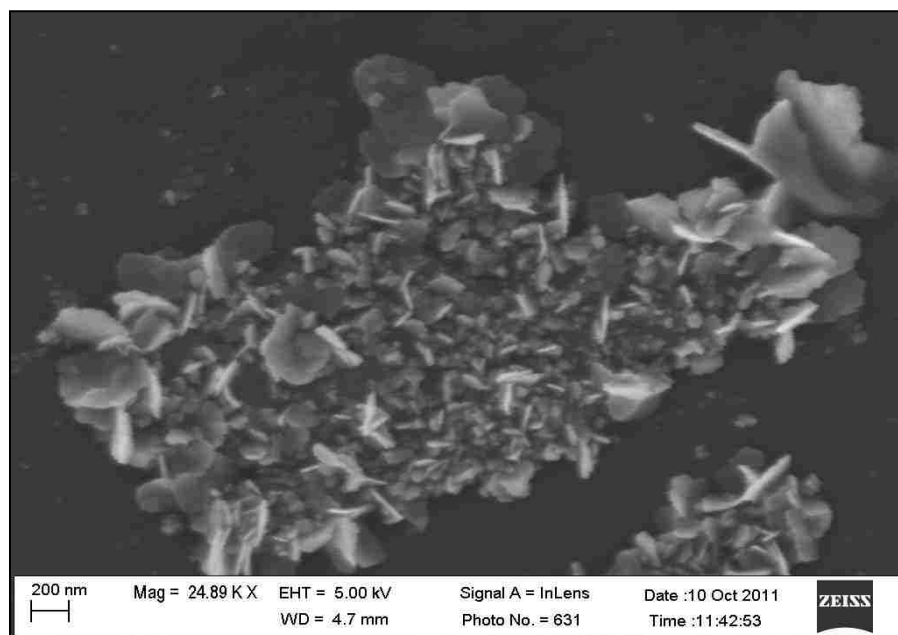


Figure 14 - SEM Image of AgSiNP/NG50 at pH 4

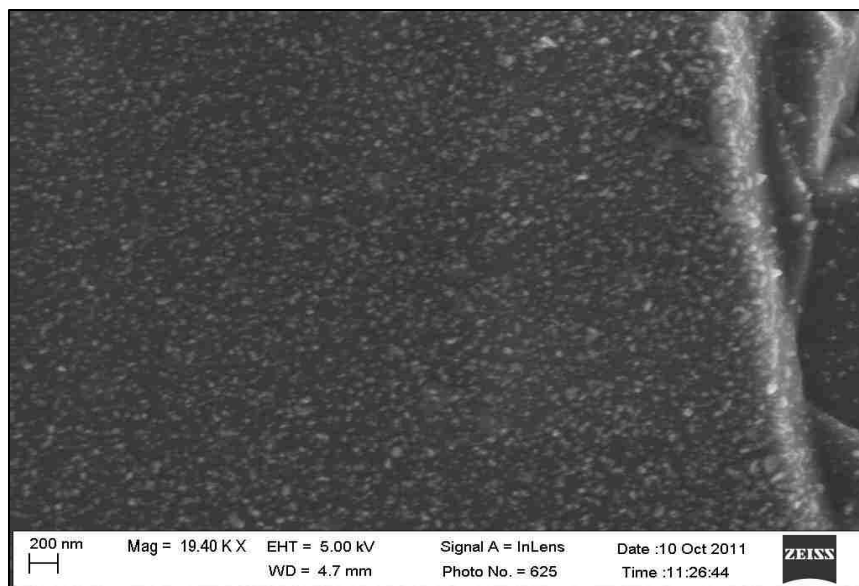


Figure 15 - SEM Image of AgSiNP/NG50 at pH 7

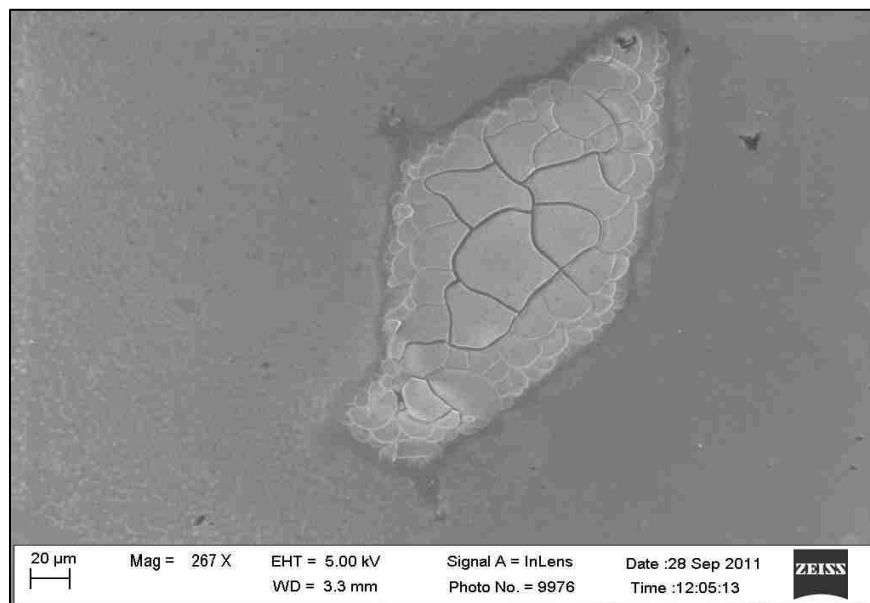


Figure 16 - SEM Image of SiNG at pH 4

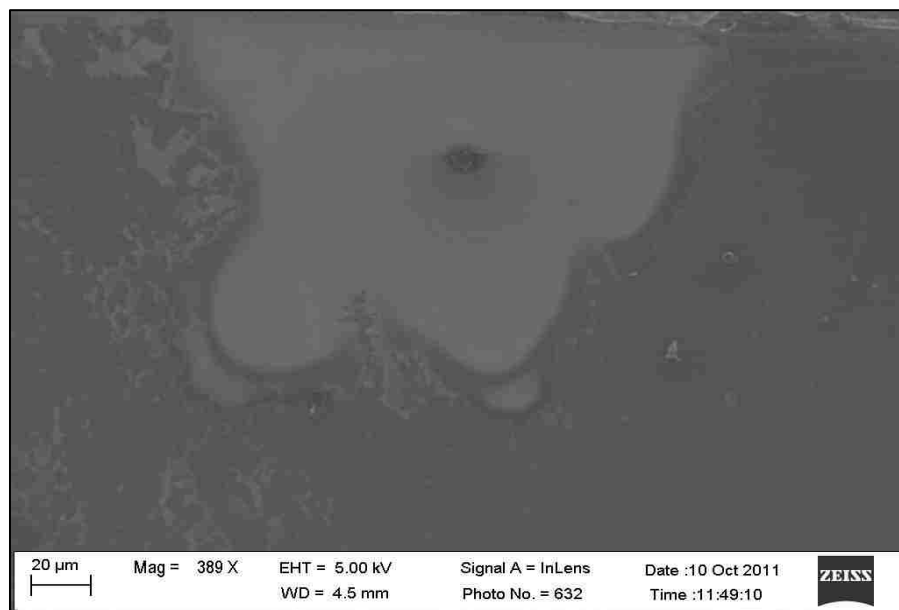


Figure 17 - SEM Image of SiNG at pH 7

From the SEM images, it can be seen that the sol particle formations occurred at higher pH. At lower pH i.e. 4, there are formations of either aggregates or flake like silica structure as seen in AgSiNP/NG50 pH 4 (figure 12). Small particulate features can also be seen in the background as well as inside the flakes. For SiNG without silver there is plain gel formation with some very less sol –particles in background.

4.2. Confirming the production of Silver Nanoparticles

4.2.1 UV-Visible spectroscopy

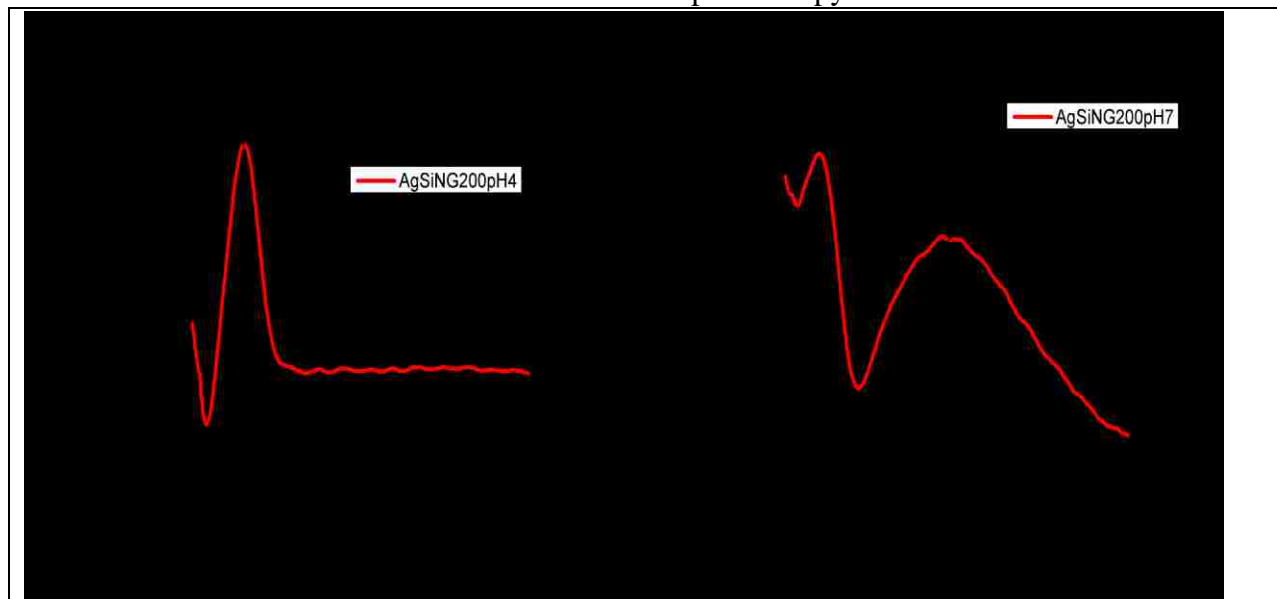


Figure 18 - UV-Vis spectroscopy of A) AgSiNP/NG200 pH 4 B) AgSiNP/NG200 pH 7

We can study the UV-Vis spectroscopy of AgSiNP/NG 200 from figure 18. It is seen that at pH 4 one peak is observed at 300nm. Whereas at pH 7 two peaks are seen one at 296nm and other at 419nm. The peak observed at 300 or 296nm is due to the Ag ion cluster formation (26). The peak at 419nm is the surface Plasmon resonance (SPR) absorption peak which is a characteristic peak of silver as well as silver oxide nanoparticles (46). Also a slight shift of the silver ions peak can also be observed from the change in pH.

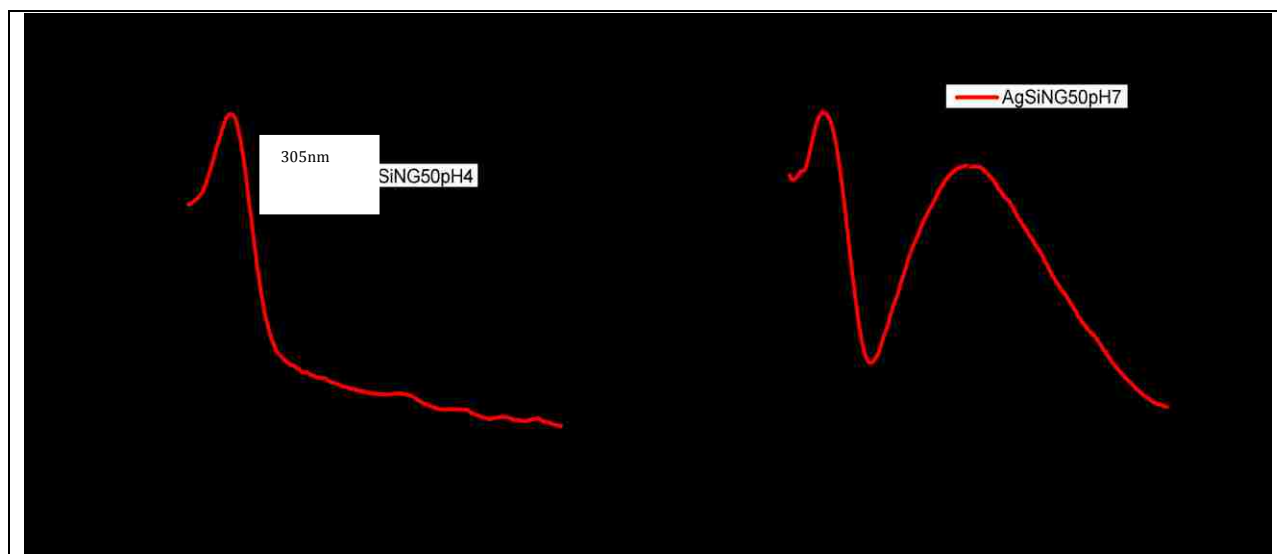


Figure 19 - UV-Vis spectroscopy of A) AgSiNP/NG50pH 4 B) AgSiNP/NG50 pH 7

AgSiNP/NG 50 formulation at pH 4 does not show any significant surface plasmon absorption peak characteristic to the formation of Ag nanoparticles, but a peak characteristic to silver ion clusters can be seen at 305nm. At pH 7 formulation a very clear surface plasmon absorption band can be seen at 421nm. Also a characteristic peak at 295nm can be seen because of presence of silver ion cluster. Surface plasmon absorption is responsible for yellow/brown coloration of Ag nanoparticles and Ag nanoparticle containing materials.

Thus from UV-Vis absorption spectra the formation of silver nanoparticles can be seen at pH 7 of both formulations because of the formation of surface Plasmon resonance. From 420nm surface Plasmon absorbance it can be concluded that the average particle size of the silver nanoparticle must be around 20-25nm. Also the presence of silver ion cluster peak shows that there are silver ions embedded in the gel matrix along with silver nanoparticles.

4.2.2 High Resolution Transmission electron Microscopy

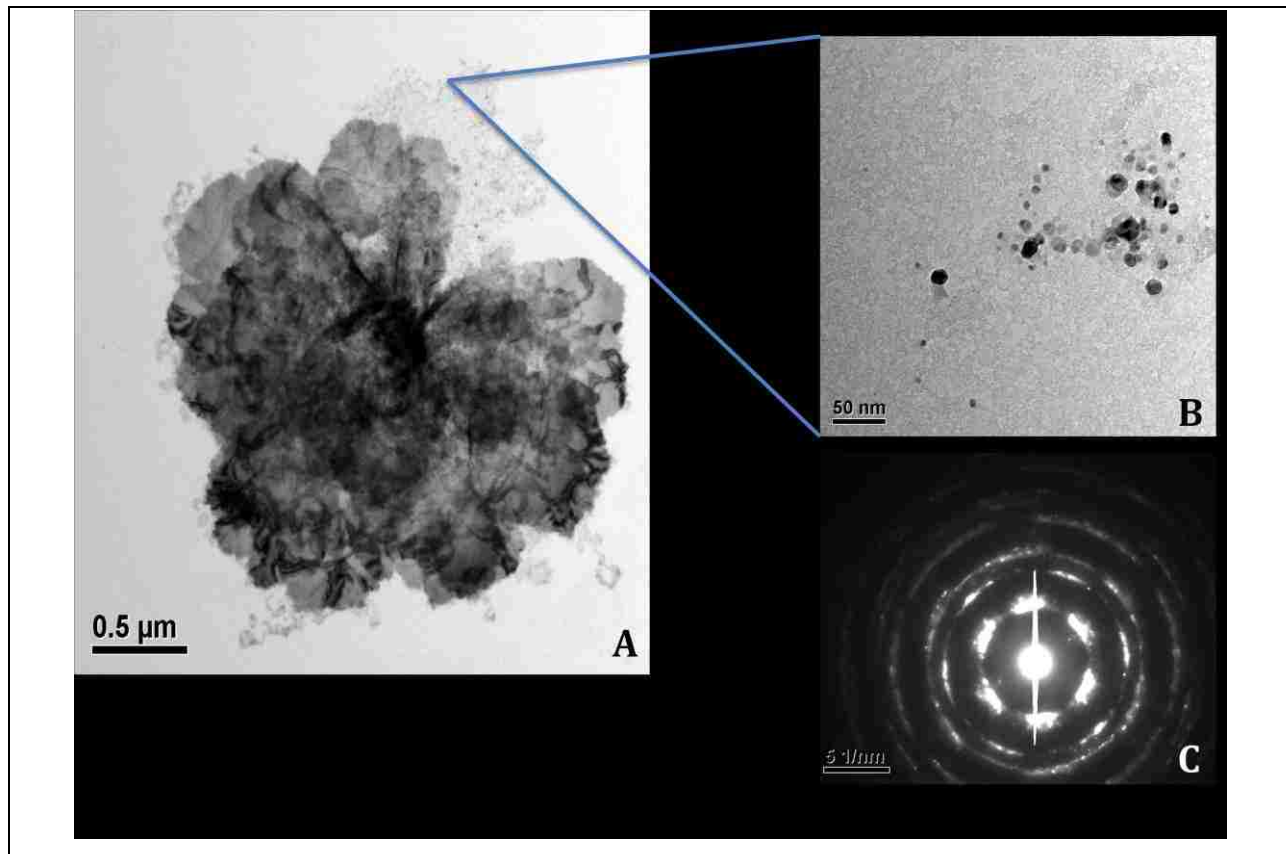


Figure 20 - HRTEM Image of AgSiNP/NG200 A) Formation of silver NpS uniformly in gel as seen at low magnification B) Formation of silica nanoparticles around 18nm in size is seen surrounded by amorphous silica C) The diffraction pattern confirming the presence of crystalline material (Silver) by d-spacing of analysis.

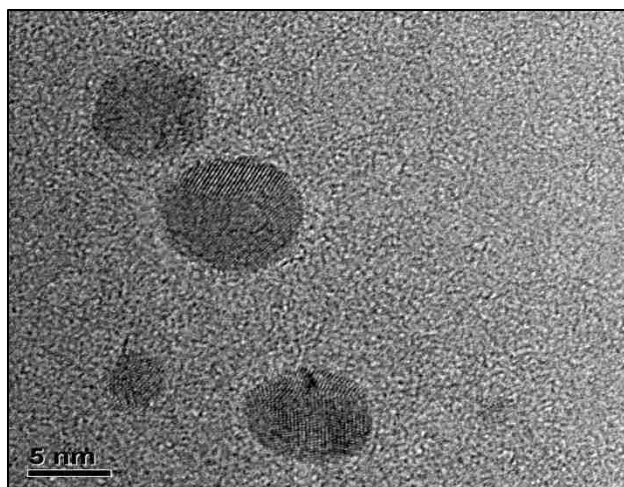


Figure 21 - HRTEM high magnification image of AgSiNP/NG200 pH 7 shows silver spherical silver nanoparticle crystal structure with silica matrix in background with average size ranging from 1 to 10nm.

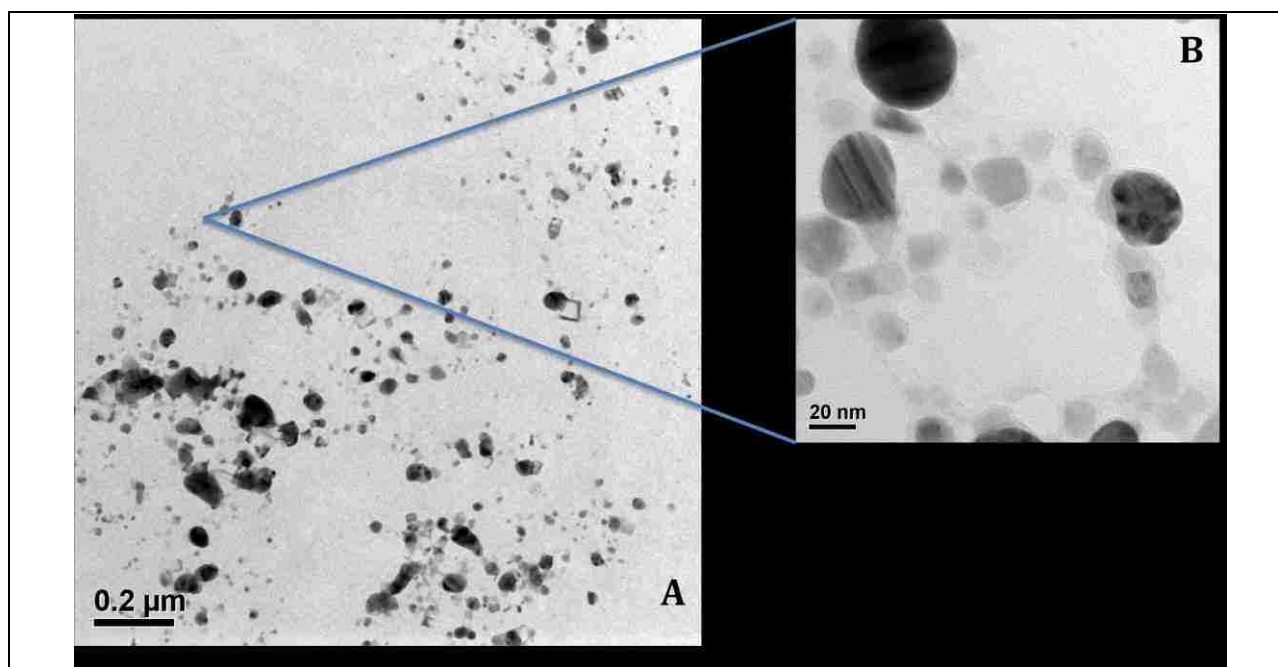


Figure 22 - HRTEM of AgSiNP/NG200 pH 4. This shows uniformly distributed silver nanoparticles through the silica matrix A) Low magnification showing uniform distribution of particles of different sizes average size being 30nm and B) showing high magnification of the nanoparticles embedded in silica gel at lower pH 4.

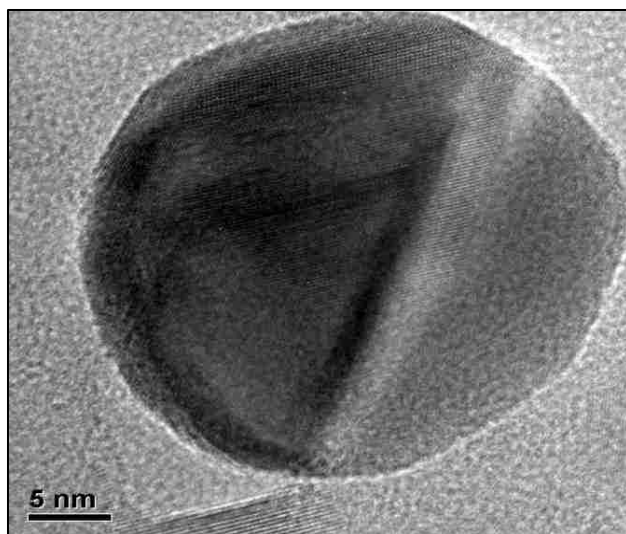


Figure 23 - Highly crystalline highly magnified silver nanoparticle can be seen in AgSiNP/NG200 pH 4.

The HRTEM micrographs show that there is formation of uniformly distributed silver nanoparticles through the matrix of silica gel of both AgSiNP/NG200 pH 7 and AgSiNP/NG200 pH 4. . It is seen that no aggregation of the particles are formed and the average size of the particle is around 25nm. In order to analyze the elemental silicon and silver composition in the matrix surrounding the silver nanoparticles we did energy dispersive X-ray spectroscopy (EDAX). From STEM images, we were able to select an area to be analyzed. For our information we selected one area of AgSiNP/NG200 pH 4 on the silver nanoparticle and another area outside the silver nanoparticle.

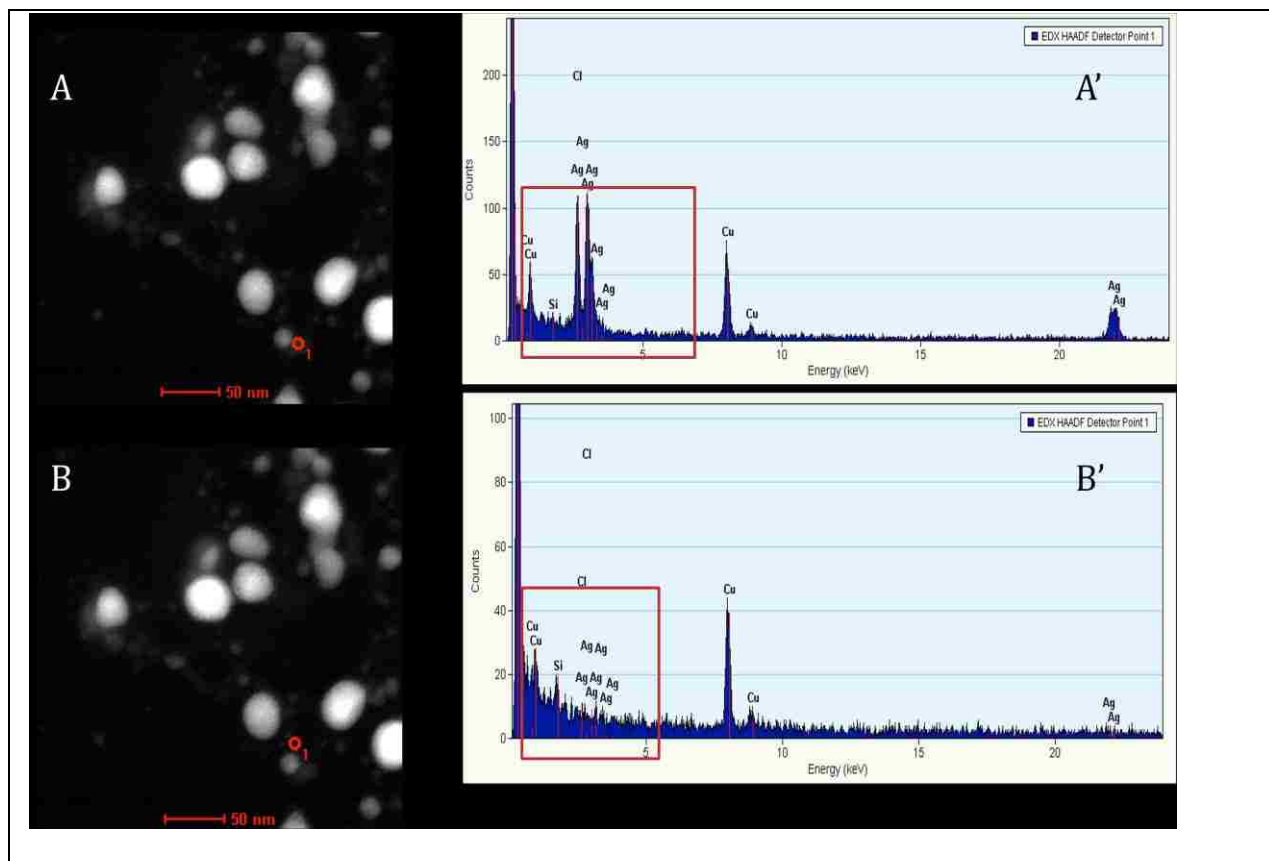


Figure 24- HR-TEM EDAX for AgSiNP/NG200 pH 4 A) Selected area for diffraction (with nanoparticle) A') EDAX analysis of the area shown in A. B) Selected area for diffraction (outside particle) B') EDAX analysis of the area shown in B.

From the elemental analysis we can see that when EDAX was done on the silver nanoparticle there is very strong peak of elemental silver, whereas there is also a small peak of silica stating that there is a layer of silica on the nanoparticle. From figure 24 B it is seen that when the position is changed to the area around the particle there is stronger peak of silica as well as some elemental silver can also be seen. This states that the silver in ionic form is also present in the silica matrix as shown in UV-Vis spectra for AgSiNP/NG200 pH 4 (figure 18)(26). The copper peak seen is because of the copper grid on which the sample was placed for HRTEM analysis.

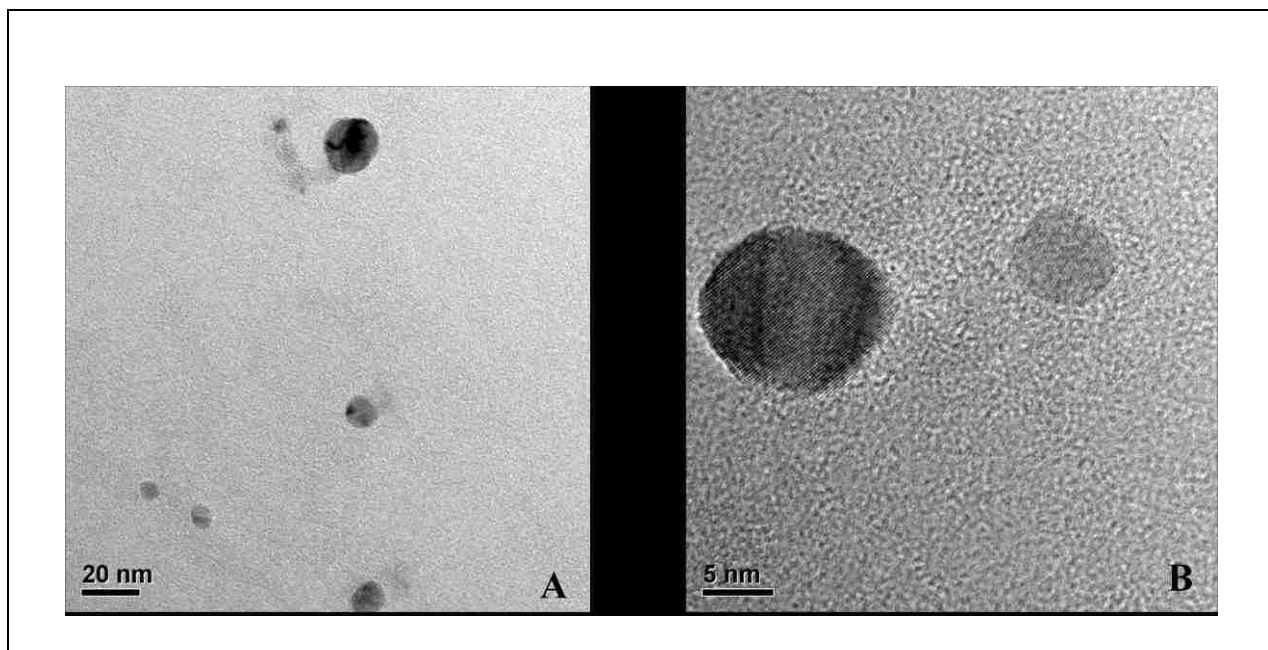


Figure 25 - HRTEM of AgSiNP/NG50 pH 7-particle A) low magnification B) high magnification

From figure 25 it is clearly seen that the silver nanoparticles are also present in AgSiNP/NG50, which are enclosed in the silica matrix. The approximate size of the silver nanoparticle is around 10-20 nm. Since the concentration of silver nitrate was low in this formulation less formation of silver nanoparticles is seen than compared to AgSiNP/NG200. We performed EDAX for this material to find the elemental composition of silver and silica.

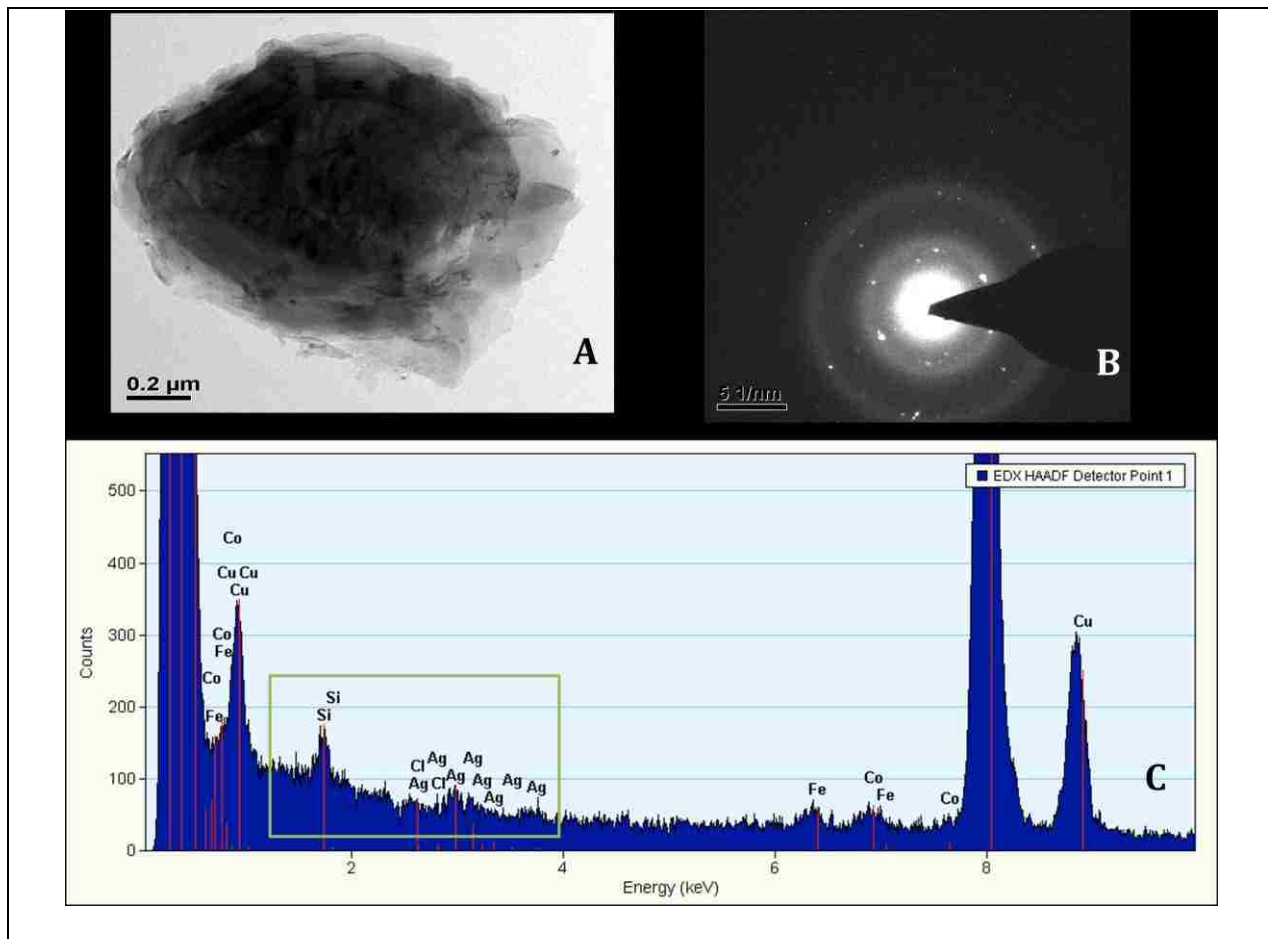


Figure 26 - HRTEM of AgSiNP/NG50 pH 7 A) low magnification image of the gel B) Crystalline diffraction pattern of AgSiNP/NG50 pH 7 B) EDAX of ASiNG50 pH 7 taken from a point in image A.

Here it shows that there is more silica gel formation than the formation of silver nanoparticles. From fig 26 (A) it can be clearly seen that there is a gel formation with small particles entrapped in the gel matrix. To analyze the particle we did X-ray diffraction and we found the presence of highly crystalline material in the diffraction (figure 26 B). The diffraction corresponds to that seen for silver nanoparticles. From EDAX (figure 26 C) it can be seen that both silica and silver are present in elemental form. Copper peak is seen because of the copper grid used.

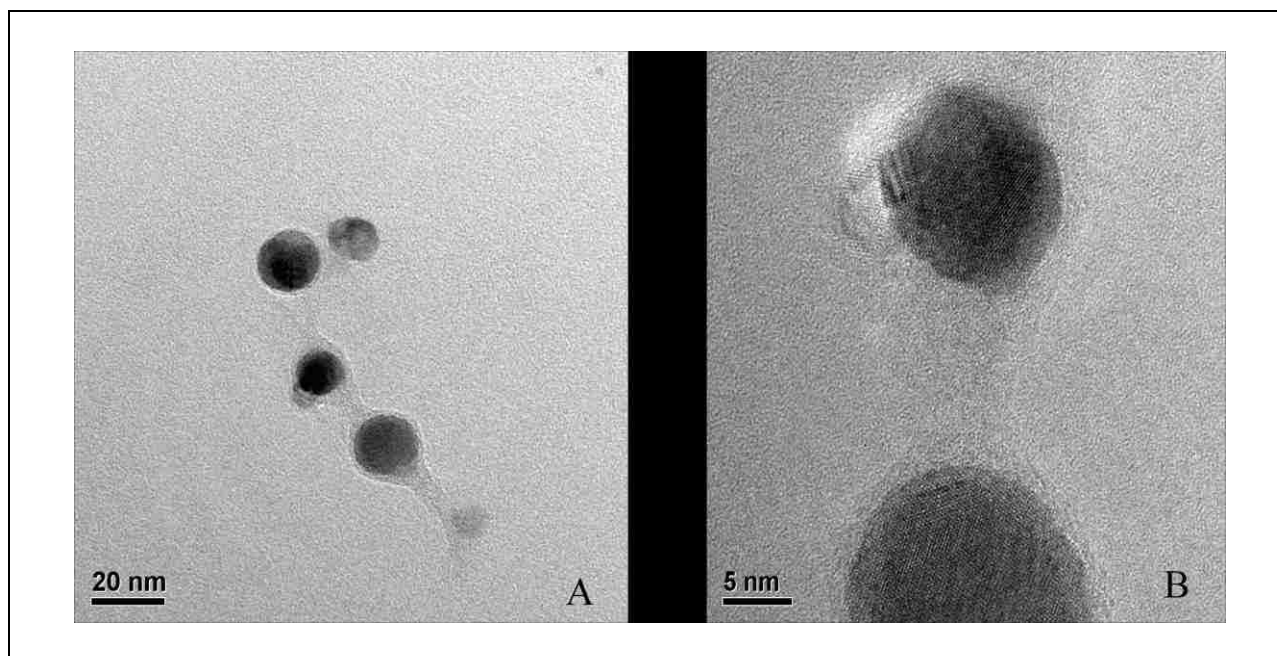














Figure 27 - HRTEM image for AgSiNP/NG50 pH 4 A) Low magnification B) high magnification

Figure 27 shows formation of silver nanoparticles of approximately 20nm in size for AgSiNP/NG50 pH 4. One can clearly see that amorphous silica material is enclosing the silver nanoparticle. Thus from HRTEM results we can state that there is formation of silver nanoparticles in both the formulation AgSiNP/NG200 and AgSiNP/NG50 at both pH 4 and pH 7. These results do not match the results from UV-Vis spectroscopy since there is no surface Plasmon resonance characteristic to silver nanoparticles observed in both formulations at pH 4. There is some phenomenon occurring because of the enclosing of silica matrix around the silver nanoparticles that plays role in shifting the SPR absorption.

4.3 Anti-bacterial Studies

4.3.1 Well Diffusion Method

Samples	E.coli	B.subtilis	S.aureus
AgSiNP/NG200pH 7	9mm 	10mm 	12mm 
AgSiNP/NG200 pH 4	9mm 	10mm 	10.5mm 
Silver Nitrate 200 pH 7	8mm 	9mm 	9mm 
Silver Nitrate 200 pH 4	8mm 	9mm 	9mm 
SiNG pH 7	0mm	0mm	0mm

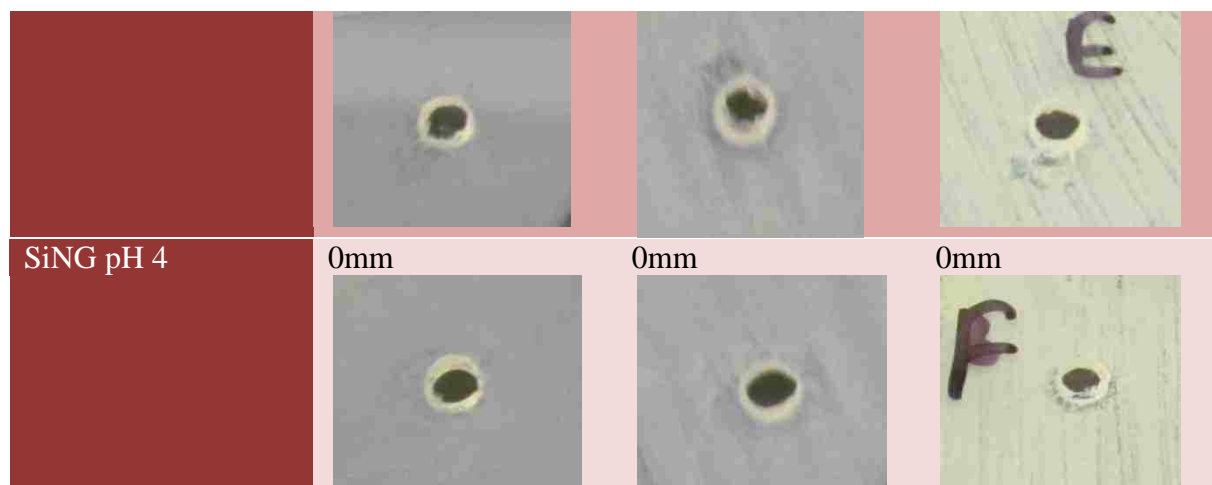


Table 1 - Well diffusion zones for AgSiNP/NG200

From the well diffusion method it can be seen that AgSiNP/NG200 can give good zone of clearance against all three bacteria. There is no zone of clearance seen for SiNG formulations.

Samples	E.coli	B.subtilis	S.aureus
AgSiNP/NG50pH 7	9mm 	9mm 	10mm
AgSiNP/NG50 pH 4	9mm 	8mm 	9mm
Silver Nitrate 50pH 7	8mm 	8mm 	8mm










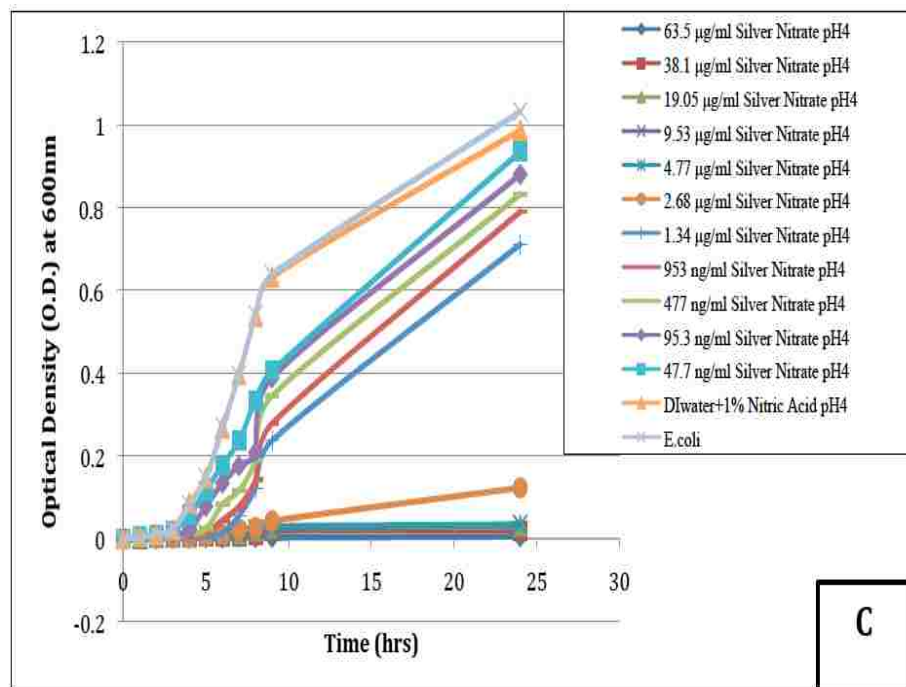
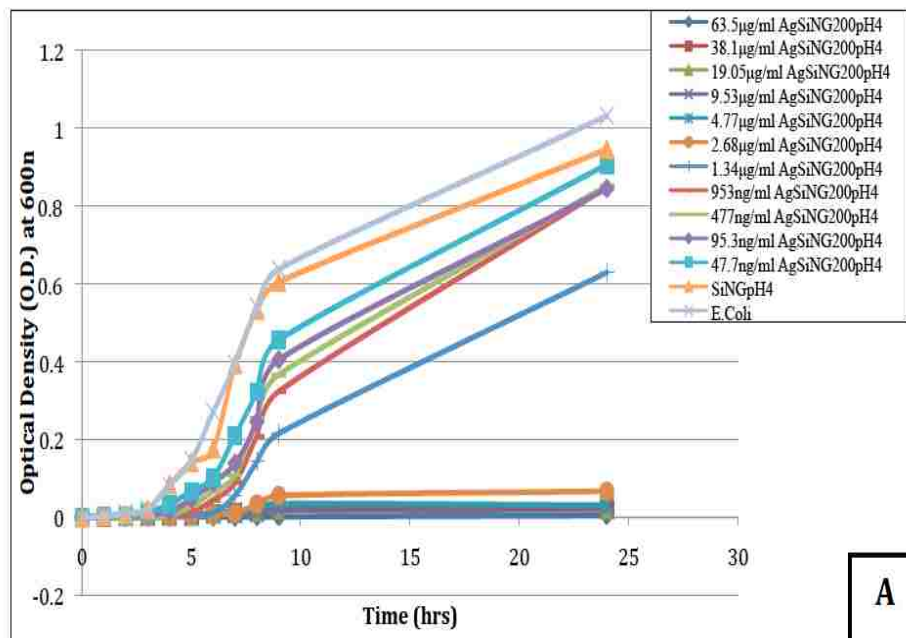
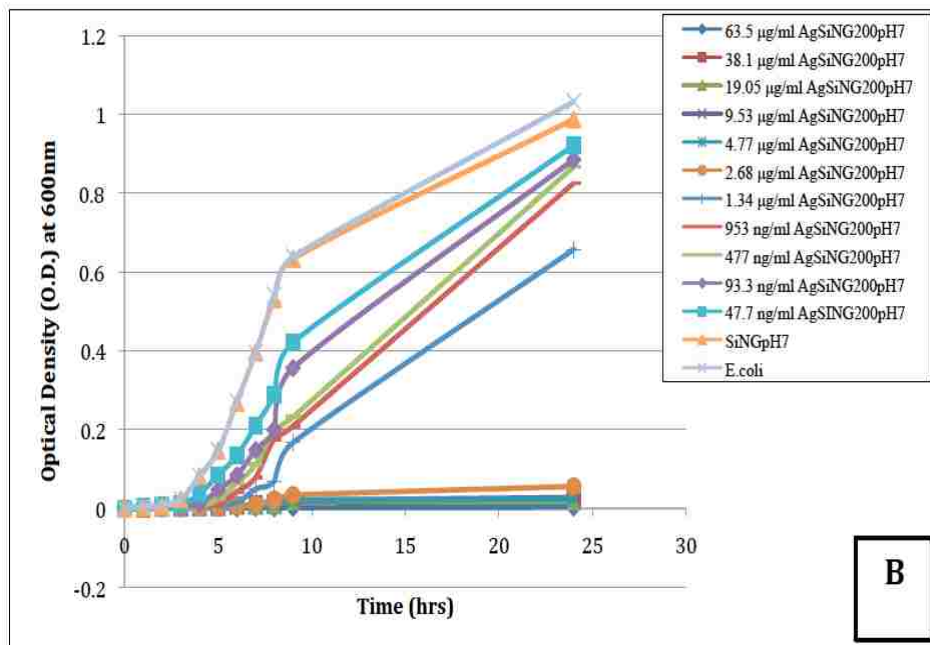
Silver Nitrate 50 pH 4	8mm 	7.5mm 	8mm 
SiNG pH 7	0mm 	0mm 	0mm 
SiNG pH 4	0mm 	0mm 	0mm 

Table 2 - Well diffusion zones for AgSiNP/NG50

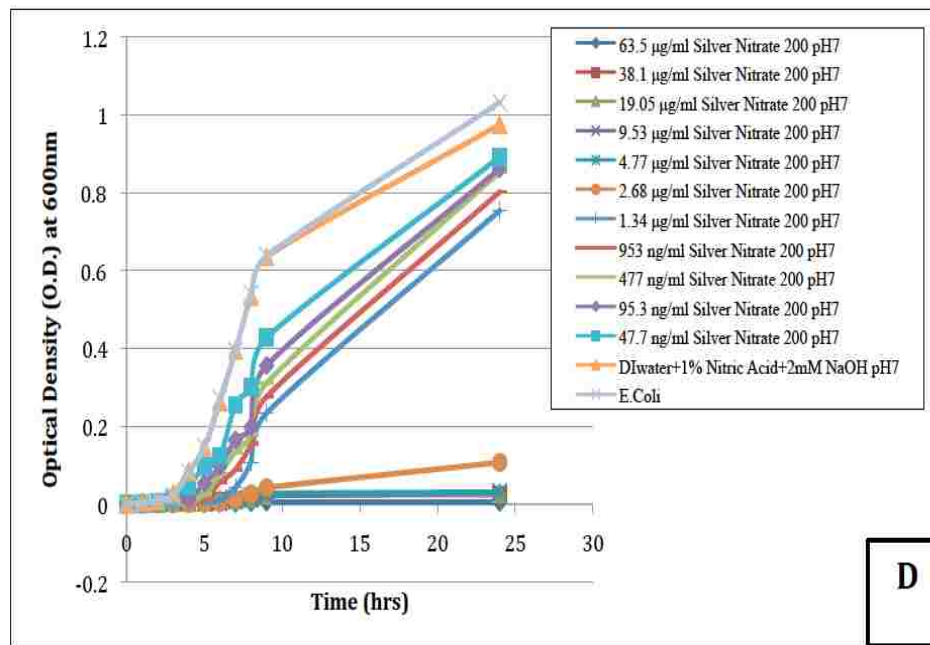
AgSiNP/NG50 has low loading of silver as compared to AgSiNP/NG200 but from the diffusion assay it is seen that AgSiNP/NG50 gives equivalent zone of clearance to that of AgSiNP/NG200. The well diffusion method was done confirm the action of AgSiNP/NG at both pH 7 and pH 4 against three bacteria *E.coli*, *B.subtilis* and *S.aureus*. From the results it can be seen that the material can effectively diffuse out of the well into agar and cause zone of clearance. These results were not seen when disc diffusion assay was used because of adherence of the material to the cellulose fibers of the disc so it was not able to diffuse out in the agar(47). The control silver nitrate also gives equivalent zone of clearance so it can be seen that silica gel does not interrupts the action of silver nanoparticles present in them. Silica gel by itself does not show any zone of clearance thus it can be said that the gel itself is just working as a delivery agent but silver is the main active component.

4.3.2 Bacterial Growth inhibition assay in broth using turbidity





B



D

Figure 28 - Growth curve of *E. coli* in presence of A) AgSiNP/NG200 pH 4 B) AgSiNP/NG200 pH 7 C) Silver Nitrate 200 (381µg/ml metallic silver content) pH 4 D) Silver Nitrate 200 (381µg/ml metallic silver content) pH 7.

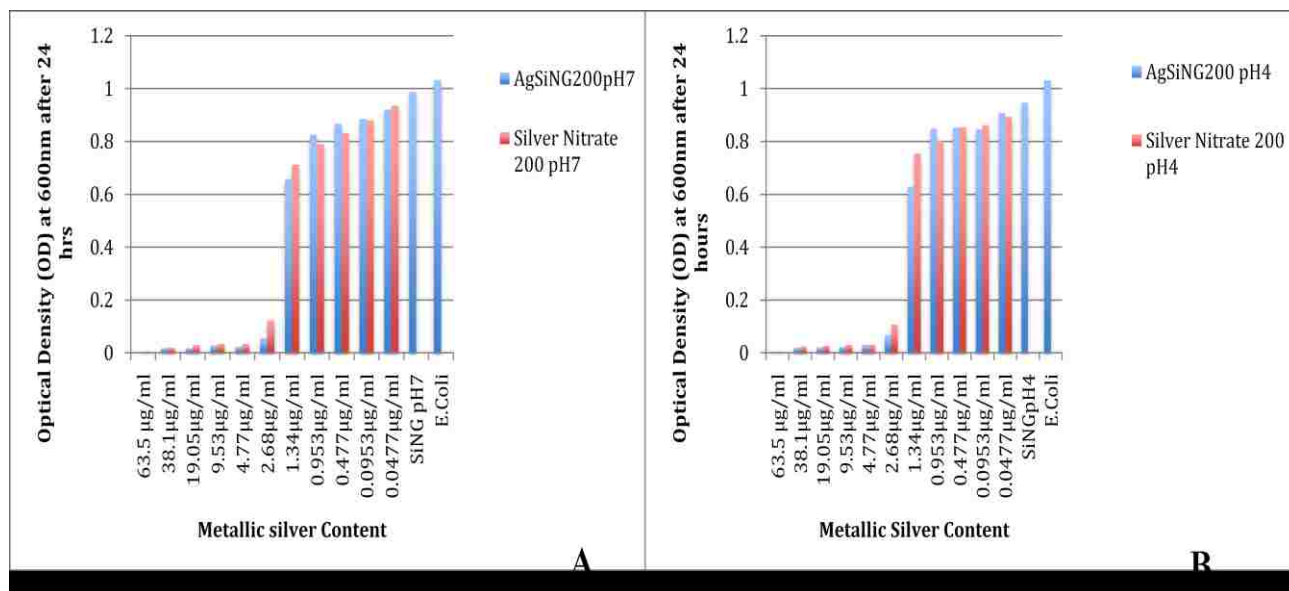
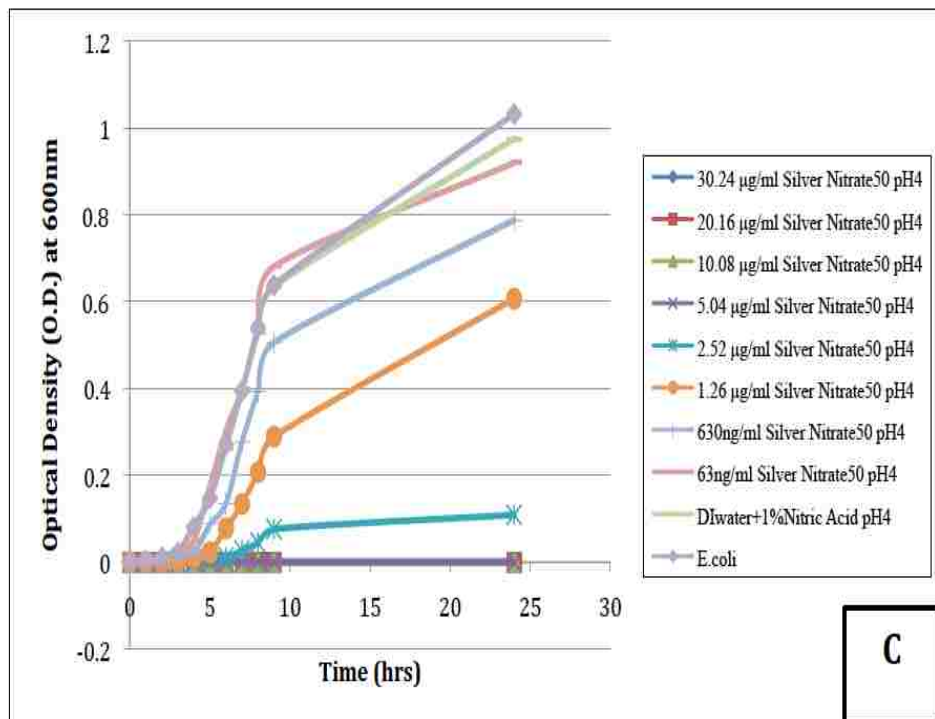
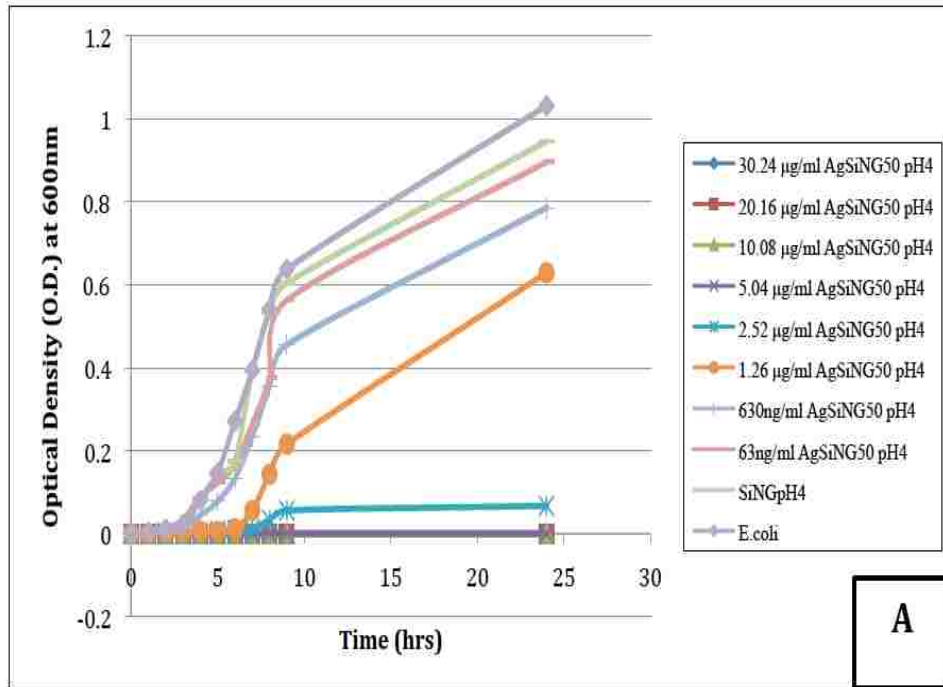
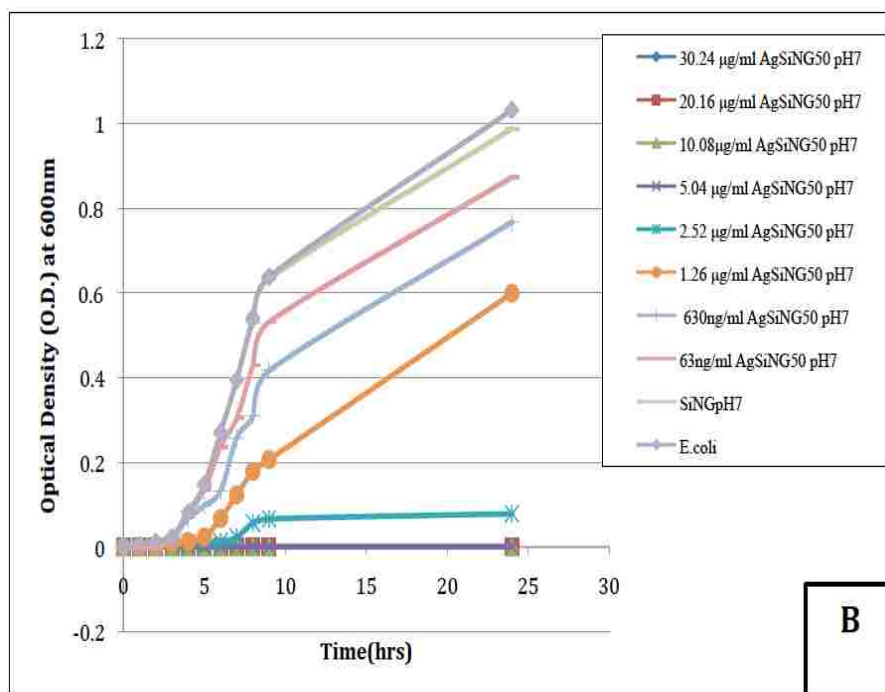


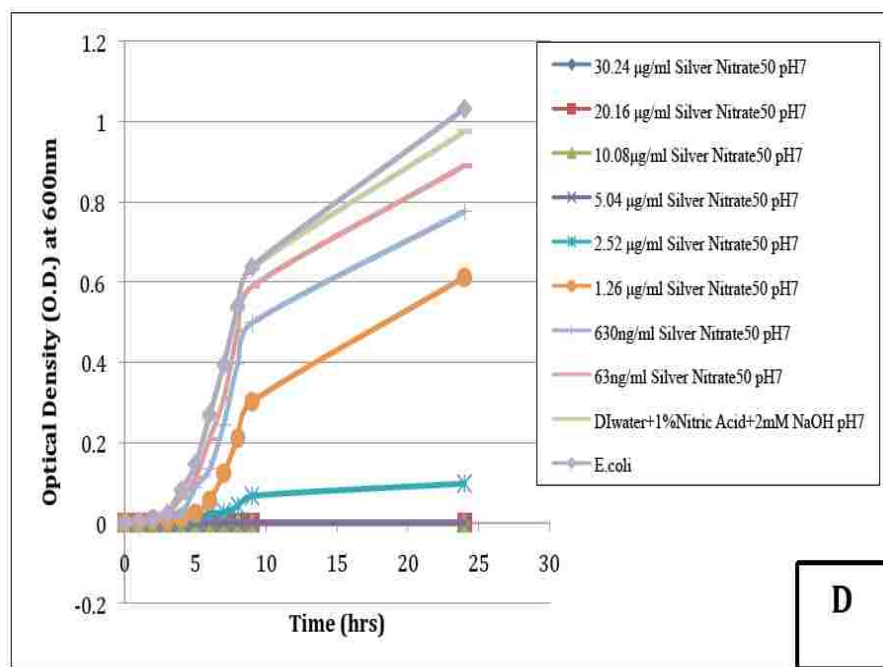
Figure 29 - Comparative end point growth inhibition of *E. coli* by A) AgSiNP/NG200 pH 7 Vs Silver Nitrate 200 pH 7 B) AgSiNP/NG200 pH 4 Vs Silver Nitrate 200 pH 4

From the growth curve of *E. coli* in presence of AgSiNP/NG200 pH 7 and pH 4 no difference in inhibition is seen stating that both the materials are equivalently effective against gram negative *E. coli*. The inhibition of growth of *E. coli* was seen at 2.68ppm for both AgSiNP/NG200 as well as the negative control silver nitrate having same metallic concentration. The growth of *E. coli* was not inhibited by SiNG formulations at both pH 7 and pH 4.





B



D

Figure 30 - Growth curve of *E.coli* in presence of A) AgSiNP/NG50 pH 4 B) AgSiNP/NG50 pH 7 C) Silver Nitrate 50 (100.8µg/ml metallic silver content) pH 4 D) Silver Nitrate 50 (100.8µg/ml metallic silver content) pH 7.

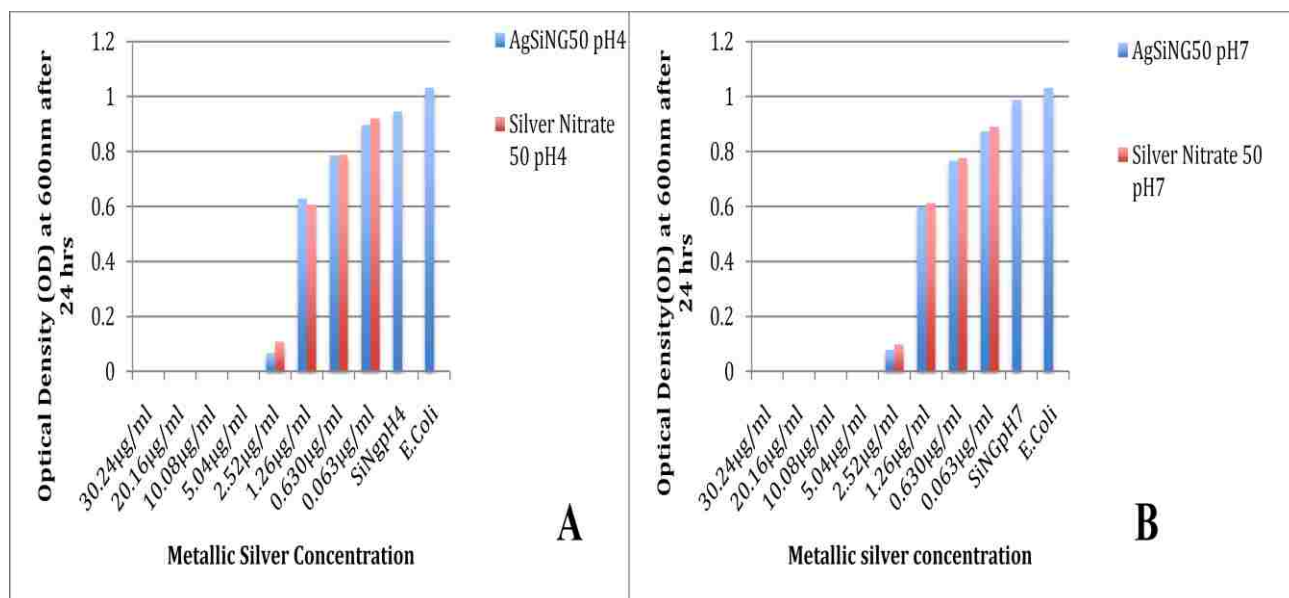
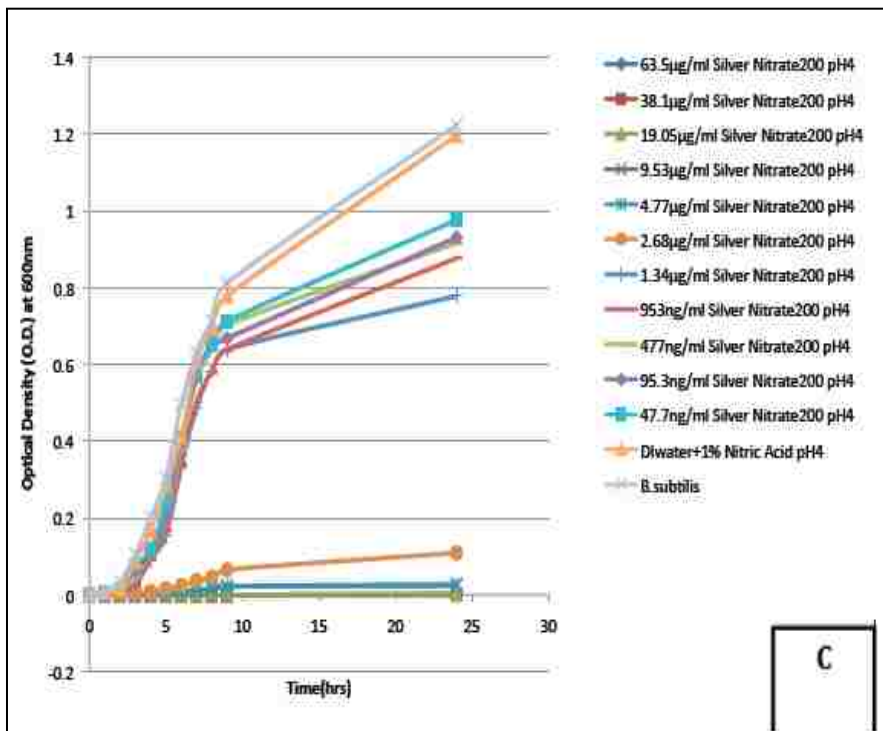
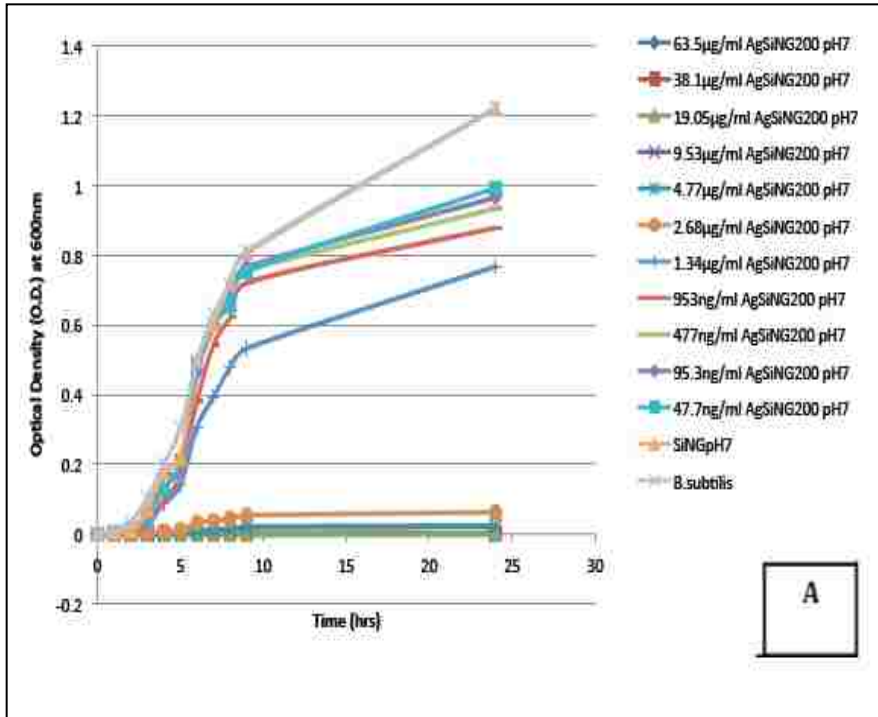


Figure 31 - Comparative end point growth inhibition of *E.coli* by A) AgSiNP/NG50 pH 4 Vs Silver Nitrate 50 pH 4 B) AgSiNP/NG50 pH 7 Vs Silver Nitrate 50 pH 7.

AgSiNP/NG 50 formulations at both pH 7 and pH 4 were able to inhibit the growth of *E.coli* equivalently. The metallic silver content of 2.52ppm was able to inhibit the growth of gram-negative *E.coli* in presence of both AgSiNP/NG50 as well as silver nitrate with same pH and metallic silver concentration. Silica gel at both pH 7 and pH 4 did not show any inhibition action against the bacteria.



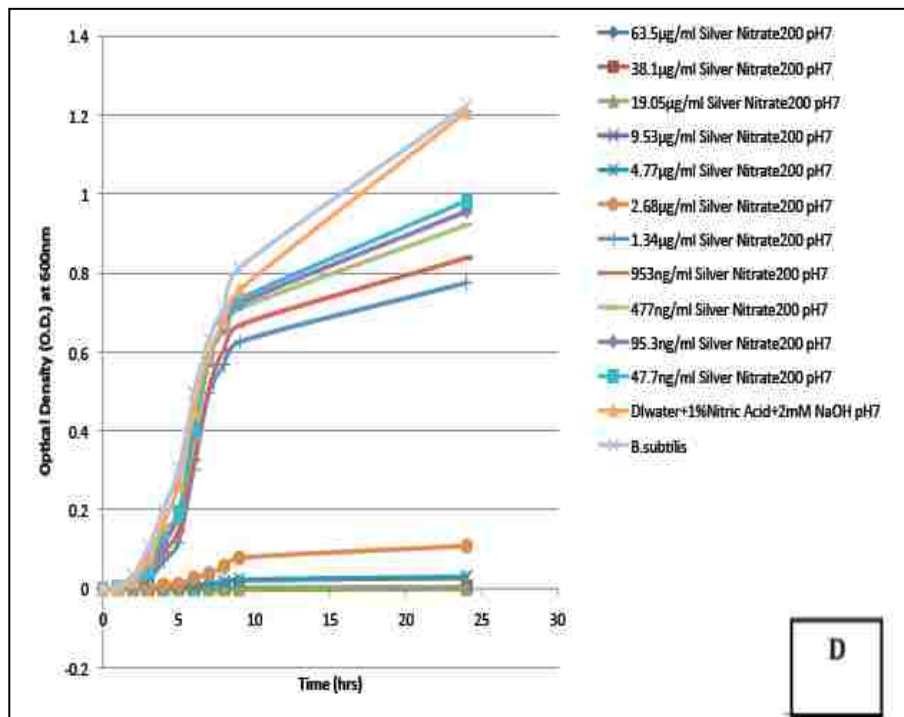
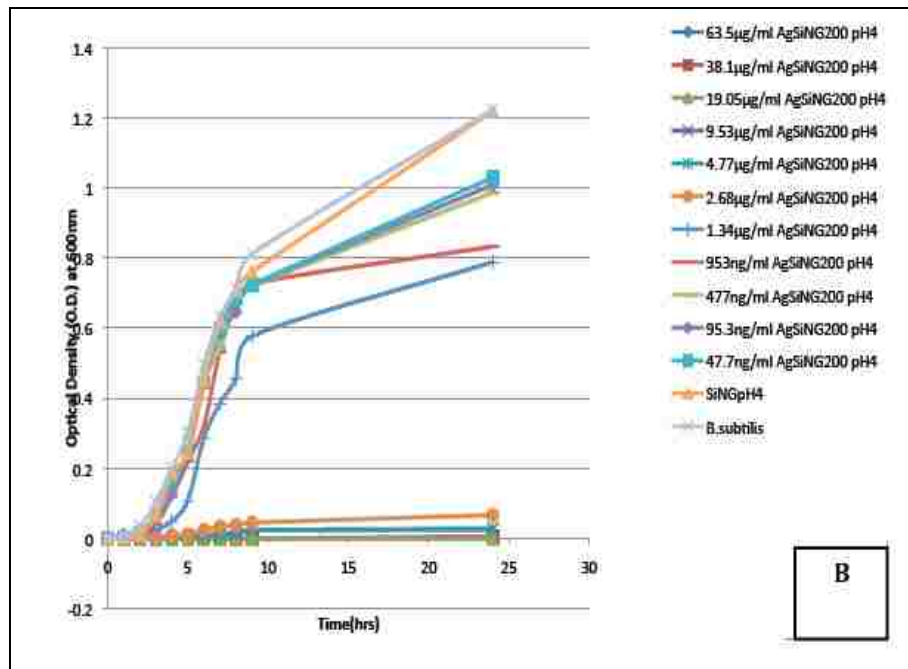


Figure 32 - Growth curve of *B. subtilis* in presence of A) AgSiNP/NG200 pH 4 B) AgSiNP/NG200 pH 7 C) Silver Nitrate 200 (381µg/ml metallic silver content) pH 4 D) Silver Nitrate 200 (381µg/ml metallic silver content) pH 7.

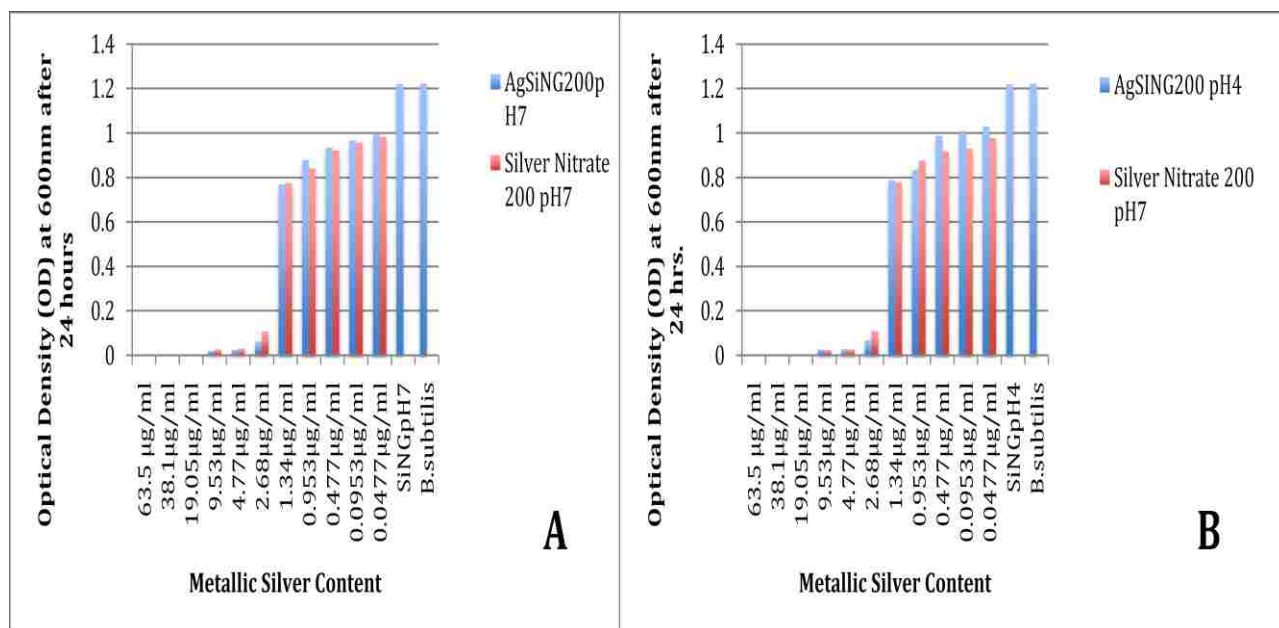
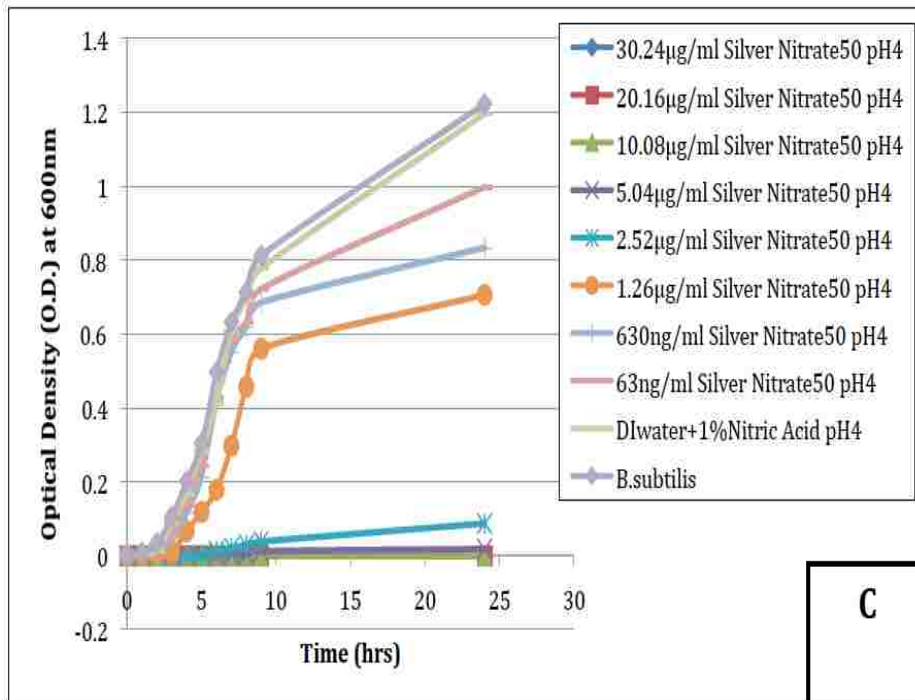
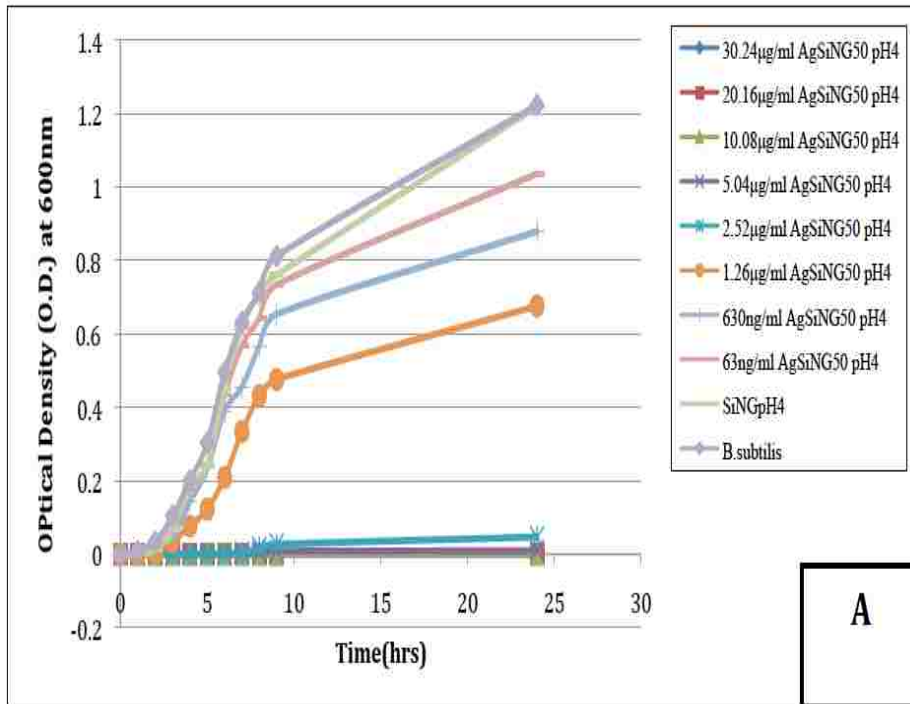


Figure 33 - Comparative end point growth inhibition of *B. subtilis* by A) AgSiNP/NG200 pH 7 Vs Silver Nitrate 200pH 7 B) AgSiNP/NG200pH 4 Vs Silver Nitrate 200pH 4

The growth of gram-negative *B. subtilis* was successfully inhibited by AgSiNP/NG200 formulation at both pH 7 and pH 4. The formulation AgSiNP/NG 200 was able to inhibit the growth of the bacteria at 2.68ppm, so was silver nitrate at the same metallic concentration and both the pH 7 and pH 4. Silica gel did not show any inhibition in growth compared to the blank.



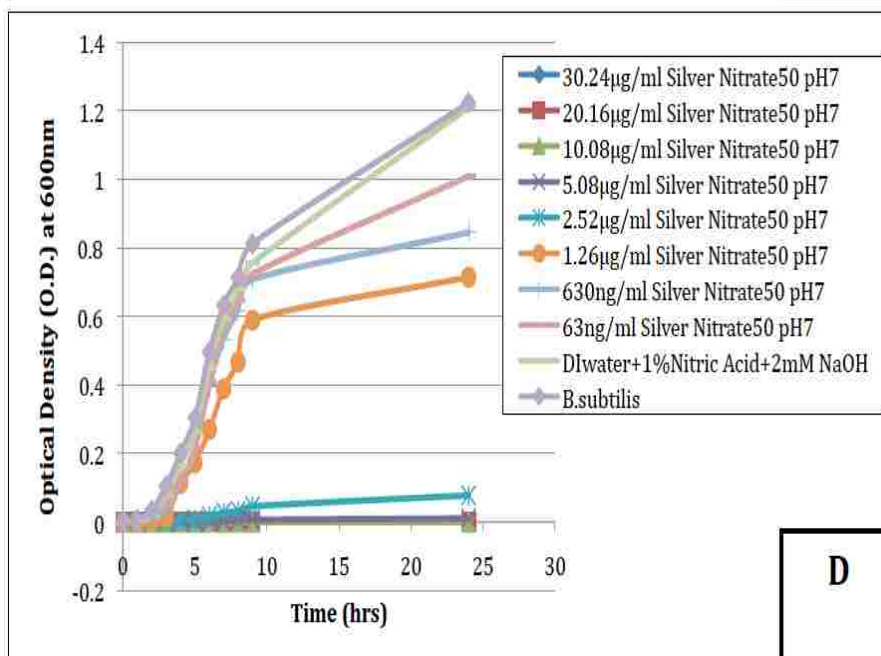
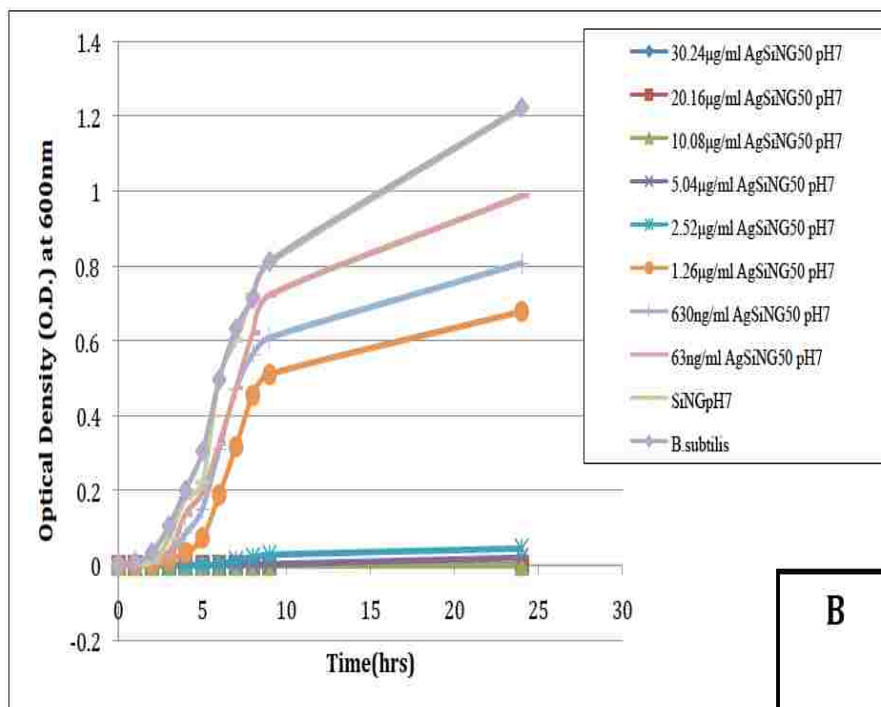


Figure 34 - Growth curve of *B. subtilis* in presence of A) AgSiNP/NG50 pH 4 B) AgSiNP/NG50 pH 7 C) Silver Nitrate 50 (100.8µg/ml metallic silver content) pH 4. D) Silver Nitrate 50 (100.8µg/ml metallic silver content) pH 7.

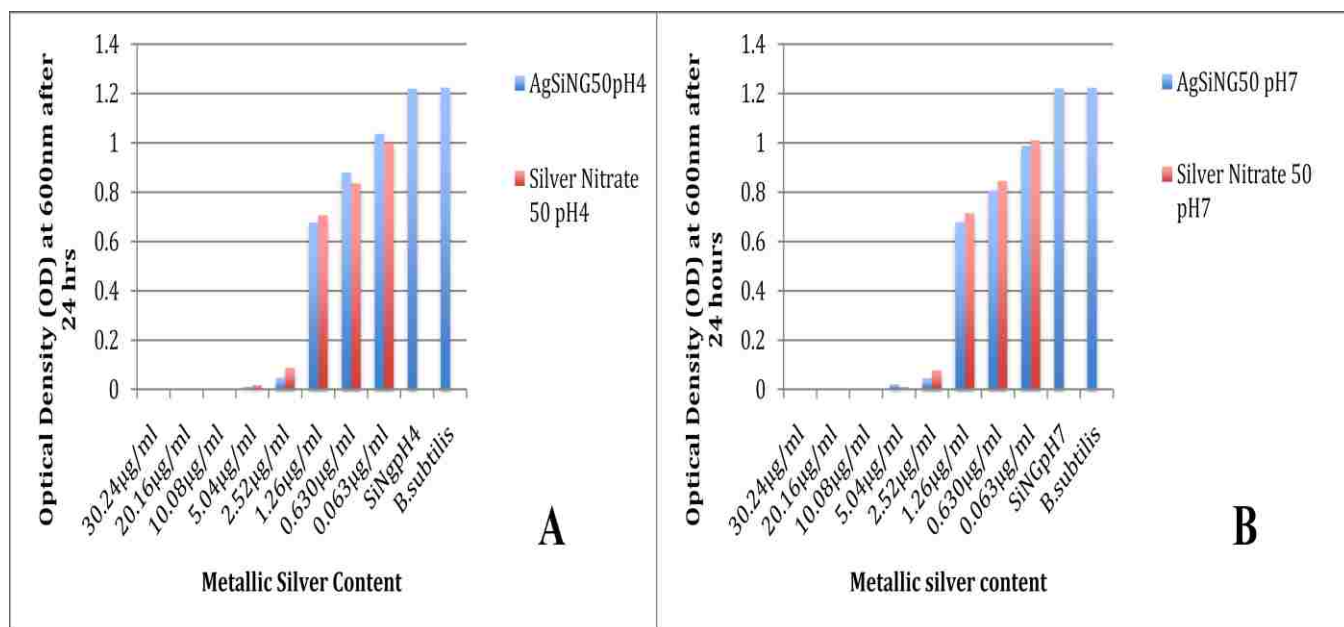
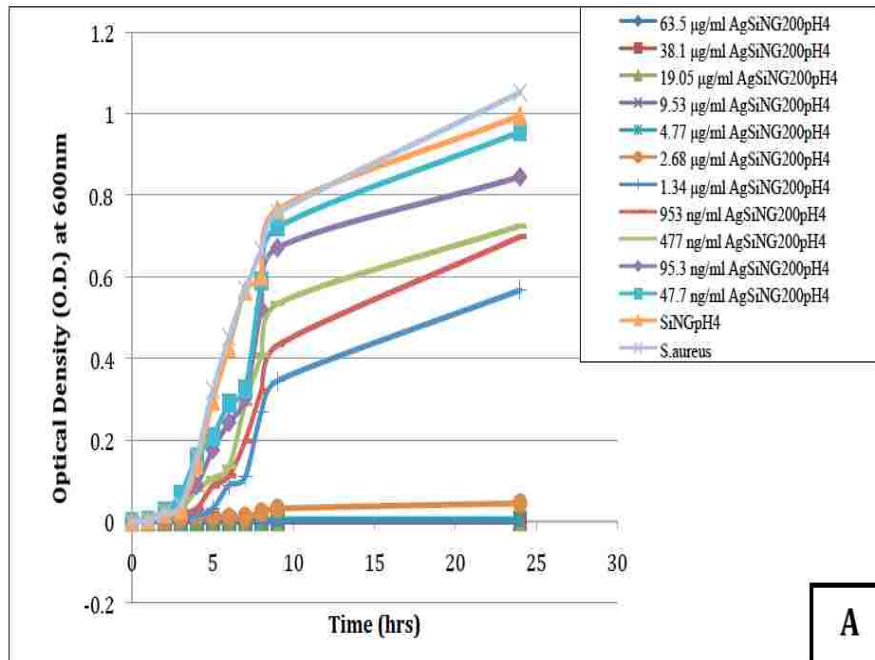
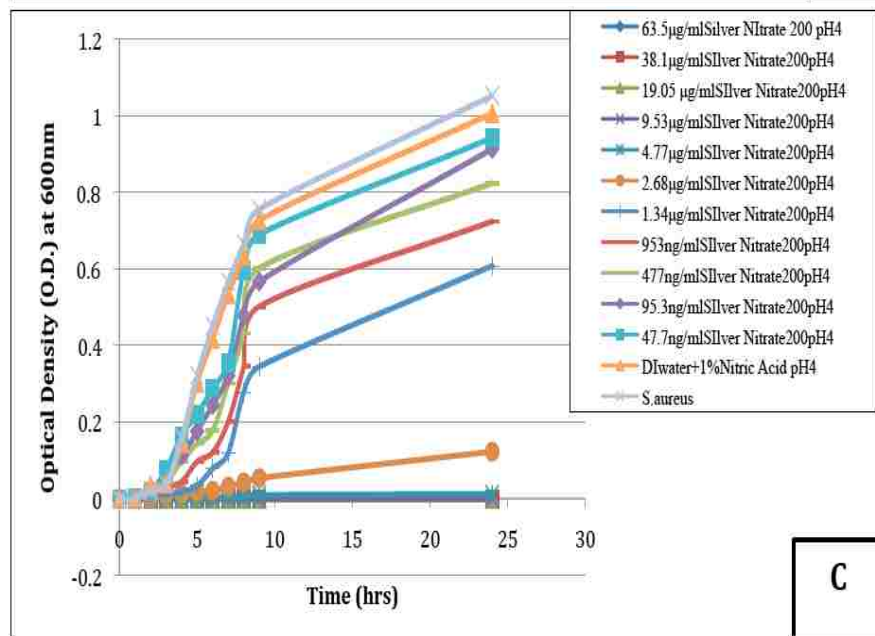


Figure 35- Comparative end point growth inhibition of *B. subtilis* by A) AgSiNP/NG50 pH 4 Vs Silver Nitrate 50pH 4 B) AgSiNP/NG50pH 7 Vs Silver Nitrate 50pH 7

From the growth curve obtained from growing *B. subtilis* in presence of AgSiNP/NG50 at both pH 7 and pH 4, one can see that there is no difference between the different pH formulations. *B. subtilis* grew well in both pH 7 and pH 4 SiNG in comparison to blank, thus silica does not provide any antibacterial efficacy. The growth inhibition was seen at 2.68 ppm. Silver Nitrate at same metallic silver concentration and pH showed similar antibacterial efficacy as that of AgSiNP/NG50 towards *B. subtilis*.



A



C

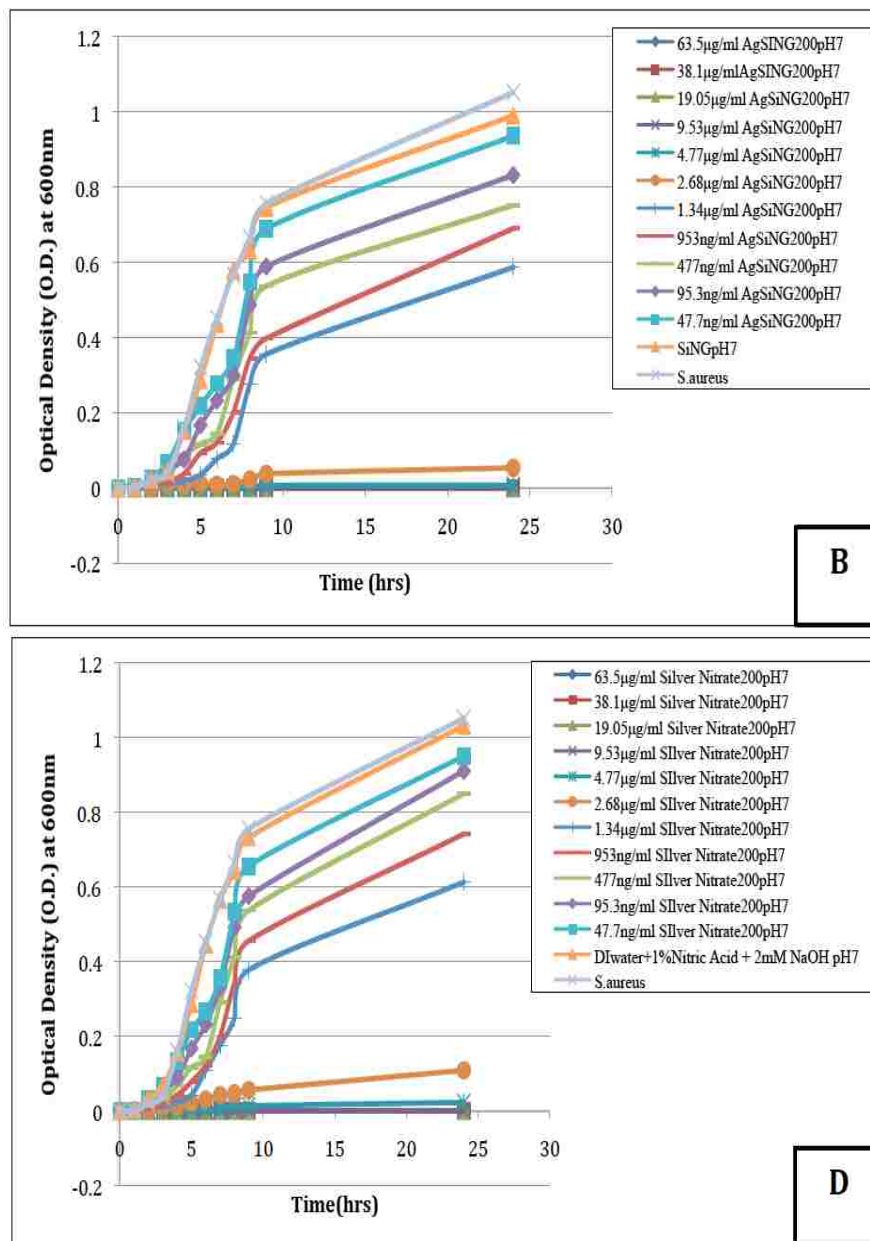


Figure 36 - Growth curve of *S.aureus* in presence of A) AgSiNP/NG200 pH 4 B) AgSiNP/NG200 pH 7 C) Silver Nitrate 200 (381µg/ml metallic silver content) pH 4. D) Silver Nitrate200 (381µg/ml metallic silver content) pH 7.

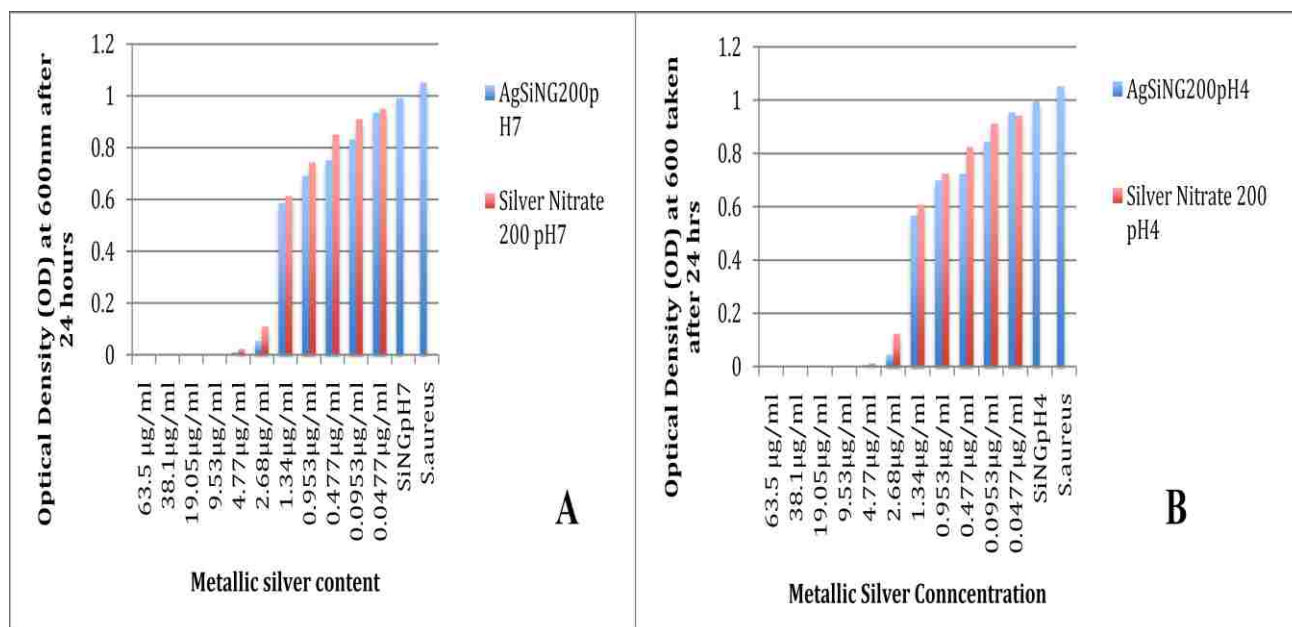
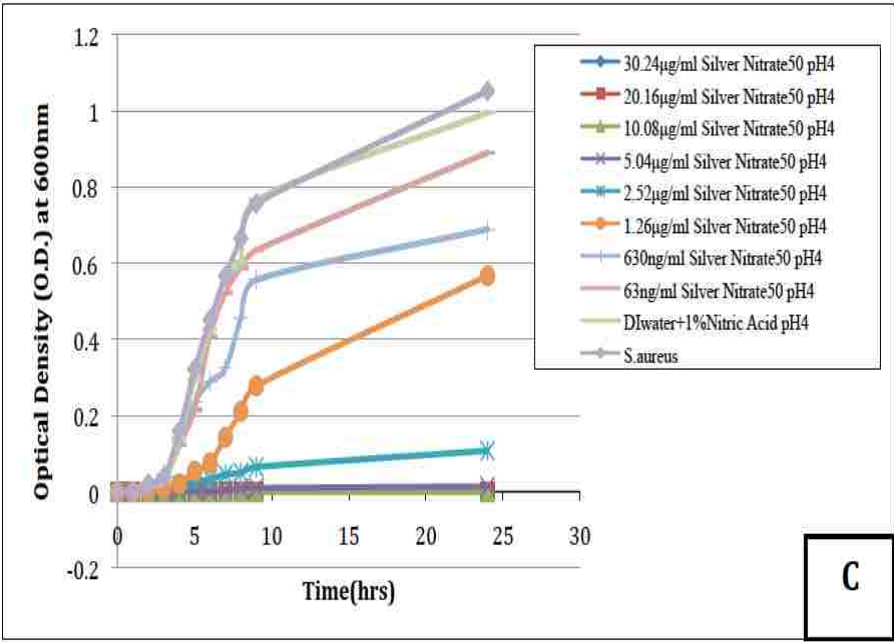
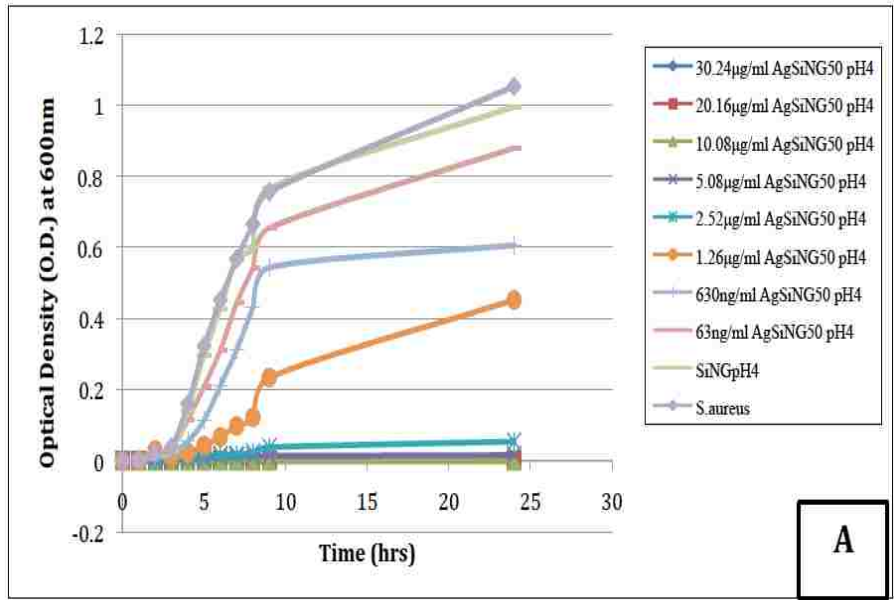


Figure 37 - Comparative end point growth inhibition of *S.aureus* by A) AgSiNP/NG200 pH 7 Vs Silver Nitrate 200pH 7 B) AgSiNP/NG200pH 4 Vs Silver Nitrate 200 pH 4

The formulation AgSiNP/NG200 was able to inhibit the growth of *S.aureus* at both pH4 and pH7 successfully. The metallic silver content required to inhibit total growth of *S.aureus* was 2.68ppm. There was no significant difference between the inhibition of silver nitrate salts to that of AgSiNP/NG formulation at same metallic content and same pH. Silica at both pH 7 and pH 4 did not show any significant inhibition of growth.



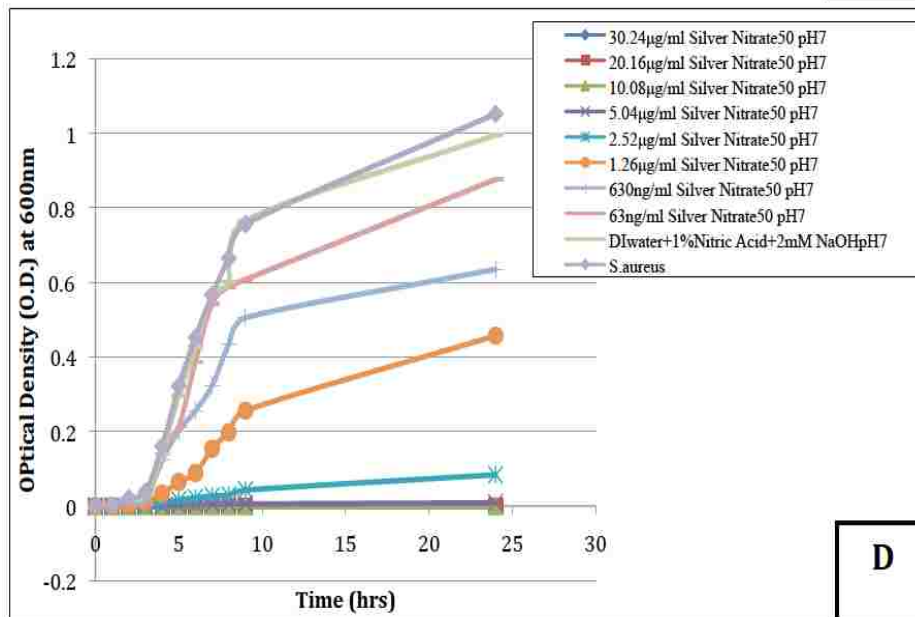
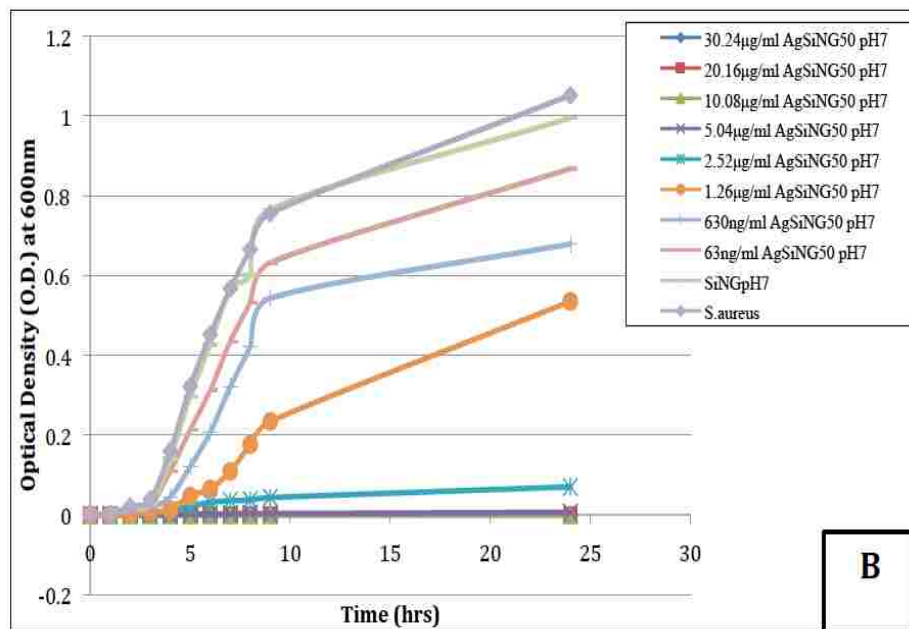


Figure 38 - Growth curve of *S.aureus* in presence of A) AgSiNP/NG50 pH 4 B) AgSiNP/NG50 pH 7. C) Silver Nitrate50 (100.8µg/ml metallic silver content) pH 4. D) Silver Nitrate50 (100.8µg/ml metallic silver content) pH 7.

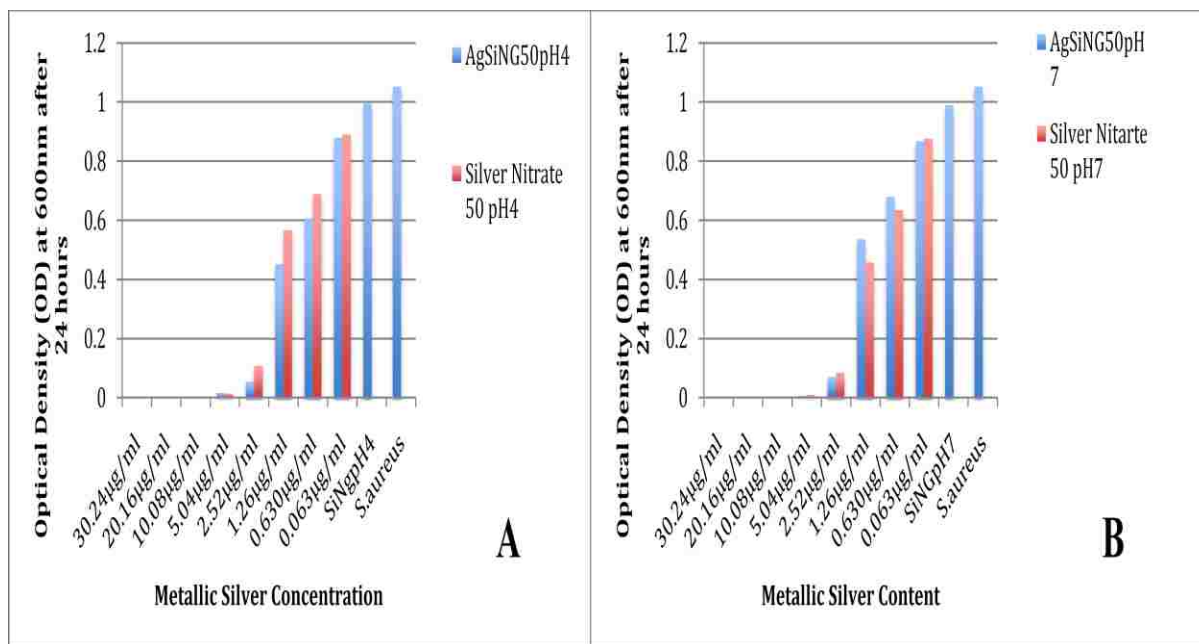


Figure 39 - Comparative end point growth inhibition of *S.aureus* by A) AgSiNP/NG50 pH 4 Vs Silver Nitrate 50pH 4 B) AgSiNP/NG50pH 7 Vs Silver Nitrate 50pH 7

AgSiNP/NG50 showed good inhibition for the growth of *S.aureus* in broth at both pH 7 and pH 4. Silver Nitrate showed same efficacy of growth inhibition as seen for AgSiNP/NG 50. 2.52 ppm of silver was able to inhibit the growth of *S.aureus*. Silica was not able to inhibit the growth of the bacteria.

4.3.3 Minimum Inhibitory Concentration assay using resazurin indicator

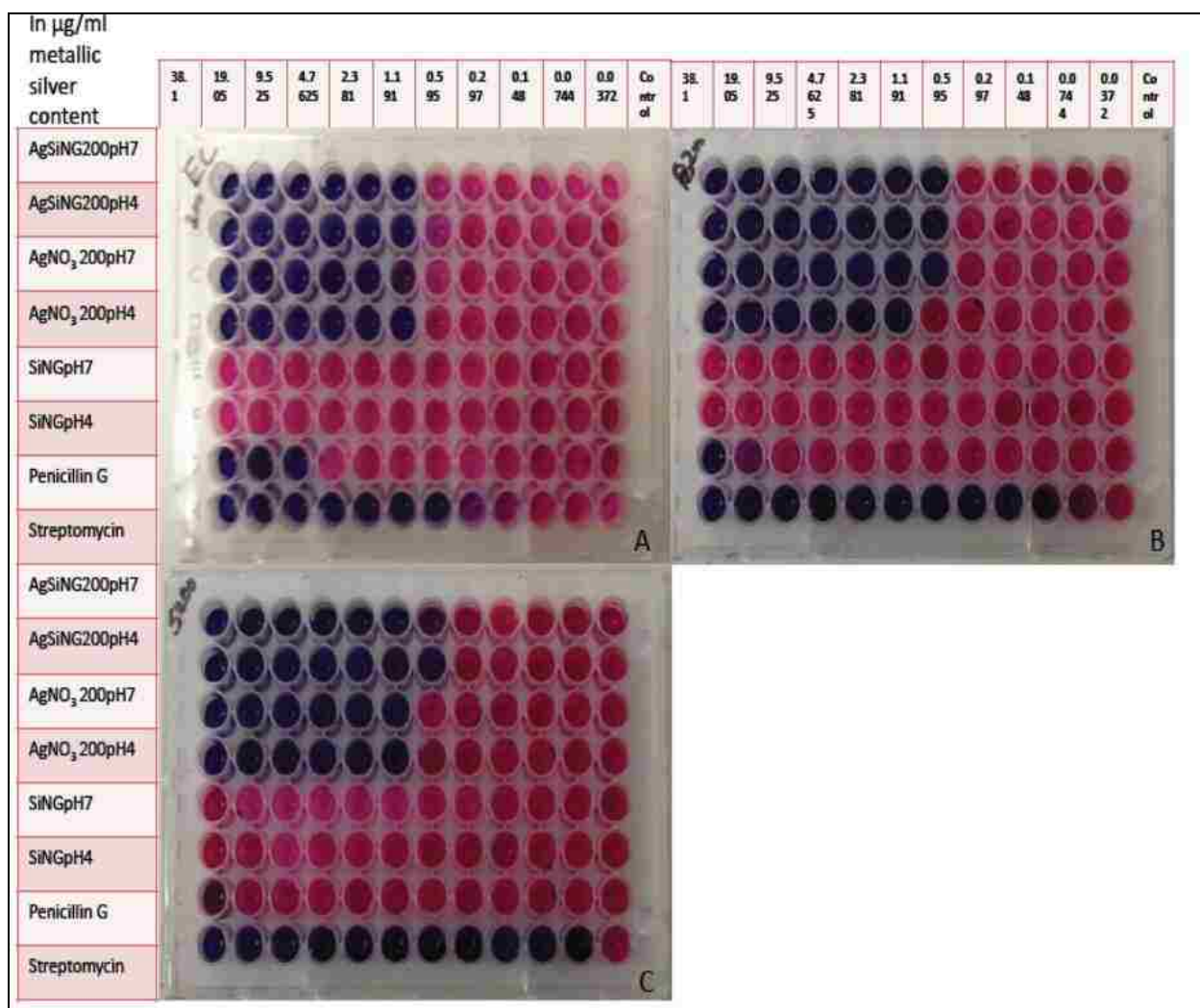


Figure 40 - Resazurin assay for AgSiNP/NG200 A) *E.coli* B) *B.Subtilis* C) *S.aureus*.



Figure 41- Resazurin assay for AgSiNP/NG50 for A) E.coli B) B.subtilis C) S.aureus.

From the resazurin assay test, one can see that the MIC values vary for each bacterium. From the result it could be concluded that the MIC from AgSiNP/NG200 and AgSiNP/NG50 is in range from 1ppm to 0.5 ppm, which is the acceptable range for MIC of silver nanoparticles. The results here show inhibition at lower ppm because the amount of nutrient broth added is comparatively lower than that used in the growth curve assay. The following results were obtained from the average of triplicate.

Sample	E.Coli (ppm)	B.subtilis (ppm)	S.aureus (ppm)
AgSiNP/NG200 pH 7	0.773	0.992	0.992
AgSiNP/NG200 pH 4	0.773	0.992	0.992
AgNO ₃ 200 pH 7	1.191	1.389	1.191
AgNO ₃ 200 pH 4	1.191	1.389	1.389
AgSiNP/NG50 pH 7	0.787	0.787	1.05
AgSiNP/NG50 pH 4	0.787	0.918	1.05
AgNO ₃ 50 pH 7	1.009	1.009	1.311
AgNO ₃ 50 pH 4	1.009	1.311	1.311
SiNGpH 7	-	-	-
SiNGpH 4	-	-	-
Penicillin-G	208.33	333.33	333.33
Streptomycin	36.455	26.385	25

Table 3 - Average MIC obtained from resazurin assay

4.3.4 BacLight® LIVE/DEAD assay

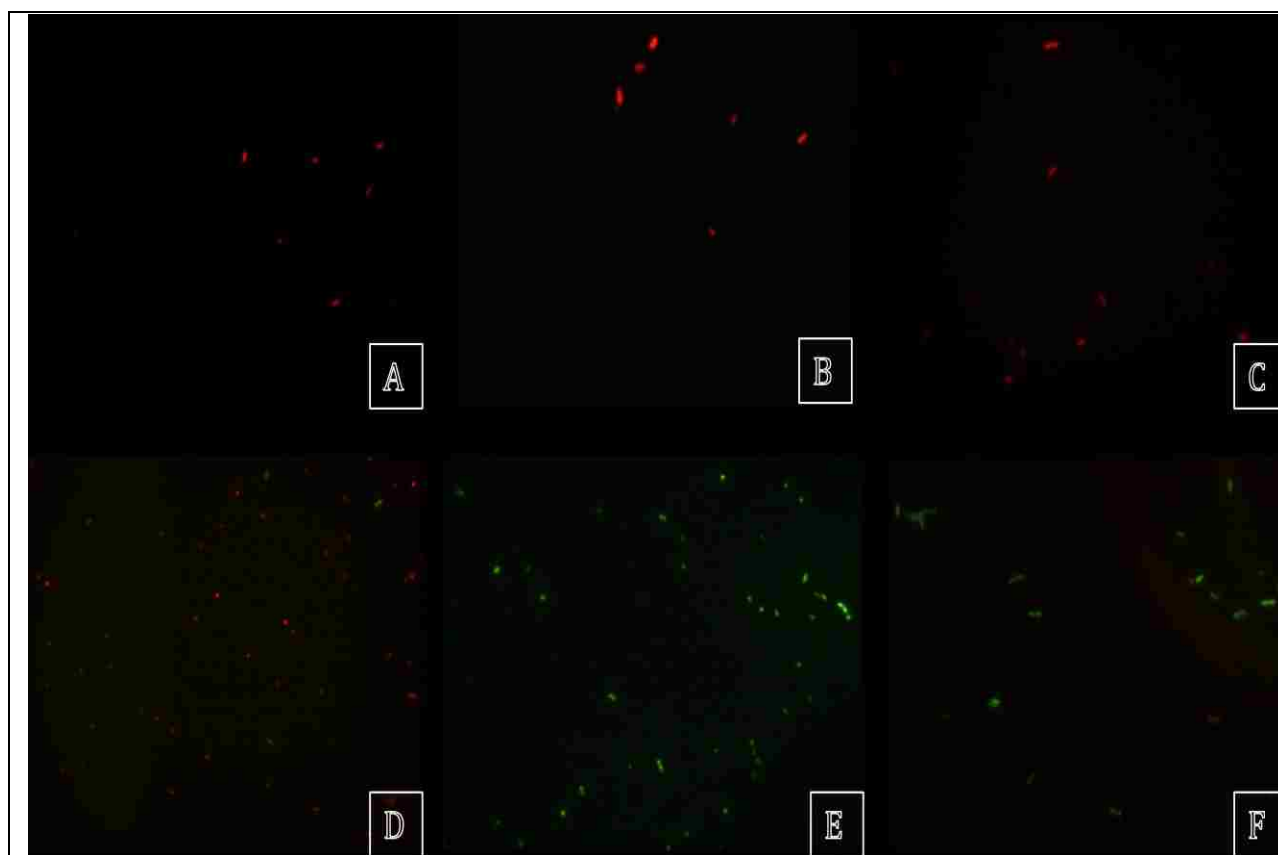


Figure 42 - *E.coli* treated for 2 hours with A) AgSiNP/NG200 pH 7 B) AgSiNP/NG200 pH 4 C) AgNO₃ pH 7 D) AgNO₃ pH 4 E) SiNG pH 4 F) Untreated cells.

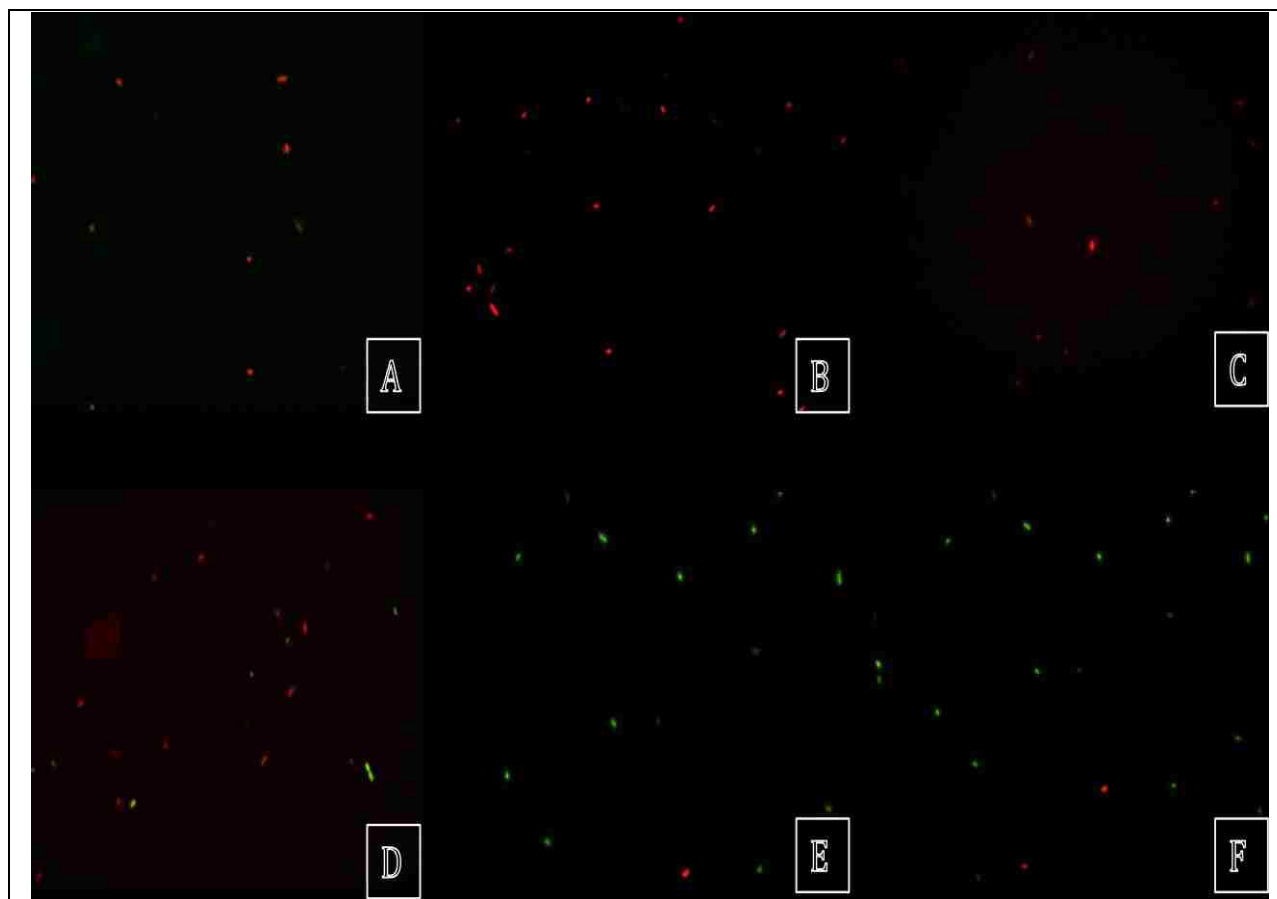


Figure 43 - *B.subtilis* treated for 2 hours with A) AgSiNP/NG200 pH 7 B) AgSiNP/NG200 pH 4 C) AgNO₃ pH 7 D) AgNO₃ pH 4 E) SiNG pH 4 F) Untreated cells.

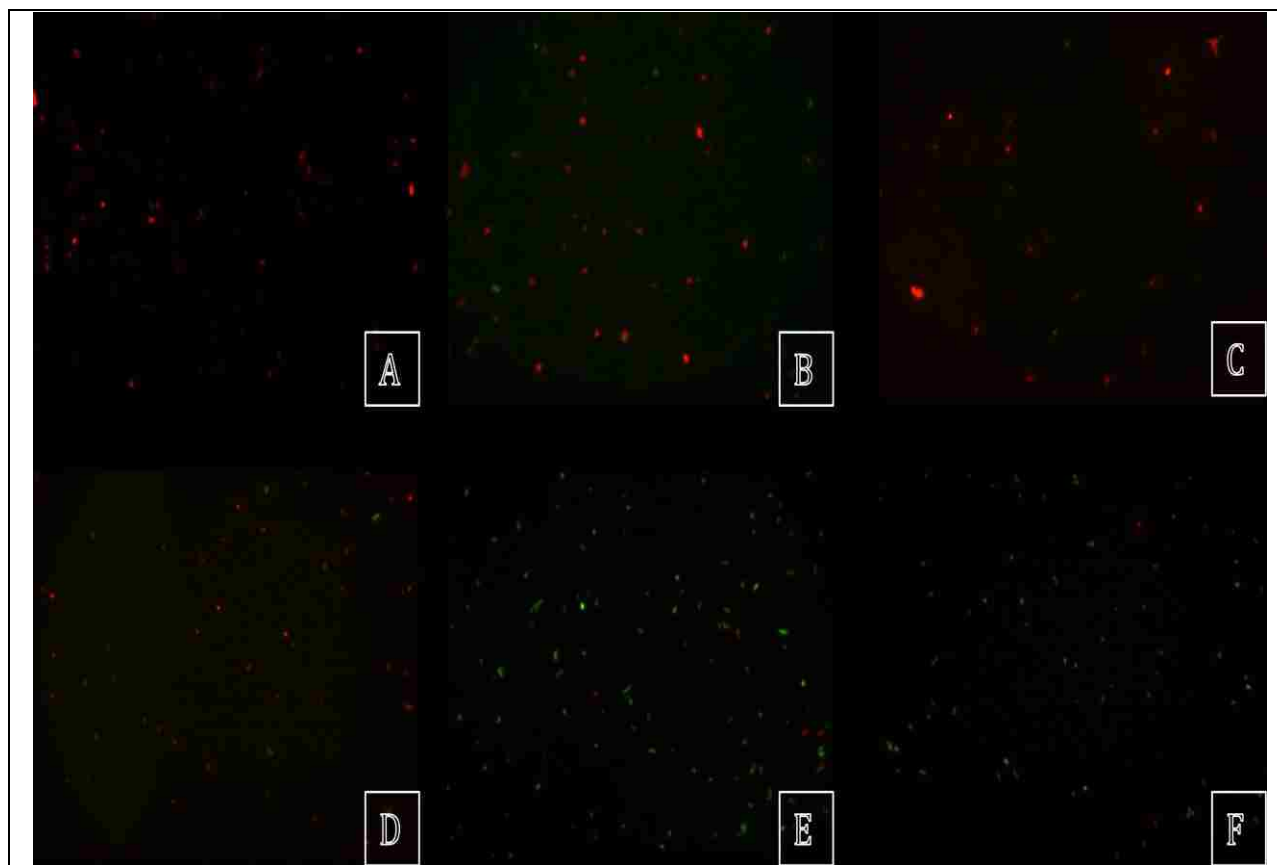


Figure 44 - *S.aureus* treated for 2 hours with A) AgSiNP/NG200 pH 7 B) AgSiNP/NG200 pH 4 C) AgNO₃ pH 7 D) AgNO₃ pH 4 E) SiNG pH 4 F) Untreated cells.

From figure 42, 43 and 44 it can be seen that the cells treated with silver containing silica gels as well as silver nitrate are stained red, showing that the propidium iodide is able to enter the cells because of cell membrane disruption. Whereas the cells treated with just SiNG and the untreated cells shows green color thus proving that they have intact membrane and no propidium iodide has entered in the cell to stain their nucleus and are live cells. From this result we can say that AgSiNP/NG was able to kill the bacteria in 2 hours of incubation.

CHAPTER 5 DISCUSSION

We synthesized four silver containing silica nanogel formulations AgSiNP/NG200 and AgSiNP/NG50 with different silver loading (3.52mM and 1mM loading respectively). Both these formulations were further classified according to their pH value. The AgSiNP/NG200 pH 4 showed transparent colorless formulation. AgSiNP/NG200 pH 7 showed yellowish-brown color formation. AgSiNP/NG 50 at pH 4 showed colorless transparent formulation. AgSiNP/NG 50 at pH 7 showed a slight yellowish color formation few weeks after synthesis.

From the results of DLS, AFM and SEM there was clear indication that by adding silver in the preparation of sol-gel itself there was formation of silica-silver sol particles which remained as particles at neutral pH whereas at lower pH sol particles formed gel since aggregation of silica particles could be seen. The presence of particles was because of increase in activity of silica-silver interaction at the higher pH, the silver did not allow silica to grow and thus particles approximately at the size from 100-200nm were seen in both AgSiNP/NG200 and AgSiNP/NG50 at pH 7. SEM did show very small sol-gel formation for SiNG at both pH and the rest of the sol was converted to gel this could be because the silica sol particles were free to condense with each other (20). No solvent was used in this process.

Surface Plasmon Resonance (SPR) absorption was seen in the UV-Vis spectroscopy for both formulations at pH 7 at around 420 nm. The presence of the SPR peak indicated that at pH 7 there was production of silver nanoparticles in the gel formulation at around 10-20nm. These samples were yellowish brown in color due SPR absorption of the silver nanoparticles. The presence of color could also be because of silver oxide nanoparticles due to interaction of silver with sodium hydroxide, which was used to raise the pH to 7 (48). The SPR was not seen for pH

4 formulations, which were colorless and transparent solutions. A peak at 296-300nm was also seen in the UV region for all the four formulations, characteristic to Ag^+ , Ag^{2+} , Ag^{3+} ion cluster peak (36). Also slight peak shift can be observed for the ion cluster peak for the formulations at pH 4 and pH 7. As a result it could be seen that the silver is present in the formulations at pH 4 in ionic form and in pH 7 formulations in nanoparticulate form.

HRTEM was carried out for both the formulations at both pH 7 and pH 4. From HRTEM results it was clearly seen that silver nanoparticles were present in all the formulations at pH 4 as well as pH 7. Uniformly distributed, non-aggregated, highly crystalline, spherical silver nanoparticles can be seen from the sizes of 10-25nm. These nanoparticles were enclosed by the silica nanogel. More nanoparticles were seen in AgSiNP/NG200 formulation than compared to AgSiNP/NG50 formulations. From the diffraction pattern of the silver nanoparticles it could be seen that elemental silver nanoparticles as well as silver oxide nanoparticles were present at pH 7, whereas that for pH 4 formulations only elemental silver nanoparticles were seen.

Silica acts as a reducing agent. Data suggested that; silica reduced silver ions to elemental silver, leading to formation of silver nanoparticles which were embedded within the silica matrix(17). TEOS hydrolysis produces silica, water and ethanol. Ethanol also helps to reduce the silver salts; since no ethanol was added as a solvent in this formulation ethanol produced by TEOS hydrolysis could have played some role in facilitating the formation of silver nanoparticles. The EDAX spectra also showed the presence of silica around the silver nanoparticle, also silica was seen when the analysis was done on the surface of silver nanoparticle stating that silica has enclosed the silver nanoparticles in its matrix.

Literature shows that silver-silica formulation is able to adhere strongly to cellulose fibers(47), thus the disc diffusion assay did not work since the material was not able to diffuse out of the disc. Thus we had to follow more traditional well diffusion assay. From the well diffusion assay one can see that there is formation of zone of clearance for both the formulations of AgSiNP/NG at both pH 7 and pH 4. The zone of clearance was equivalent to silver nitrate solutions at the same metallic silver concentration. The presence zone of clearance indicated that the entrapment of silver in silica did not reduce its antibacterial property. Overall, slow release of the Ag⁺ ions took place, thus prolonging the antibacterial property of the material. Silica nanogel by itself did not show any zone of clearance. This showed that silica nanogel does not have any anti-bacterial effect. Silver-silica gel was also able to diffuse out in agar leading to antibacterial activity.

From growth inhibition assay in broth using turbidity, it was seen that AgSiNP/NG200 at both pH 7 and pH 4 were able to inhibit the growth of all the three microorganisms at 2.68µg/ml of metallic silver content. Silver Nitrate was also able to inhibit the growth at that same metallic silver concentration. As a result one could see that AgSiNP/NG200 has same antibacterial efficacy as seen for silver nitrate salt at similar concentration and pH. Similarly, it was seen that for AgSiNP/NG50 the growth was inhibited at 2.52 µg/ml of the metallic silver. Silver nitrate at the same metallic silver concentration also showed inhibition at the same concentration of metallic silver. It is reported that Ag⁺ ions are released from the silica matrix when suspended in aqueous medium (17, 38, 42, 49). This ion released from the silica matrix produces antibacterial effect of the material.

From the resazurin MIC assay it could be seen that the MIC of AgSiNP/NG 200 were better than that seen for AgSiNP/NG 50. This could be due to the increase in loading of the silver particle in the gel. Again there was no significant difference seen in the results obtained from silver nitrate salt. The similarity in antibacterial efficacy of silver nitrate and AgSiNP/NG could be because of the availability of free silver ions in its biologically active form in silver nitrate solution (38) whereas silver entrapped in silica gel releases silver ions at much controlled rate, concluding that even if silver nitrate shows equivalent amount of growth inhibition, its effect is short lived, but in case of AgSiNP/NG formulation because of the controlled release of ions the antibacterial effect is going to be prolonged.

From the BacLight™ assay after two hours of incubation of the bacteria with AgSiNP/NG completely dead cells were seen under microscope (propidium iodide stained-red). From this result one could say that there is bactericidal effect of AgSiNP/NG since it ruptures the cell membrane allowing propidium iodide to enter the cell to stain the nucleus. Whereas the cells which were either treated with SiNG as well as untreated cells shows green fluorescent staining from STYO9 indicating that they had intact cell membranes; thus, the cells were alive.

CHAPTER 6. CONCLUSION

The AgSiNP/NG materials have been synthesized using sol-gel method. Materials were characterized using various microscopic and spectroscopic techniques. In all of these materials silver nanoparticles were formed and these nanoparticles were embedded in silica matrix as characterized by the HRTEM. UV-Vis results confirmed characteristic SPR absorption of silver nanoparticles and presence of ionic silver. Colorless AgSiNP/NG formulations were obtained at pH 4.0 at which minimal or characteristic SPR absorption was found. The non-color formation in pH 4 formulations suggests that silica coating (a dielectric material) is able to shift the SPR towards the UV region. All the four materials showed excellent antibacterial activity against gram-negative *E.coli* and gram-positive *B.subtilis* and *S.aureus*. Loading of silver in AgSiNP/NG formulations did not compromise antibacterial properties of the silver.

The AgSiNP/NG containing formulation can be successfully used to produce touch-safe (antibacterial) non-color forming surface. A number of potential applications including antibacterial coating on medical instruments, textiles, glass & ceramic substrates, plastics and paints could be realized using AgSiNP/NG materials. Strong antibacterial properties against *S.aureus* could lead to development of a spray-formula to be used in health care facilities to minimize Methicillin-Resistant Staphylococcus *Aureus* (commonly known as MRSA) infections.

REFERENCES

1. Singh, M.; Singh, S.; Prasad, S .; Gambhir, I.S., Nanotechnology in medicine and anti bacterial effect of silver nanoparticles. *Digest Journal of Nanomaterials and Biostructures* **3**, 115 (2008).
2. Nishida, H.; Risemberg, H.M., Silver nitrate ophthalmic solution and chemical conjunctivitis. *Pediatrics* **56**, 368 (1975).
3. Charles L. Fox, J., Silver Sulfadiazine-A new topical therapy for Pseudomonas in burns. *AMA Arch Surg* **96**, 184 (1968).
4. Bowen, D.L.; Fung, M.C., Silver Products for meicinal indiations: risk assessment. *Journal of Toxicology* **34**, 119 (1996).
5. Samuel, U.; Guggenbichler, J.P., Prevention of catheter-related infections: The potential of a new nano-silver impregnated catheter. *International Journal of Antimicrobial Agents* **23**, 75 (2004).
6. Ahearn, D.G.; May, L.L.; Gabriel, M.M., Adherence of organisms to silver-coated surfaces. *Journal of Industrial Microbiology & Biotechnology* **15**, 372 (1995).
7. Lohmeier-Vogel, E.M.; Lee, H.; Trevors, J.T.; Slawson R.M., Silver Resistance in Pseudomonas Stutzeri. *Biometals* **7**, 30 (1994).
8. Bragg, P.D.; Rainnie, D.J., The effect of silver ions on the respiratory chain of E.coli. *Can J Microbiol* **20**, 883 (1974).
9. Rogers, K.S., Variable sulfahydryl activity toward silver nitrate by reduced glutathionine and alcohol, glutamate and lactate dehydrogenases. *Biochim Biophys Acta* **263**, 309 (1972).

10. Yakabe, Y.; Sano, T.; Ushio, H.; Yasumaga, T., Kinetic studies of the interaction between silver ion and deoxyribonucleic acid. *Chem Lett* **4**, 373 (1980).
11. Coward, J.S.; Carr, H.S.; Rosenkranz H.S., Silver Sulfadiazine: effect of the ultrastructure of *Pseudomonas aeruginosa*. *Antimicrobial Agents Chemotherapy* **3**, 621 (1973).
12. Silver, S.; Phung, L.; Silver, G., Silver as biocides in burn and wound dressings and bacterial resistance to silver compounds. *Journal of Industrial Microbiology & Biotechnology* **33**, 627 (2006).
13. Li, X.Z.; Nikaido, H.; Williams, K.E., Silver resistant mutants of *Escherichia coli* display active efflux of Ag⁺ and are deficient in porins. *J Bacteriol* **179**, 6127 (1997).
14. Nair, L.S.; Cato L.T., Silver Nanoparticles: Synthesis and Therapeutic Applications. *Journal of Biomedical Nanotechnology* **3**, 301 (2007).
15. Furno F.; Morley, K.S.; Wong B.; Sharp, B.L.; Arnold, P.L.; Howdle, S.M.; Bayston, R.; Brown P.D.; Winship P.D.; Reid H.J., Silver Nanoparticles and polymeric medical devices: A new approach to prevention of infection? *J. of Antimicrobial Chemotherapy* **54**, (2004).
16. Hu, S.; Zhao, B.; Xu, W.; Li, B.; Fan, Y., Surface enhanced raman spectroscopy study on the structure changes of 4-mercaptopyridine adsorbed on silver substrates and silver colloids. *Spectrochem. Acta, Part A* **58**, (2002).
17. Kim, Y.H., Lee, D.K., Cha, H.G., Kim, C.W., & Kang, Y.S., Synthesis and characterization of antibacterial Ag-SiO₂ nanocomposite. *The Journal of Physical Chemistry C* **111**, 3629 (2007).

18. Patakfalvi R.; Viryani, Z.; Dekany, I., Kinetics of silver nanoparticle growth in aqueous polymer solutions. *Colloid polymer sci.* **283**, (2004).
19. Jia, H.; Zeng, J.; Song, W.; An, J.; Zhao, B., Preparation of silver nanoparticles by photoreduction for surface enhanced Raman scattering. *Thin Solid Films* **496**, (2006).
20. Gupta, R.; Kumar, A., Bioactive materials for biomedical applications using sol-gel technology. *Biomedical Materials* **3**, 1 (2008).
21. Ebelmen, M.; *Ann. Chim. Phys.* **16**, (1846).
22. Kim, Ki Do; Kim, Hee Talk, Formation of Silica Nanoparticles by Hydrolysis of TEOS Using a Mixed Semi-Batch/Batch Method. *Journal of Sol-Gel Science and Technology* **25**, 183 (2002).
23. C. J. Brinker, Hydrolysis and condensation of silicates: Effects on structure. *Journal of Non-Crystalline Solids* **100**, 21 (1988).
24. Farady, M. *Philos. Trans. R. Soc. London* **147**, 145 (1857).
25. Wiley, B.J.; Im, S. H.; Li, Z.Y.; McLellan, J.; Siekkinen, A.; Xia, Y., Maneuvering the surface plasmon resonance of silver nanostructures through shape-controlled synthesis. *J. Phys. Chem. B* **110**, 15666 (2006).
26. Li, Z.; Gu, A.; Zhou, Q., Growth of spindle-shaped silver nanoparticles in SDS solution. *Cryst. Res. Technol.* **44**, 841 (2009).
27. Huang, H.H.; Ni, X.P.; Loy, G.H.; Chew, C.H.; Tan, K.L.; Loh, F.C.; Deng, J.F.; Xu, G.Q., Photochemical formation of silver nanoparticles in poly (N-vinylpyrrolidone). *Langmuir* **12**, 909 (1996).

28. Pastoriza-Santos, I.; Liz-Marzan., L.M., Formation of PVP-Protected Metal Nanoparticles in DMF. *Langmuir* **18**, 2888 (2002).
29. Yin, B.; Ma, H.; Wang, S.; Chen, S., Electrochemical Synthesis of Silver Nanoparticles under Protection of Poly(N-vinylpyrrolidone). *Journal of Physical Chemistry B* **107**, 8898 (2003).
30. Toshikazu, T., Antimicrobial agent composed of silica-gel with silver complex. *Inorg Mater* **6**, 505 (1999).
31. Podsiadlo, P.; Paternel, S.; Rouillard, J.M.; Zhang, Z.; Lee, J.; Lee, J.W.; Gulari, E.; Kotov, N.A., Layer-by-layer assembly of nacre-like nanostructured composites with antimicrobial properties. *Langmuir* **21**, 11915 (2005).
32. Lee, D.; Cohen, R.E.; Rubner M.F., Antibacterial properties of Ag nanoparticle loaded multilayers and formation of magnetically directed antibacterial microparticles. *Langmuir* **21**, 9651 (2005).
33. Zhang, L.Z.; Yu, J.C.; Yip, H.Y.; Li, Q.; Kwong, K.W.; Xu, A.W.; Wong, P.K., Ambient Light Reduction Strategy to Synthesize Silver Nanoparticles and Silver-Coated TiO₂ with Enhanced Photocatalytic and Bactericidal Activities. *Langmuir* **19**, 10372 (2003).
34. Yeo, S.Y.; Jeong, S.H., Preparation and characterization of polypropylene/silver nanocomposite fibers. *Polymer International* **52**, 1053 (2003).
35. Park S.J.; Jang Y.S., Preparation and characterization of activated carbon fibers supported with silver metal for antibacterial behavior. *J Colloid Interface Sci* **261**, 238 (2003).
36. Jeon, H.J.; Yi, S.C.; Oh, S.G., Preparation and antibacterial effects of Ag–SiO₂ thin films by sol–gel method. *Biomaterials* **24**, 4921 (2003).

37. Kawashita, M.; Tsuneyama, S.; Miyaji, F.; Kukobu, T., Antibacterial silver-containing silica glass prepared by sol-gel method. *Biomaterials* **21**, 393 (2000).
38. Egger, S.; Lehmann, R.P.; Height, M.J.; Loessner, M.J.; Schuppler, M., Antimicrobial properties of a novel silver-silica nanocomposite material. *Applied and Environmental Microbiology* **75**, 2973 (2009).
39. Jiang, Z.J.; Lui, C.Y., Seed-Mediated Growth Technique for the Preparation of a Silver Nanoshell on a Silica Sphere. *J Phys Chem B* **107**, 12411 (2003).
40. Jasiorski, M.; Leszkiewicz, A.; Brzezinski, S.; Bugla-Płoskon'ska, G.; Borak, B.; Malinowska, G.; Karbownik, I.; Baszczuk, A., Textile with silver silica spheres: its antimicrobial activity against Escherichia coli and Staphylococcus aureus. *J Sol-Gel Sci Technol* **51**, 330 (2009).
41. Quang, D.V.; Sarawade, P. B.; Hilonga, A.; Kim, J.K.; Chai, Y.G.; Ryu, J.Y.; Kim, S.H.; Kim, H.T., Preparation of silver nanoparticle containing silica micro beads and investigation of their antibacterial activity. *Applied Surface Science* **257**, 6963 (2011).
42. Min, S.; Yang, J.; Kim, J. Y.; & Kwon, Y., Development of white antibacterial pigment based on silver chloride nanoparticles and mesoporous silica and its polymer composite. *Microporous and Mesoporous Materials* **128**, 19 (2010).
43. Schillinger, U.; Lucke, F.K., Antibacterial activity of lactobacillus sake isolated from meat. *Applied and Environmental Microbiology* **55**, 1901 (1989).
44. Rastogi, S.K.; Rutledge, V.J.; Gibson, C.; Newcombe, D.A.; Branen, J.R.; Branen, L.A., Ag colloids and Ag clusters over EDAPTMS-coated silica nanoparticles: synthesis,

- characterization, and antibacterial activity against Escherichia coli. *Nanomedicine: Nanotechnology, Biology, and Medicine* **7**, 305 (2010).
45. Sarker, S.D.; Nahar, L.; Kumarasamy, Y., Microtitre plate-based antibacterial assay incorporating resazurin as an indicator of cell growth, and its application in the in vitro antibacterial screening of phytochemicals. *Methods* **42**, 321 (2007).
 46. Rentería-Tapia, V., Synthesis, optical properties, and modeling of silver core/silver oxide shell nanostructures in silica films. *Proc. SPIE* **6641**, 66411W (2007).
 47. Nischala, K.; Rao, T.N.; Hebalkar, N., Silica-silver core-shell particles for antibacterial textile applications. *Colloids and surfaces B. Biointerfaces* **82**, 203 (2011).
 48. Tripathi, S.; Mehrotra, G.K.; Dutta, P.K., Chitosan–silver oxide nanocomposite film: Preparation and antimicrobial activity. *Bulletin of Materials Science* **34**, 29 (2011).
 49. Melaiye, A.; Sun, Z.; Hindi, K.; Milsted, A.; Ely, D.; Reneker, D. H.; et al., Silver(I)-imidazole cyclophane gem-diol complexes encapsulated by electrospun tecophilic nanofibers: Formation of nanosilver particles and antimicrobial activity. *Journal of American Chemical Society* **127**, 2285 (2005).